MIT Open Access Articles

Light-Controlled Radical Polymerization: Mechanisms, Methods, and Applications
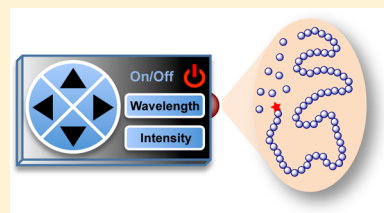
CHEMICAL REVIEWS

Review

Light-Controlled Radical Polymerization: Mechanisms, Methods, and Applications

Mao Chen,[†,§] Mingjiang Zhong,[†,‡,§] and Jeremiah A. Johnson[*,†]

[†]Department of Chemistry and [‡]Department of Chemical Engineering, Massachusetts Institute of Technology, 77 Massachusetts Avenue, Cambridge, Massachusetts 02139, United States

ABSTRACT: The use of light to mediate controlled radical polymerization has emerged as a powerful strategy for rational polymer synthesis and advanced materials fabrication. This review provides a comprehensive survey of photocontrolled, living radical polymerizations (photo-CRPs). From the perspective of mechanism, all known photo-CRPs are divided into either (1) intramolecular photochemical processes or (2) photoredox processes. Within these mechanistic regimes, a large number of methods are summarized and further classified into subcategories based on the specific reagents, catalysts, etc., involved. To provide a clear understanding of each subcategory, reaction mechanisms are discussed. In addition, applications of photo-CRP reported so far, which include surface fabrication, particle preparation, photoresponsive gel design, and continuous flow technology, are summarized. We hope this review will not only provide informative knowledge to researchers in this field but also stimulate new ideas and applications to further advance photocontrolled reactions.

## CONTENTS

1. INTRODUCTION

1.1. General Introduction

Controlled/living radical polymerization (CRP) has revolutionized polymer science by enabling the user-friendly synthesis of polymers with precise average molar masses, diverse compositions, and well-defined architectures.[1−8] It has offered new

opportunities to directly incorporate various functional groups into polymers, which can provide fascinating new properties or facilitate subsequent derivatization for applications of interest. With this powerful innovation, scientists are able to access advanced materials with nearly infinite possibilities of polymer backbone structures, functionalities, and properties, which has benefited numerous fields including nanotechnology, biomedicine, energy, and defense.[9] Building on these achievements, in recent years researchers have sought to further expand the utility of CRP reactions through the development of externally regulated and/or switchable polymerizations.[10] Today, light,[11,12] applied voltage,[13–15] chemical redox triggers,[16–18] and mechanical force[19,20] have been successfully utilized as stimuli for CRP as well as other living polymerization reactions.[21]
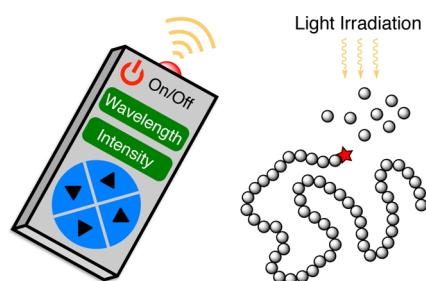

Figure 1. Photocontrolled radical polymerizations offer a range of attractive features for polymer synthesis and advanced materials design.

Due to its low cost and ubiquity, light is perhaps the most attractive external regulator for a chemical reaction. Notably, photosynthesis, the process by which plants convert solar energy into carbohydrate molecules and eventually biopolymers, gives rise to all life on Earth.[22] In greatly oversimplified terms, photosynthesis is nature's photocontrolled chemistry. Seeking to emulate this complex and sophisticated process from nature, scientists have developed methods for harnessing the energy of light to induce novel chemical reactions, thereby producing useful molecules and materials. These innovations have also led to successful strategies for photocontrolled switching of reactions between "on" and "off" states, which provides the unique capability to temporally and spatially control chemical reactivity.[10] Light has proven particularly useful in the context of radical polymerizations;[23] photoinduced radical polymerization is now routinely used for the synthesis of commercial adhesives, coatings, and resins, for additive manufacturing, and for photolithography.[24–31] However, most of the widely used photopolymerization reactions are not completely switchable with light, and they are not "living" polymerizations. The development of living photocontrolled radical polymerization, i.e., processes that lead to high chain end fidelity and the ability to reinitiate polymer chains over several cycles, offers many potential advantages in the above-mentioned applications as well as unprecedented novel applications.

Understanding what makes a photocontrolled polymerization living or not requires consideration of the paradigms of organic photochemistry. In general terms (Scheme 1), a photochemical reaction begins when a ground state molecule R absorbs a photon ($h\nu$) of sufficient energy to excite an electron from the molecule's HOMO into a higher lying orbital. Regardless of which higher lying orbital is initially populated, Kasha's rule

Scheme 1. Simplified Paradigm of Organic Photochemistry
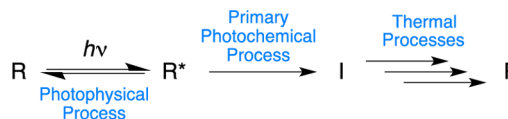
stipulates that rapid thermal relaxation will produce the first singlet excited state molecule R*.[32] This excited species can then undergo either photophysical or photochemical transformations. In the context of traditional photoinitiated free radical polymerization, the desired primary photochemical processes generate free radicals from the absorbing species, and these radicals undergo thermal propagation reactions in the presence of suitable monomers M to yield products P (in this case polymers). Since the radicals initiated are not instantly and reversibly consumed in the reaction system, they can continually propagate before they terminate via thermal biradical reactions that can occur in the presence or absence of light. Thus, the growth of individual polymer chains is not switchable between "on" and "off" states, and such polymerizations are not technically living. In recent years, several elegant strategies for imparting living behavior to radical polymerization have been reported. In subsequent sections of this review, the specific mechanistic strategies used to develop photocontrolled, living radical polymerizations (photo-CRPs) are described in detail. Though many of these methods and strategies are still relatively new, we anticipate continued growth of this area as increasingly controlled polymerizations and novel applications of living photopolymers are developed.

Motivated by potential applications of living photopolymers, there has been an explosion of interest in photo-CRP in recent years. There are now photo-CRP methods that resemble the most well-known thermal CRP methods such as atom transfer radical polymerization (ATRP), single electron transfer living radical polymerization (SET-LRP), nitroxide-mediated radical polymerization (NMP), and reversible addition–fragmentation chain-transfer (RAFT) polymerization, as well as other classes of CRP reactions.[1–8] These methods allow access to polymers with different architectures and functionalities, predictable and precise molecular weights, and desirable physical and/or chemical properties. A large scope of compounds such as α-bromo carbonyl compounds, perfluoroalkyl iodides, thiocarbonylthio compounds, trithiocarbonates, organometalloids, and nitroxides can be employed as initiators or crucial intermediates during photo-CRP, and in many cases polymers with high structural fidelity and narrow molar mass distributions can be obtained. A very broad scope of vinyl-containing monomers including (meth)acrylates, acrylamides, styrene (St), vinyl esters, N-vinyl amides, acrylonitrile (AN), etc., have been successfully polymerized by photo-CRP methods to yield polymers with a wide variety of properties. Block copolymers and other complex polymer compositions and architectures have also been prepared using these techniques. To meet diverse requirements for applications, metal-catalyzed/mediated, trace metal containing, and metal-free photo-CRP reaction systems have been developed. Furthermore, the well-documented advantages of continuous-flow photochemistry techniques have been adapted to photo-CRP to enable rapid scale-up of photo-CRP reactions. Additionally, the temporal and spatial control of photo-CRP has been used to demonstrate new methods of templation and compartmentalization. Using light as an orthogonal trigger for photo-CRP, multicomponent reaction systems can be rationally

designed to produce smart advanced materials. As a consequence, the seemingly simple innovation of photo-CRP will potentially spawn new applications in areas such as coatings, microelectronics, printing, adhesives, nanoparticle functionalization, drug delivery, and gel fabrication.

Since a number of excellent reviews on photoinitiated/induced polymerization have been presented from the perspectives of reaction mechanisms, polymer backbones, reagents/catalysts, or applications, etc.,[23−31,33] this review highlights the use of light as an external control to regulate controlled, living radical polymerizations (i.e., photo-CRP), as well as the applications of photo-CRP that have appeared so far.

1.2. Simplified Catalogue of Photo-CRP

Generally, in a photo-CRP process, the excited state species R* undergoes either a chemical bond cleavage event or an electron or energy transfer step to initiate downstream reactions that ultimately provide polymers. During these processes, R (the absorbing species) can play the role of an initiator or a catalyst. Despite the flurry of recent interest in this field, all reported photo-CRP reactions can be divided into two categories based on the primary photochemical process involved: (1) intramolecular photochemical process (e.g., bond cleavage or energy transfer) or (2) photoredox process (Scheme 2). In the former group,

Scheme 2. Representative Polymerization Mechanisms Involving (A) an Intramolecular Photochemical Process and (B) a Photoredox Process[a]
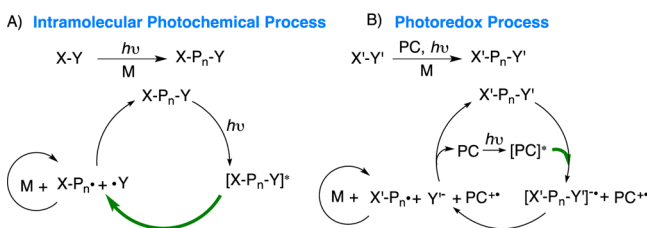
[a]The arrow representing the primary photochemical process is colored in green. In A, the primary photochemical process is a homolytic bond cleavage event or, in a few cases, intramolecular energy transfer followed by bond cleavage (these polymerizations are described in section 3 of this review). In B, the primary photochemical process is single electron transfer (SET) between a photoredox catalyst (PC) and a suitable donor or acceptor (these processes are described in section 4 of this review). To our knowledge, all existing photo-CRP methods fall into one of these two categories.

fragmentation reactions of excited state species are common primary photochemical reactions; in the latter, photoinduced single electron transfer (SET) is always the primary photochemical process. In sections 3 and 4 of this review we highlight the variety of photo-CRP reactions that are accessed via these general reaction manifolds. We consider the subtleties of each polymerization mechanism; specific differences are also discussed. Our goal is to unify the seemingly large number of photo-CRP reactions that are known and to place these strategies in the context of established organic photochemistry and thermal CRP methods. In some cases, we recommend specific terminology for methods based on their mechanistic similarities to other systems. Most importantly, we hope to outline the basic paradigms in this field and provide motivation for new developments.

A typical photo-CRP based on an intramolecular photochemical process is depicted in Scheme 2A. Here, the absorbing species X−Y acts as an initiator as well as a reversible terminator.

Homolytic cleavage of the excited initiator ([X−Y]*) or polymeric initiator ([X−P_n−Y]*) generates a radical (X$^\bullet$ or X−$P_n$$^\bullet$) that can undergo either propagation or recombination with Y$^\bullet$. Thus, the primary photochemical process is homolytic bond cleavage of the light-absorbing species, the latter of which is directly incorporated into the polymer chain. Good control of these polymerizations can be effectively realized in the absence of catalysts or other additives given that other criteria are satisfied (vide infra).

In the photoredox CRP case (Scheme 2B), the absorbing species PC is a "photoredox catalyst". A PC is a species that undergoes photoinduced SET to or from an appropriate initiator to generate radical species that then propagate. For example, in Scheme 2B the PC transfers an electron to an initiator (X′−Y′) or a polymeric initiator (X′−P_n−Y′) (also referred to as an "oxidative quenching" process since the PC is oxidized and no longer in an electronically excited state after SET to the initiator) to produce [X′−P_n−Y′]$^{-\bullet}$ and oxidized catalyst PC$^{+\bullet}$. Note: nearly all examples of photoredox-based photo-CRP methods reported so far are based on an oxidative quenching mechanism, though one example with a reductive quenching mechanism, i.e., SET from initiator to PC*, is discussed below in section 4.1.1. The active radical anion intermediate then undergoes thermal fragmentation to produce a radical X′$^\bullet$ or Y′−$P_n$$^\bullet$. The radical species can then either propagate to yield polymer or regenerate a macroinitiator and ground state PC via combination with Y′$^-$ and SET to PC$^{+\bullet}$. Note that these types of photo-CRP reactions could either occur via a "closed" cycle mechanism where growing polymers are only deactivated/reactivated by the PC or proceed via radical chain processes where [X′−P_n−Y′]$^{-\bullet}$ transfers an electron not back to PC$^{+\bullet}$ but instead to another ground state X′−Y′ or X′−P_n−Y′. These two mechanistic possibilities have well-known analogues in traditional SET-based substitution reactions: they resemble the canonical SET versus $S_{RN}1$ substitution mechanisms. Given this precedent, it is not surprising that radical chain processes (similar to $S_{RN}1$) also appear in photoredox catalysis reactions involving small molecules.[34] In the case of photoredox-CRP, the radical chain process would resemble degenerative chain transfer, which if operative could provide additional control over the chain growth. We note, however, that to date these details have not been elucidated experimentally.

A key advantage of photoredox processes is that the PC is responsible for light absorption; the initiator and polymer chains do not necessarily need to have any absorbing group, and the PC is not incorporated into the polymer chain. Effective PCs typically have excited states that are relatively long lived (e.g., for Ir(ppy)$_3$, τ = 1900 ns, where ppy stands for 2-phenylpyridine ligand;[35] for Ru(bpy)$_3$$^{2+}$, τ = 1100 ns, where bpy stands for 2,2′-bipyridine ligand[36]), thus ensuring efficient SET. It should also be noted that the details of photoredox reactions are generally governed by thermal reactions of radical anions/cations. Light is simply a very convenient (and catalytic) method for inducing SET, though many of these reactions could presumably be conducted with other sources of electrons (e.g., electrochemically).

As in all CRP processes, the key to excellent control in both of the above classes of photo-CRP reactions is to ensure that the growth of polymer chains is reversibly and efficiently terminated by reactions between initiator fragments (the reaction between X−$P_n$$^\bullet$ and Y$^\bullet$ in intramolecular photochemical processes and the proposed reaction between X′−$P_n$$^\bullet$, Y′$^-$, and PC$^{+\bullet}$ in photoredox reactions). Thus, unlike traditional photoinitiated polymer-
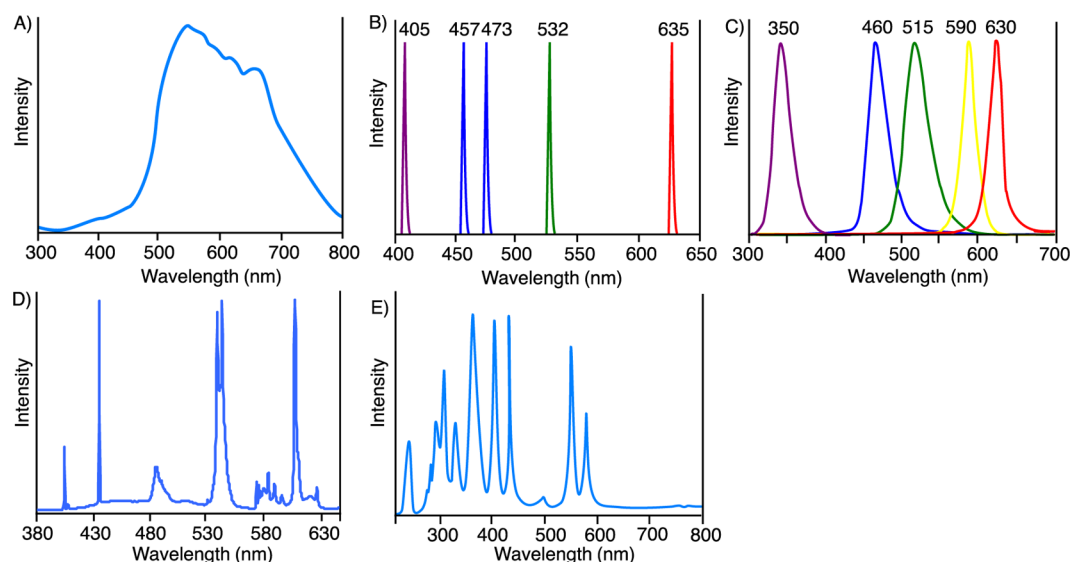
Figure 2. Typical emission spectra of (A) halogen lamps, (B) laser diodes at 405 (purple), 457 (blue), 473 (blue), 532 (green), and 635 nm (red), (C) UV lamp centered at 350 nm (left) and LEDs centered at 460 (blue), 515 (green), 590 (yellow), and 630 nm (red), (D) household CFLs, and (E) high-pressure mercury plasma arc-discharge lamp. Reproduced with permission from ref 30. Copyright 2015 Elsevier.

izations, where light induces growth of polymer chains that terminate irreversibly upon removal of the light source, the reversible recombination feature of photo-CRP means that simply re-exposing the system to light can continue the growth of the same polymer chains. Notably, neither of the processes described in Scheme 2 requires addition of exogenous radical sources (such as azobis(isobutyronitrile) (AIBN), which is often used in RAFT polymerization). Thus, they minimize the formation of dead chains and improve the structural fidelity of the polymer products.

2. LIGHT SOURCES FOR PHOTO-CRP

Enabled by modern technologies such as light-emitting diodes (LEDs), various light sources for photo-CRP are now readily available. For traditional photoinitiated polymerizations, light sources having emission in the range of ~150−700 nm were normally used; many methods required 254 nm or shorter wavelength high-energy ultraviolet (UV) light. Enabled by the characteristic functional groups of photo-CRP initiators or PCs, which are typically excited by light in the range between 350 and 700 nm, the usage of high-energy UV light can be avoided in photo-CRP conditions. For these reactions, halogen lamps, household compact fluorescent lamps (CFLs), laser diodes, LEDs, and black light UV lamps are all cheap and practical light sources. Representative emission spectra of some exemplar irradiation devices are presented in Figure 2. Also, sunlight has been directly employed in a few examples of photo-CRP. Among these light sources, halogen lamps, household CFLs, and sunlight provide polychromatic emission; laser diodes provide mono-chromatic light; LEDs and black light UV lamps are used as quasi-monochromatic light sources. These sources can typically provide light intensity from 2 to 100 mW/cm^2, which of course depends on the light source as well as the distance between the emission source and the reaction vessel. Though light sources are readily available, one potential drawback of photo-CRP is that it can be difficult to scale; a larger reaction requires a corresponding larger or more intense light source to maintain identical conditions, which is particularly important in polymerization where time and light intensity can critically impact molecular

weight and molar mass distribution Đ (Đ refers to "molar mass dispersity", which is a measure of the distribution of molecular masses in a given polymer sample calculated by dividing the weight-average molar mass M_w by the number-average molar mass M_n). To address this challenge, researchers have utilized continuous-flow technology for photo-CRP (see section 5.4).

3. PHOTO-CRP VIA DIRECT PHOTOCHEMICAL PROCESSES

3.1. Thio-Compound-Mediated Processes

Perhaps the best-known CRP method that uses sulfur-based compounds (i.e., "thio compounds") is RAFT polymerization (Scheme 3). Indeed, RAFT polymerization is one of the main

Scheme 3. Mechanism for Reversible Addition−Fragmentation Chain-Transfer (RAFT) Polymerization
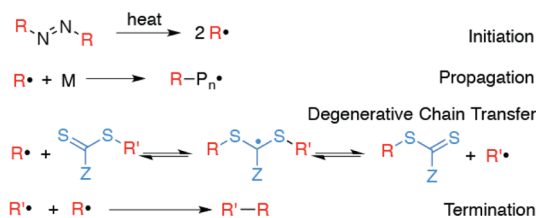
pillars of CRP.[2,37−42] In RAFT polymerization, dithioesters, dithiocarbamates, trithiocarbonates, and xanthates are widely used chain-transfer agents (CTAs or RAFT agents).[2,37−42] In these systems, the RAFT agent reacts rapidly with a free radical generated from a suitable radical initiator (e.g., AIBN or a photoinitiator in the case of "photo-RAFT"). The weakest C−S bond of the resulting stabilized radical species then breaks to generate a new propagating radical. This radical can also undergo degenerative chain transfer with another RAFT agent to induce growth of a new polymer chain (Scheme 3). Notably, each R$^•$ that derives from an initiator molecule must terminate irreversibly at the end of the RAFT polymerization, which leads to a small fraction of dead chains. However, retention of the RAFT agent within the vast majority of the polymers enables

growth of new blocks from these macro-RAFT agents, thus satisfying the criteria of a living polymerization.

Interestingly, metal-free photo-CRPs based on thio compounds are among the earliest known CRP methods;[11,12] these methods were reported before the introduction of RAFT polymerization. In these photo-CRP reactions, thio compounds are used as initiator-transfer-agent-terminators (iniferters) in a process that is mechanistically distinct from RAFT polymerization.[43,44] Thiocarbonylthio, trithiocarbonates, and disulfides with suitable UV absorption ranges are typical photoiniferters. As shown in Scheme 4, these iniferters undergo bond cleavage under

Scheme 4. Mechanism for Photo-CRP Using Iniferters
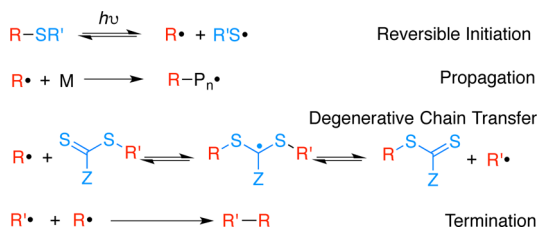
irradiation to generate R$^\bullet$ and R′S$^\bullet$ radicals that initiate polymerization; ideally this event is reversible. Then these propagating radicals can undergo degenerative chain transfer with iniferters *that were not previously cleaved by photolysis*, which is similar to the RAFT-equilibrium process. Finally, the sulfur radical of the cleaved iniferter can combine with the radical end of a growing polymer chain to regenerate a dormant macroiniferter that can later be reactivated by absorption. Though bimolecular termination reactions are possible, these can be mitigated by control of light intensity (i.e., amount of radicals generated). On the basis of this mechanism, it becomes clear that in iniferter systems no exogenous radical initiators are needed; photo-cleavage of the iniferter provides the radical source for initiation, and this radical generation is ideally reversible. Thus, despite the fact that many researchers refer to both reactions as photo-RAFT polymerizations, there is a clear distinction between RAFT polymerizations initiated by an exogenous photoinitiator (herein referred to as photo-RAFT) and photoiniferter polymerizations. In the photo-RAFT case, just as with standard thermally initiated

RAFT, the initiator-derived radicals must ultimately terminate irreversibly, and thus, with each on/off cycle some fraction of chains cannot continue growth. In theory, photoiniferter polymerization can be cycled indefinitely, though this may not be possible in practice due to undesired side reactions that lead to termination.

3.1.1. Thiocarbonylthio Used as a Photoiniferter. In 1982, Otsu and co-workers seminally reported photo-CRP when they introduced the iniferter concept.[11,12,44] In these experiments, tetraethylthiuram disulfide (TTDS), dibenzoyl disulfide (DBDS), and *S*-benzyl *N,N*-diethyldithiocarbamate (BDT) iniferters (see Scheme 5 for structures of representative iniferters) were synthesized and applied to the polymerization of methyl methacrylate (MMA) and St under UV irradiation. A linear relationship between M_n and monomer conversion was observed, thus suggesting a well-controlled polymerization process.

Later, Tardi, Lambrinos, and co-workers explored this photopolymerization using *p*-xylylene bis(*N,N*-diethyldithiocarbamate) (XDT) as an iniferter to produce polymers (ca. Đ = 1.7−2.3) with *n*-butyl acrylate (*n*BA) as a monomer.[45] However, they found this system showed significant loss of active end groups from the growing chain as dithiocarbamate groups were partially degraded during polymerization. Thus, full control over the molar masses of the polymers was problematic. It was also claimed that this polymerization had a partially living character in the early stage, but that control disappeared progressively at later times due to unspecified termination reactions.

Bowman and co-workers presented a kinetic study of the bulk photopolymerization of methacrylates with XDT.[46] Under the conditions studied, the photoiniferter polymerization mechanism involved two termination pathways: (1) carbon−carbon radical termination and (2) carbon−dithiocarbamyl radical termination. When the conversion of monomer was low, pathway 1 was the predominant termination mechanism, due to the low viscosity of the polymerizing system. As the viscosity increased at higher conversion pathway 2 began to dominate.

Employing a dithiocarbamates, e.g., 2-(*N,N*-diethyldithiocarbamyl)isobutyric acid (DTCA) and (4-cyano-4-diethyldithiocarbamyl)pentanoic acid (CDPA) as iniferters, the Ishizu group investigated photo-CRP of 2-hydroxyethyl

Scheme 5. Chemical Structures of Selected Iniferters Used in Photo-CRPs
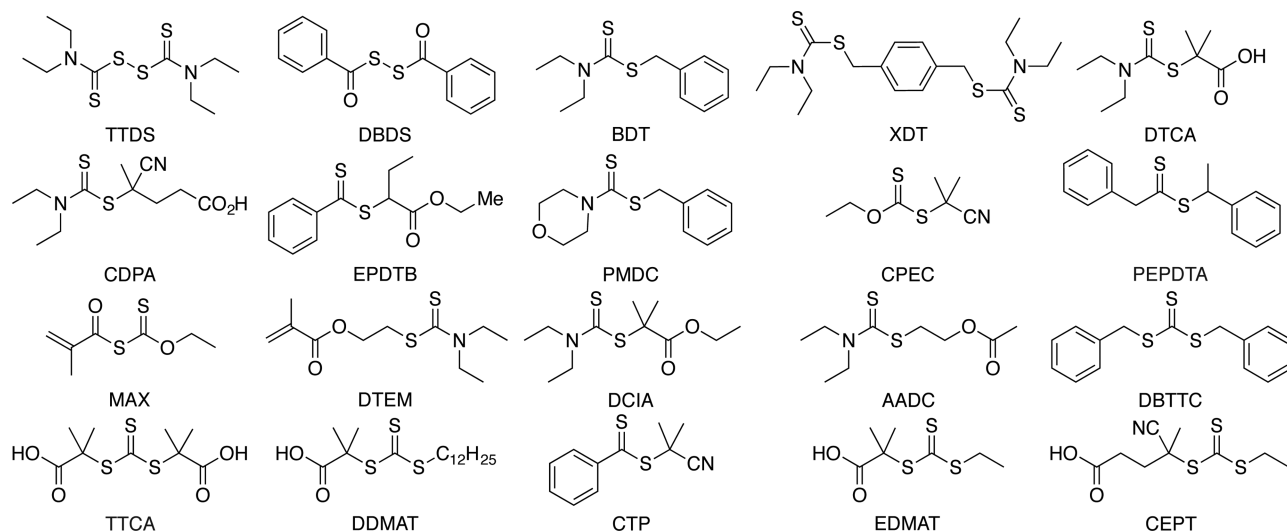
methacrylate (HEMA), methyl acrylate (MA), methacrylic acid (MAA), and St under UV light (ca. $Đ$ = 1.2–2.1).[47−50] Amphiphilic block polymers were also prepared by using thiocarbonylthio-containing poly(HEMA) as a macroiniferter. While the use of CDPA as an iniferter could provide living polymerization of a variety of monomers at low conversions, non-pseudo-first-order kinetics were observed in the polymerization of St in the presence of DTCA. By making the sodium salt of DTCA, this group also realized the photo-CRP of *N*-isopropylacrylamide (NiPAAm) in aqueous medium (ca. $Đ$ = 1.6–2.1).[48]

The Pan group developed a new dithiobenzoate iniferter, i.e., 1-(ethoxycarbonyl)prop-1-yl dithiobenzoate (EPDTB), to facilitate the copolymerization of St and maleic anhydride (MAh) at 310 nm.[51] The results of microstructural analysis indicated that the copolymer had strictly alternating structure of two different monomers as is expected for radical copolymerization of St and MAh (ca. $Đ$ = 1.1–1.2).

Yagci and co-workers designed the dithiocarbamate phenacyl morpholine-4-dithiocarbamate (PMDC), which was used for the photo-CRP of St (up to 50% conversion) under 350 nm irradiation (ca. $Đ$ = 1.3).[52] The end-group fidelity of these macroiniferters was demonstrated by growing copolymers. The authors also pointed out that this reaction proceeded via both reversible deactivation and RAFT-equilibrium mechanisms as described in Scheme 4.

Kwark and co-workers designed *S*-2-cyano-2-propyl-*O*-ethyl xanthate (CPEC) as an iniferter, which was used for photo-CRP of vinyl acetate (VAc) at 60 °C under UV irradiation.[53] While the chain ends were not perfectly stable toward UV irradiation, adding more CPEC could increase the degree of control over the photopolymerization.

Davis, Rizzardo, and co-workers found that employing 1-phenylethyl phenyldithioacetate (PEPDTA) as an iniferter could generate well-defined poly(St) with molecular weights close to theoretical values under 365 nm irradiation when conversions were up to 30%.[54] The molar mass distribution became broad after extending the irradiation time. According to these results, they suggested that the appropriate selection of iniferters could reduce degradation during polymerization. GC/MS analysis of the residue from the UV-irradiated neat iniferter revealed the presence of 1-phenylethyl and benzyl radical decomposition products, thus suggesting the existence of side reactions during polymerization with this agent.

Ajayaghosh and Francis prepared a xanthate-derived photoiniferter, *S*-methacryloyl *O*-ethyl xanthate (MAX), bearing an electron-deficient polymerizable double bond, which is capable of distinguishing between MMA and St during reactions.[55−57] With this iniferter, polymerizations of an electron-poor acrylate and an electron-rich alkene were performed in controlled fashion at 350 nm. However, molar mass distributions increased significantly with extended reaction times, suggesting irreversible termination. As shown in Scheme 6, this photoiniferter, which played a dual role as both iniferter and monomer, facilitated the synthesis of hyperbranched polymer architectures.

Later, the Ishizu group designed another dual-role iniferter 2-(*N*,*N*-diethyldithiocarbamyl)ethyl methacrylate (DTEM) (Scheme 6). Kinetic studies using 2-(*N*,*N*-diethyldithiocarbamyl)isobutyric acid ethyl ester (DCIA) and acetic acid 2-(*N*,*N*-diethyldithiocarbamyl)ethyl ether (AADC) as model compounds indicated that the polymerization of this dual-mode iniferter and monomer proceeded with pseudo-first-order

Scheme 6. Employing Dual-Role Iniferter Monomers To Grow Branched Polymers via Photo-CRP
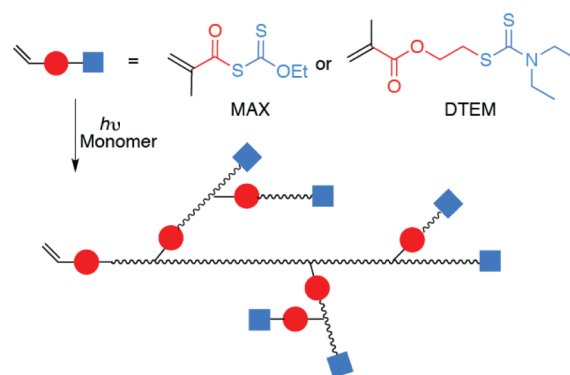
kinetics.[58] Thus, this polymerization provided hyperbranched polymer products in a controlled fashion.[59,60]

Pan, You, and co-workers developed the novel photoiniferter dibenzyl trithiocarbonate (DBTTC).[61] With this agent, monomers of St, MA, and *n*BA were successfully polymerized under the irradiation of an 8 W UV mercury lamp. This process displayed typical characteristics of CRP including precisely controlled molar mass, linear increase of M_n with monomer conversion, and narrow molar mass distribution (ca. $Đ$ = 1.1–1.2). Triblock copolymers poly(MA)-*block*-poly(St)-*block*-poly-(MA), with narrow molar mass distribution (ca. $Đ$ = 1.2) and well-defined structures, were prepared from macroiniferter.

Polyacrylamide with controlled molar mass distribution (ca. $Đ$ = 1.1–1.2) and somewhat controlled tacticity was prepared by Li and co-workers using photo-CRP in the presence of DBTTC and Y(OTf)$_3$.[62] The authors suggested that the moderate isotacticity of the polyacrylamide was due to coordination of Y(OTf)$_3$ with the last two amide groups in the growing radical chain. As determined by ^{13}C nuclear magnetic resonance (NMR) analysis, the isotactic sequence of dyads (m), triads (mm), and pentads (mmmm) was 0.32%, 50.95%, and 29.97%, respectively. Interestingly, the meso tacticity increased gradually during propagation, and the later polymerization stage afforded higher isotacticity.

Using *S*,*S*-bis(α,α′-dimethyl-α″-acetic acid) trithiocarbonate (TTCA) as a photoiniferter, Barner and co-workers developed a facile photo-CRP of acrylic acid (AA) in aqueous solution at ambient temperature under UV irradiation ($Đ$ = 1.04–1.11).[63] As demonstrated by their results, this reaction system could control the polymerization effectively at conversions as high as 50%. The same iniferter was also reported by Ran and co-workers for the photo-CRP of St and *n*BA.[64]

3.1.1.1. A More Complete Mechanism for Thiocarbonylthio Iniferter-Based Photo-CRP. On the basis of the above examples, it is clear that there is a strong dependence on irradiation time, conversion, and iniferter structure on the livingness of photo-iniferter polymerizations. Though the mechanism shown in Scheme 4 provides for living photo-CRP in principle, a refined mechanism for trithiocarbonate-mediated iniferter polymerization that explains certain experimental observations was proposed in 2013 by Bai, Du, and co-workers.[65] In this work, the authors investigated the mechanism of photopolymerization of MA under long-wavelength UV irradiation in the presence of *S*-dodecyl-*S*′-(α,α′-dimethyl-α″-acetic acid) trithiocarbonate (DDMAT) by in-situ ^{1}H NMR spectroscopy. They systematically studied the influence of light intensity, wavelength, and iniferter concentration on the photo-CRP reaction. Importantly,

their results demonstrated that good control of the polymerization was critically related to the concentration of the iniferter. For example, well-controlled polymerization was successfully achieved by using a high concentration of DDMAT ([DDMAT] = 7.25 mM) where a ratio of 1/400 of DDMAT/MA was used; much less control was achieved at lower DDMAT concentrations. The authors proposed an intriguing mechanism to explain these results (Scheme 7).[65] In this mechanism, the

Scheme 7. Proposed Mechanism for Photo-CRP with DDMAT Iniferter under UV Irradiation That Explains the Relationship between Living Character and DDMAT Concentration[65] [a]
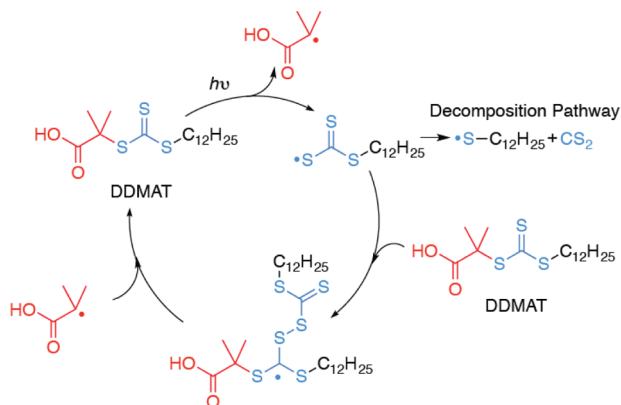

[a]Adapted from ref 65. Copyright 2013 American Chemical Society.

photolysis of DDMAT generates a carbon radical and a trithiocarbonate-based sulfur radical as expected for iniferter polymerization (see Scheme 4). One potential mode of irreversible termination in this system is loss of CS_2 from the newly formed trithiocarbonate-based radical. To explain why high DDMAT concentration gave increased control, the authors proposed a novel step wherein this trithiocarbonate-based radical combines with a molecule of DDMAT to afford a heteroatom-stabilized carbon radical that is reminiscent of the dormant radical in RAFT polymerization. Importantly, this reaction would be second order in DDMAT and thus would be expected to depend critically on DDMAT concentration. This new radical could fragment or produce two DDMAT molecules by reacting with a carbon radical generated in the first step. With this elegant proposal, the impact of DDMAT concentration can be readily explained as a competition between this favorable second-order trithiocarbonate-based radical + DDMAT coupling reaction and the first-order loss of CS_2 from the trithiocarbonate-based radical, namely, when the concentration of DDMAT was low, the trithiocarbonate-based radical could not be trapped and it decomposed irreversibly to a thiyl radical and a CS_2 molecule. We note that presumably light intensity would have a similar effect: high intensity reduces the DDMAT concentration by photolysis. This work provides important insights into the results of previous photoiniferter and photo-RAFT reactions that used UV or short-wavelength visible light: trithiocarbonate decomposition in both cases can be avoided by ensuring the presence of a high concentration of trithiocarbonate species in solution to trap photogenerated trithiocarbonate radicals.

On the basis of the realization that decreased light intensity could provide greater control in iniferter-based photo-CRP and to realize photocontrolled growth of end-linked polymer gels, the Johnson group used a bis-norbornene trithiocarbonate (Scheme

8) to investigate photo-CRP of NiPAAm under low-intensity, long-wavelength UV irradiation.[66] Under optimal conditions, M_n

Scheme 8. Photo-CRP of NiPAAm with Bis-Norbornene TTC as an Iniferter
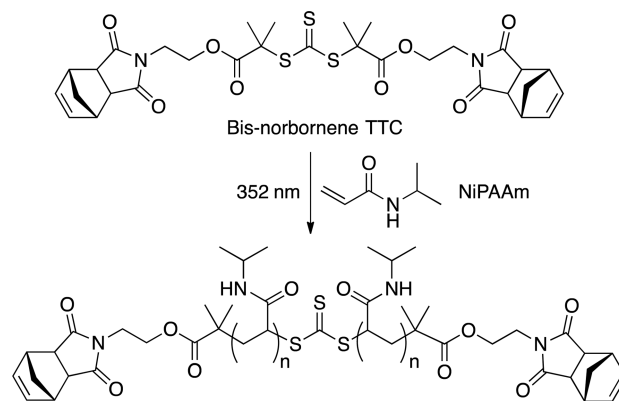
increased linearly with monomer conversion up to 86% in this system. The dispersity index of the polymers remained low throughout the entire process. Importantly, though the reaction time increased, decreased dispersity indices were obtained when the reaction vials were placed at longer distances from the light source, suggesting that reduced irradiation intensity does indeed provide increased control in this system. Characterization methods such as matrix-assisted laser desorption/ionization time-of-flight (MALDI-TOF) mass spectroscopy and ^1H NMR spectroscopy were employed to verify the structure of poly-(NiPAAm) obtained from bis-norbornene TTC. On/off experiments were performed by iteratively switching the UV irradiation. These results showed that the polymerization was efficiently reactivated across several irradiation cycles, and the M_n versus monomer conversions displayed a linear relationship during the on/off studies, representing a successful photo-controlled process.

3.1.2. Photo-RAFT Polymerizations with Demonstrated On/Off Behavior. The combination of RAFT agents with exogenous photoinitiators (i.e., photo-RAFT) is also widely used for photo-CRP; however, it is important to understand the distinctions between RAFT and iniferter polymerizations (see discussion above). The key distinction between photo-RAFT and general RAFT is the use of a photoinitiator (rather than a thermal initiator) to provide a radical source (Scheme 9). Nonetheless, photo-RAFT is still RAFT in the sense that irreversible radical generation initiates the polymerization, which is fundamentally different than the reversible activation possible in iniferter polymerization. In this section we highlight examples where on/off behavior was reported in photo-RAFT systems. We note that in photo-RAFT there is no mechanism for reinitiation

Scheme 9. Proposed Mechanism for Photo-RAFT with Exogenous Photoinitiators
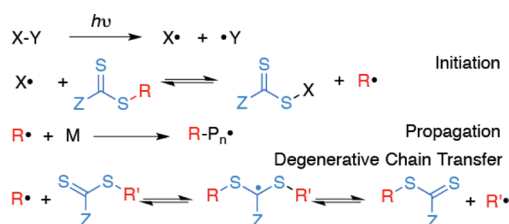
of irreversibly terminated polymer chains. Thus, one would expect that low molecular weight impurities might build up over many reaction cycles. Nonetheless, as long as a small number of radicals are generated with each irradiation cycle it is possible to observe apparent on/off behavior because the fraction of dead chains is presumably very small. To further complicate matters, simultaneous iniferter and photo-RAFT processes are likely occurring in these systems when both the thio compound and the photoinitiator absorb at similar wavelengths. Thus, a full appreciation of the mechanistic details of both methods (as outlined in Schemes 7 and 9) is required to fully explain the observed data. We also note here that demonstrations of on/off photocontrol in all photo-CRP systems should include plots of conversion, molar mass, *and* molar mass distribution as a function of the number of irradiation cycles, because monomer conversion may increase with each new irradiation, but this does not mean that all existing polymer chains continue to grow. For example, due to a fraction of irreversibly terminated chains in photoiniferter and photo-RAFT polymerizations, the dispersity index could increase with increasing number of cycles.

Cai and co-workers realized the photo-RAFT of primary amine-functionalized acrylamide monomers using cyanopentanoic acid dithiobenzoate (CTP) and (2,4,6-trimethylbenzoyl)-diphenylphosphine oxide (TPO) initiator under visible light, which provided a facile method for the synthesis of primary amine-functionalized polymers at room temperature.[67] This photopolymerization system afforded well-controlled molar mass distributions in acidic aqueous media. An acceleration effect on the reaction was observed by adding less polar alcohol solvents into the aqueous system. Furthermore, this reaction could be switched on and off over three cycles.

With the employment of an unsymmetrically substituted trithiocarbonate S-dodecyl-S′-(α,α'-dimethyl-α''-acetic acid) trithiocarbonate (DDMAT) and photoinitiator TPO, Cai and co-workers developed a photo-RAFT method to produce well-defined poly(St) and its functional derivatives including poly(vinylbenzyl chloride), poly(N,N-diethyl vinylbenzyl-amine), and poly(vinylbenzyl alcohol) using a high-pressure mercury lamp equipped with a filter to remove <320 nm light.[68] Their results indicated that photodegradation of trithiocarbonate functional groups (likely the result of direct photolysis as desired in the iniferter mechanism) and irreversible termination reactions of the resulting radicals were significantly suppressed with DDMAT under long-wave irradiation conditions. However, when vinylbenzyl alcohol (VBA) was employed as a monomer, a slight shoulder peak was observed by gel permeation chromatography (GPC) analysis at conversions over 50%. Nonetheless, kinetic investigations were used to confirm the controlled behavior of these processes. This photopolymerization system also offered direct access to all-styrenic block copolymers under mild conditions.

Combining S-ethyl-S′-(α,α'-dimethyl-α''-acetic acid) trithiocarbonate (EDMAT) and TPO, the Cai group developed a photo-RAFT reaction that could be conducted in acidic aqueous solution under visible-light irradiation.[69] Their results indicated that EDMAT was stable in acidic aqueous solutions but that it underwent decomposition in alkali solutions. The well-controlled process was demonstrated by employing periodic on/off experiments. Using the same trithiocarbonate compound, this group attempted to polymerize the ionic monomer N-(2-aminoethyl) acrylamide hydrochloride (AEAM) through visible-light irradiation in water, enabling the synthesis of polymers with structures tuned from homopolymers to random, block,

random−block, and block−random−block copolymers.[70] The polymerization process could again be suspended and restarted immediately for 3 times by cycling exposure to light. The authors also found that the reaction behavior with trithiocarbonates or dithioesters was significantly dependent on the UV−vis irradiation wavelength.[71,72] Under long-wave UV irradiation, trithiocarbonates (e.g., DDMAT) only underwent slight decomposition, whereas dithioesters were not stable toward these conditions. Improvement of these processes can be achieved by cutting off short-wavelength irradiation or by simply using lower intensity light and higher trithiocarbonate concentration.

A recyclable solid-state photochemical initiator based on the surface modification of $Nb(OH)_5$ was prepared and successfully applied to cyclable photo-RAFT reactions by Liu and co-workers.[73] Enabled by the visible-light absorbance of niobium compounds, the photopolymerization process could proceed with 420 nm irradiation in the presence of the trithiocarbonate CEPT. Notably, when the conversion of NiPAAm reached 86%, this method could still afford the polymer with a narrow molar mass distribution ($Đ = 1.17$). In addition, this polymerization process was controlled between on and off by cycling the irradiation for 6 times.

3.2. Nitroxide-Mediated Processes

Like RAFT polymerization and ATRP, NMP represents one of the pillars of CRP.[5,74,75] After Georges and co-workers reported the first NMP system that used benzoyl peroxide as the initiator and TEMPO as a mediator to achieve well-controlled polymerization of styrene,[76] discrete alkoxyamine compounds capable of reversible activation were developed[5,77] for NMP as shown in Scheme 10A. Under thermal conditions, alkoxyamines can

Scheme 10. Mechanism of Nitroxide-Mediated Radical Polymerization under (A) Thermal Conditions and (B) Light Irradiation Conditions
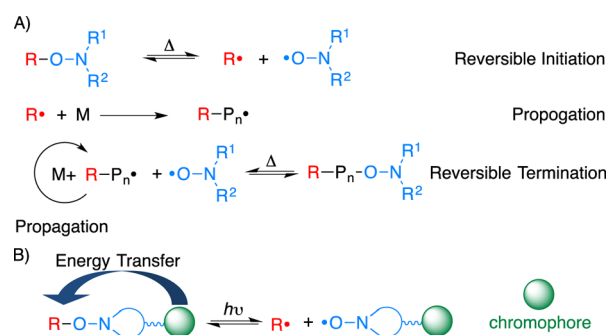
undergo homolysis of the C−O bond without a catalyst or an external additive to generate a carbon radical ($R^\bullet$) and a stable nitroxide radical ($^\bullet O-NR^1R^2$). The $R^\bullet$ species undergoes further propagation in the presence of monomers. During chain growth, the polymeric radical $R-P_n^\bullet$ is reversibly terminated by the persistent radical[78] $^\bullet O-NR^1R^2$ to produce the dormant species $R-P_n-ONR^1R^2$, thus providing a means for control of the radical polymerization process. Similar to $R-O-NR_1R_2$, the dormant species can also undergo reversible initiation under thermal conditions, which facilitates further propagation.

Motivated by the development of thermal NMP, Scaiano and co-workers reported in 1996 that carbon-centered radicals and stable radicals 2,2,6,6-tetramethyl-1-piperidinyloxy (TEMPO) were generated from irradiation of corresponding alkoxyamines

Scheme 11. Chromophore-Containing Alkoxyamine Compounds for Photo-NMP
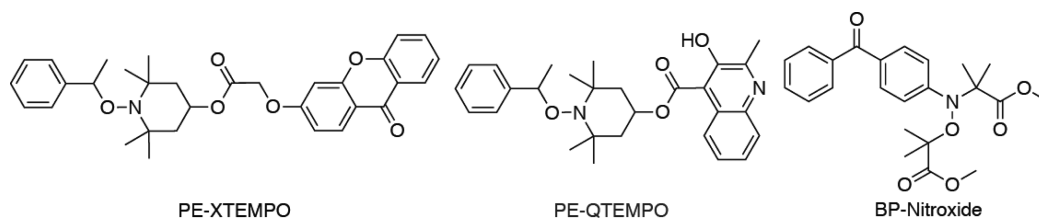
in the presence of xanthone derivatives as photosensitizers.[79] This process was proposed to occur via intermolecular energy transfer from the absorbing xanthone derivative to the alkoxyamine. Although no polymerization reaction was investigated in this study, the authors clearly recognized the potential for photo-CRP, and this work provided the theoretical basis for subsequent photo-NMP reactions (vide infra).

Building on this work, the nitroxide-mediated photopolymerization (photo-NMP) methods described below use alkoxyamines connected to a suitable sensitizer (shown in green in Scheme 10B). Irradiation of the chromophore followed by *intramolecular* energy transfer to the alkoxyamine leads to bond cleavage and formation of the requisite carbon and nitroxide radicals typical of NMP. It must be noted that living photo-NMP is not as developed as other strategies discussed in this review. Furthermore, *intermolecular* energy transfer to induce alkoxyamine decomposition (as studied in Scaiano's work that did not involve polymerization) has not, to our knowledge, been successfully realized in photo-NMP. If it were then potentially "energy transfer catalysts" (i.e., sensitizers) could be employed much like photoredox catalysts (see Scheme 2 and section 4 of this review).

The Neckers group synthesized a variety of chromophore–alkoxyamine conjugates and explored their utility in photo-NMP.[80] Although photopolymerization of MMA was realized by using PE-XTEMPO (Scheme 11) as a photoinitiator, the polymer obtained was not photoreactive, which suggested nonliving polymerization behavior. Significantly shortened triplet lifetimes were observed for the chromophore–alkoxyamine conjugates compared to the free chromophores, which suggested that the alkoxyamine quenched the excited chromophores as expected.

Goto and Scaiano reported a new quinolone–alkoxyamine derivative, PE-QTEMPO (Scheme 11), that they investigated for photo-NMP of Sty monomer.[81] Ten percent conversion was observed after irradiation for 2 h to yield poly(St) with a relatively broad molar mass distribution (M_n = 2700 g/mol, Đ = 1.60).

In an effort to increase the energy transfer efficiency in these types of systems, Guillaneuf, Gigmes, and Lalevée developed a new class of alkoxyamines where the sensitizing chromophores were directly connected to the aminoxyl component electronically.[82–84] In this way, the authors suggested that the photochemical and photophysical properties of the chromophores and the alkoxyamine could be influenced much more dramatically than in previous designs. On the basis of this idea, the authors reported a benzophenone-substituted nitroxide (BP-Nitroxide, Scheme 11) that facilitated photo-NMP of *n*BA.[84] In this system, the polymer molecular weight deviated significantly from the theoretical values and a broad molar mass distribution was observed (Đ > 2), suggesting limited control.

Inspired by this work, Liu and colleagues synthesized photosensitive TEMPO-based nitroxides with various chromo-phores including benzophenone, naphthalene, and quinoline.[85] As indicated by their results, efficient energy transfer to cleave the targeted C–O bond could occur. The authors reported the successful photo-NMP of MMA by combining their photosensitive nitroxide compounds as mediators with 2,2-dimethoxy-2-phenylacetophenone (DMPA) as a photoinitiator. This system displayed linear growth of the M_n with monomer conversion and narrow molar mass distributions (Đ = 1.3–1.4).

Yoshida reported the photo-CRP of various monomers accelerated by redox-active additives (e.g., iodonium salts, sulfonium salts, and iron–arene complex) with 4-methoxy-2,2,6,6-tetramethylpiperidine-1-oxyl (MTEMPO) at ambient temperature.[86–93] The living nature of these systems was confirmed with kinetics studies; however, compared to traditional NMP methods, the dispersity indices of polymers obtained via these methods were typically higher. Nonetheless, the authors showed that the polymerization could be immediately stopped and restarted by turning the light source off and on for one cycle.[87,94] The authors suggested a unique mechanism wherein the additive accelerates the polymerization rate by reversibly oxidizing the nitroxide to an oxoaminium salt.[95–97] Back electron transfer regenerates MTEMPO, which can then cap a propagating radical to reform a dormant chain. The authors propose that the photoexcited redox-active additive is responsible for MTEMPO oxidation. They suggest that the C–O bond of the MTEMPO polymer chain end is cleaved first, and free MTEMPO radical is then oxidized. There is an alternative possibility whereby the photoexcited additive could directly oxidize the dormant polymer chain, i.e., form a polymeric radical cation, which could then fragment to generate a propagating radical and an oxoaminium salt. To our knowledge, the latter mechanism has not been ruled out; if it were operative then this system should technically be classified as a photoredox polymerization where the redox-active additive is the photocatalyst and reductive quenching is the key photochemical process.

3.3. Manganese-Mediated Processes

Since the first preparation of dimanganese decacarbonyl ($Mn_2(CO)_{10}$ or $(CO)_5Mn-Mn(CO)_5$) in 1954,[98] this metal carbonyl complex has garnered broad attention[99] and been an important reagent in the organometallic chemistry of manganese. As shown in Scheme 12, unlike many other metal carbonyl compounds, there is no bridging CO ligand in $Mn_2(CO)_{10}$, and the two $Mn(CO)_5$ subunits are staggered with each other. Due to

Scheme 12. Homolysis of Dimanganese Decacarbonyl
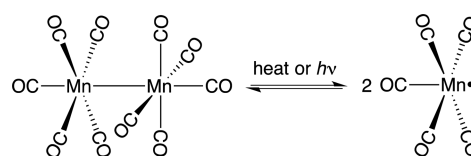
the weak Mn−Mn linkage (20−40 kcal/mol), this compound can undergo homolysis upon heating or irradiation with light, providing two $Mn(CO)_5^\bullet$ $17e^-$ metalloradicals.[100−102] The metalloradical generated can react with alkyl halide groups to produce a carbon-centered radical.[102,103] Further useful features of $Mn_2(CO)_{10}$ are its low cost and the high quantum yield of Mn−Mn bond cleavage.[104−106] Although $Mn_2(CO)_{10}/CCl_4$-initiated polymerizations were first reported about half a century ago,[99] this compound has only recently found wide application in radical polymerizations including photo-CRP.[107−110]

Kamigaito and colleagues developed highly active photo-CRP reactions using $Mn_2(CO)_{10}$ in combination with an alkyl iodide initiator (R−I in Scheme 13: 2-iodoisobutyrate) under visible-

Scheme 13. Proposed Mechanism of Photo-CRP with $Mn_2(CO)_{10}$ and R−I Initiator
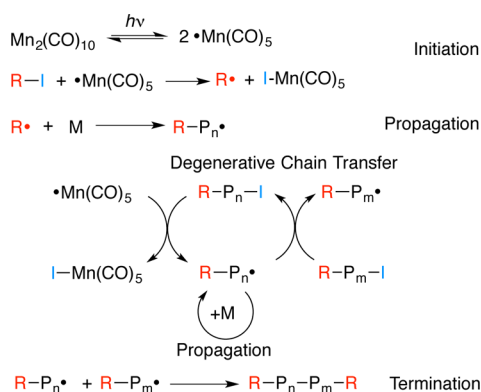
light irradiation.[108] A variety of monomers including VAc, MA, and St were polymerized efficiently with a catalytic amount of $Mn_2(CO)_{10}$ (0.025 mol % of VAc or 5.0 mol % of R−I); greater than 90% monomer conversion was achieved within 3 h for VAc monomer at 40 °C. Although the obtained molar mass distributions (ca. Đ = 1.3−1.9) were broader than other popular CRP methods, this polymerization displayed switchable behavior as demonstrated by 5 cycles of on/off experiments and the M_n increased linearly with conversion.

By introducing fluoroalcohol solvents into this system, the same authors developed a copolymerization reaction of MA and 1-hexene that enabled the synthesis of almost perfectly alternating copolymers when excess nonpolar olefins were used.[111] Kinetic analysis revealed that the relative reactivity of the MA radical to 1-hexene radical increased by about six times in the new solvent environment, which could be attributed to an H bond between the carbonyl group of MA and the alcohol group of the fluoroalcohol solvent. The enhanced reactivity of MA caused the cross-propagation to the electron-rich monomer of 1-hexene. Later, the same group reported copolymerization of MA and VAc with the $Mn_2(CO)_{10}/R$−I-promoted photo-CRP system.[112] In this work, a novel block copolymer consisting of a gradient copolymer block poly(MA-*grad*-VAc) and a homopolymer block poly(VAc) was prepared; the structure was supported by NMR analysis. Upon saponification of the ester side groups of the poly(MA-*grad*-VAc)-*block*-poly(VAc) polymer, a novel poly(MA-*co*-γ-lactone)-*block*-poly(vinyl alcohol) product was obtained that resulted from intramolecular lactonization.

A proposed mechanism for photo-CRP reactions with $Mn_2(CO)_{10}$ and initiator R−I is depicted in Scheme 13. Under visible-light irradiation, the Mn−Mn bond of $Mn_2(CO)_{10}$

compound cleaves to generate two $^\bullet Mn(CO)_5$ radicals, which are themselves unable to initiate polymerization. The metalloradical activates the C−I bond of the initiator R−I (e.g., 2-iodoisobutyrate) to produce a metal iodide compound (driven by the high bond dissociation energy of the Mn−halide) and a carbon-centered radical. The latter undergoes propagation in the presence of monomers. Kamigaito and co-workers showed that irreversible termination reactions of propagating radicals lead to an accumulation of I−Mn(CO)$_5$ and that this metal−iodide species does not contribute substantially to deactivation of the growing carbon radical species. Furthermore, the consumption of R−I follows first-order kinetics during the polymerization, and it is not affected by increasing the amount of I−Mn(CO)$_5$. These results suggest that reversible C−I bond activation takes places through a degenerative iodine transfer mechanism.[108] In this process the iodine atom at the end of an initiator or polymer chain transfers to $R-P_m^\bullet$ and thus initiates a new chain; this step is similar to the iodine transfer step known in other free radical polymerizations (see section 3.5 of this review for examples).[113] It is also similar to photo-RAFT using thio compounds (vide supra): photolysis of the Mn−Mn bond and halogen abstraction initiates the polymerization (much like a photoinitiator in photo-RAFT), and degenerative chain transfer of iodide provides control (much like sulfur-based RAFT agents).

Combining ATRP with $Mn_2(CO)_{10}$-promoted photo-CRP, the Yagci group developed a two-step procedure to produce block copolymers.[114] As shown in Scheme 14, in the first step, ω-

Scheme 14. Synthesis of Block Copolymers by Sequential ATRP and $Mn_2(CO)_{10}$-Initiated Photo-CRP
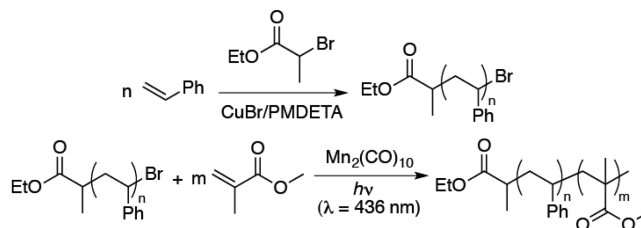
bromo-poly(St) was first synthesized via copper-catalyzed ATRP using N,N,N',N'',N''-pentamethyldiethylenetriamine (PMDE-TA) as a ligand in toluene at 110 °C. In a following step, the Br end group was chain extended with a variety of monomers such as MMA, nBA, and VAc in the presence of a catalytic amount of $Mn_2(CO)_{10}$ under visible-light irradiation. However, the fidelity of the end group was not demonstrated after polymerization with $Mn_2(CO)_{10}$. These authors also found that termination by biradical combination generated an ABA block structure. Later, the same group reported the combination of ATRP and cationic polymerization initiated by photolysis of $Mn_2(CO)_{10}$ followed by carbon radical oxidation with iodonium salts to produce block copolymers of poly(St)-*block*-poly-(cyclohexene oxide).[115] They also prepared hyperbranched polymers and linear polyethylene backbones both functionalized with bromide substituents, which allowed for postpolymerization transformations via $Mn_2(CO)_{10}$-mediated polymerization under visible light to provide polymeric materials with different properties.[116,117]

Fluorinated polymers are fundamental and important materials in a wide range of applications. While many CRP reactions of fluorinated alkene monomers such as vinylidene fluoride (VDF) have been conducted at elevated temperature

(100−250 °C) and in high-pressure reactors, new polymerization processes for fluoropolymer synthesis at ambient temperatures and in simple reaction vessels are desirable.[118−120]

On the basis of the photochemistry of $Mn_2(CO)_{10}$ and related radical reactions with alkyl halides, Asandei and co-workers reported a $Mn_2(CO)_{10}$/R−X (R−X were alkyl, semifluorinated alkyl, or perfluorinated chlorides, bromides, or iodides) system for photo-CRP of VDF (ca. $Đ$ = 1.2−1.8) under visible-light irradiation at 40 °C in low-pressure glass tubes in a variety of solvents.[121,122] To understand the mechanism of this reaction, kinetic studies, NMR experiments, control experiments, etc., were conducted. As shown in Scheme 15, similar to other

Scheme 15. $Mn_2(CO)_{10}$/R−X-Promoted Photo-CRP of VDF[121] [a]

Initiation

$Mn_2(CO)_{10} \xrightleftharpoons{h\nu} 2 \cdot Mn(CO)_5$

R−X + $\cdot Mn(CO)_5 \longrightarrow$ R• + X-$Mn(CO)_5$

Propagation

R-P_n-CH_2CF_2• $\xleftarrow{CH_2CF_2}$ R• $\xrightarrow{CH_2CF_2}$ R-P_n-CF_2CH_2•

Chain Transfer to Initiator

R-P_n-CH_2CF_2•

R-P_n-CH_2CF_2-X+ R• $\longleftarrow$ R−X $\longrightarrow$ R-P_n-CF_2CH_2-X+ R•

R-P_n-CF_2CH_2•

Iodine Degenerative Transfer

R-P_n-CH_2CF_2• + R-P_m-CH_2CF_2-I $\rightleftharpoons$ R-P_n-CH_2CF_2-I + R-P_m-CH_2CF_2•

R-P_n-CH_2CF_2• + R-P_m-CF_2CH_2-I $\rightleftharpoons$ R-P_n-CH_2CF_2-I + R-P_m-CF_2CH_2•

R-P_n-CF_2CH_2• + R-P_m-CF_2CH_2-I $\overset{X}{\rightleftharpoons}$ R-P_n-CF_2CH_2-I + R-P_m-CF_2CH_2•

Termination

R-P_n-CH_2CF_2• + R-P_m-CH_2CF_2• $\longrightarrow$ R-P_n-CH_2CF_2-CF_2CH_2-P_m-R

[a]Adapted from ref 121. Copyright 2013 American Chemical Society.

photoinitiated reactions with $Mn_2(CO)_{10}$ and organic halides (R−X), this reaction first generates carbon-centered radicals (R•). Notably, in this system there are two possible propagation pathways through two different propagating radicals, RCH_2CF_2• and RCF_2CH_2•. Subsequently, when the initiators have relatively strong R−X bonds (e.g., alkyl−I, R_F(perfluorinated alkyl)−Cl), the propagating radical chains do not undergo noticeable chain transfer with them, resulting in poly(VDF) without terminal halides (i.e., the polymerization is not living). In contrast, when the R−X bond is relatively weak (e.g., CF_3SO_2−Cl, CCl_3−Br, R_F−I), chain transfer occurs between growing radical chains and initiators, providing polymers with halogen atoms on the chain ends. In the later case, after initiators (e.g., R_F−I) are completely consumed, a reversible iodine degenerative transfer proceeds in the polymerization system,[113] producing polymers with two terminal modes (−CH_2CF_2−I and −CF_2CH_2−I), which are both able to be reactivated by •$Mn(CO)_5$ during further photopolymerization. The authors suggested that the reversible halide exchange between equally reactive propagating (R−P_n−CH_2CF_2•) and dormant (R−P_m−CH_2CF_2−I) chains enabled good control of this polymerization. Starting from poly(VDF) synthesized with this method, well-defined block copolymers with a variety of monomers such as styrene, butadiene, vinyl chloride, VAc, etc., have been prepared via a second chain extension with the same photopolymerization method (for block copolymers, ca. $Đ$ = 1.5−2.5). Very recently, these authors investigated the metal and ligand effects of various photoactive transition-metal carbonyls in conjunction with alkyl and perfluoroalkyl halides in the polymerization of VDF under visible light.[123] It was demonstrated that an iodine degenerative transfer CRP process is achieved for several metal carbonyls (the

overall qualitative order in the activity of these complexes is $Mn_2(CO)_{10} \approx Re_2(CO)_{10} \gg Cp_2Mo_2(CO)_6 \gg Cp_2W_2(CO)_6$) with different alkyl halides and perfluoroalkyl iodides. When the radical reactivation of the poly(VDF)−I chain ends was evaluated, metal complexes of $Mn_2(CO)_{10}$, $Re_2(CO)_{10}$, $Cp_2Mo_2(CO)_6$, $Cp_2W_2(CO)_6$, and $Cp_2Fe_2(CO)_4$ all provided quantitative radical activation of both types of chain ends (poly(VDF)−CH_2CF_2−I and poly(VDF)−CF_2CH_2−I).

Further demonstrating the similarity between these processes and photo-RAFT, in 2014 Zhu and colleagues applied $Mn_2(CO)_{10}$ as a photoinitiator with a RAFT agent for photo-CRP with LED (λ_{max} = 565 nm) or sunlight as light source.[124] With this method, a variety of monomers including MMA, MA, St, 2-(dimethylamino)ethyl methacrylate (DMAEMA), and N-vinylcarbazole (NVC) were polymerized in the presence of 2-cyanoprop-2-yl-1-dithionaphthalate (CPDN) RAFT agent and a catalytic amount of $Mn_2(CO)_{10}$ at 40 °C ($Đ$ = 1.10−1.37). This reaction was reported to be switchable toward LED light irradiation as shown by two cycles of on/off experiments. In addition, the fidelity of the polymer chain end was demonstrated by ^{1}H NMR analysis and chain extension experiments.

3.4. Cobalt-Mediated Processes

Since the Co^{III}−C bond is generally weak (18−40 kcal/mol), homolytic bond cleavage can be achieved under thermal or photochemical conditions[125,126] to produce a cobalt radical (also viewed as a Co^{II} species) and a carbon-centered radical, the latter of which can propagate in the presence of suitable monomers.[127−130] Importantly, the persistent cobalt radical can recombine with the growing radical chain to generate a dormant species, resulting in a reversible metal−carbon bond formation/activation process that is reminiscent of NMP. On the basis of this paradigm, polymer chemists have developed many cobalt-mediated CRP reactions.[127−131] As shown in Scheme 16, these

Scheme 16. Two Common Approaches to Co-Mediated Photo-CRP: (A) In-Situ Production of the Key Organo−Co(III) Intermediate via Use of an Exogenous Initiator and (B) Use of a Preformed Organo−Co(III) Complex[a]
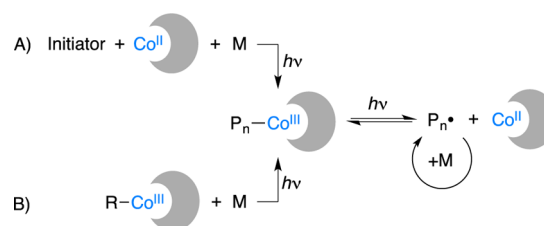
[a]In both cases the polymerization is controlled by reversible photolysis of the C−Co bond (shown on the right).

polymerizations can be generally classified into two groups: (A) In-situ formation of P_n−Co^{III} by heating or photolysis of a radical initiator (e.g., AIBN or TPO) in the presence of a Co^{II} source and a suitable monomer[129,132] or (B) polymerization from a preformed R−Co^{III} initiator. In both cases, photocontrol of the polymerization can be achieved through reversible photolysis of the C−Co bond.[129,133,134] Although photopolymerizations mediated by cobalt have been developed for more than 20 years,[129,132] there have been exciting recent advances in terms of control over molecular weight, dispersity, fidelity of the chain end, and reaction kinetics.

Using strategy A (Scheme 16), Debuigne and co-workers synthesized well-defined α-functional and α,ω-telechelic poly-

mers from Co(acac)$_2$ and a hydroxyl-functional initiator (VA-086).[135] To our knowledge, this approach represents the first example of preparing homotelechelic polymers via cobalt-mediated photo-CRP (ca. Đ = 1.1). Telechelic poly(N-vinylpyrrolidone) (NVP) was synthesized with the same photopolymerization method (Đ = 1.08), and this strategy was combined with ring-opening polymerization to access triblock copolymers containing poly(NVP) and poly(ε-caprolactone) segments. The ability to synthesize triblock copolymers suggests high end-group fidelity in the initial Co-mediated photo-CRP.

Also using strategy A (Scheme 16), Detrembleur and Lalevée realized the cobalt-mediated photopolymerization of nBA at 30 °C initiated by photolysis of AIBN.[136] In their system, when the molar mass of poly(nBA) reached above 4 000 000 g/mol, the corresponding dispersity index remained low (Đ = 1.38). Changing the photoinitiator from AIBN to phenyl bis(2,4,6-trimethylbenzoyl)phosphine oxide (Irgacure 819) resulted in a significant enhancement in the initiation efficiency (increased from <1% to 22%) during the polymerization of nBA.[136] In addition, as indicated by kinetic studies and spin-trapping experiments, they proved that the terminal C−Co bond generated in the dormant polymer chains could be cleaved by light.

The Zhu group reported that a variety of monomers including VAc, N-vinylcaprolactam (NVCL), and NVP were able to be polymerized in a controlled manner (ca. Đ = 1.1−1.3) using a Co(acac)$_2$/TPO reaction system under 365 nm irradiation.[137] Chain extension from poly(VAc) was successfully performed (original poly(VAc): $M_{n,GPC}$ = 4720 g/mol, Đ = 1.22. Chain extended poly(VAc): $M_{n,GPC}$ = 39 200 g/mol, Đ = 1.14). However, when this method was applied to St, MMA, and nBA, broader molar mass distributions were observed (Đ = ~2.1−3.2).

Cobalt porphyrins (Scheme 17A) have been investigated for many years in thermally initiated radical polymerizations. More

Scheme 17. Structures of Cobalt Porphyrins and Their Adducts
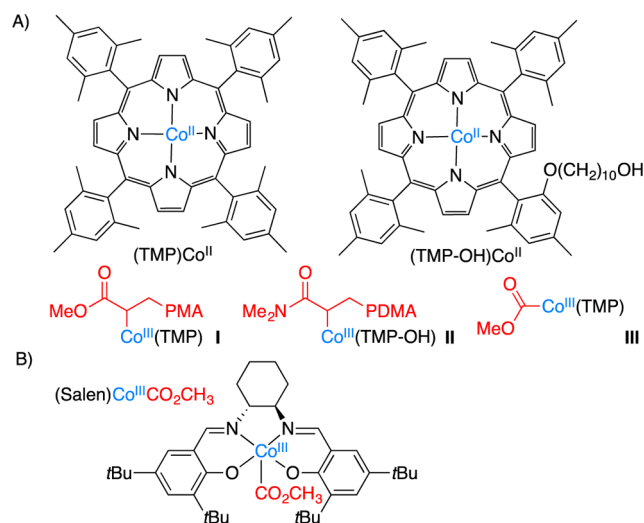
recently, organo-Co^{III} derivatives of these compounds (Scheme 17A) have been shown to be ideal candidates to achieve photo-CRP without extra additives (i.e., strategy B in Scheme 16). For example, Fu and colleagues synthesized polymer- or CO$_2$CH$_3$-bonded organocobalt(III) porphyrins as shown in Scheme 18A.[138,139] While (TMP)Co^{II} was applied for polymerization in nonpolar solvents (i.e., benzene), its derivative (TMP−OH)Co^{II}

Scheme 18. Proposed Mechanisms for the Photo-CRP of Polymer-I with Amine
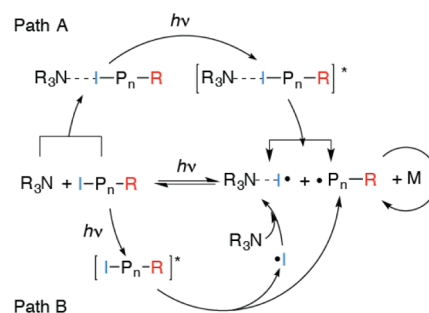
could be used in polar solvents (i.e., methanol). Since porphyrin cobalt alkyl complexes (i.e., I and II) are light and air sensitive, an air-stable organocobalt porphyrin complex III was successfully prepared (upon storage at room temperature in the dark, only 4% decomposition of III was observed in 3 months).[138] With these complexes, well-defined diblock and triblock copolymers were prepared, indicating the high fidelity of the cobalt-functionalized chain end and the strong tendency for regeneration of the terminal C−Co bond in the polymerization. Highly responsive on/off control was observed in these systems. In addition, these cobalt complexes enabled the photo-CRP of electron-deficient alkenes, such as MA, nBA, and 2-hydroxyethyl acrylate (HEA) (ca. Đ = 1.2−1.3), the polymerications of which were less controlled in the initiator-incorporated cobalt-mediated photo-polymerizations.[138,139] Later, the same group prepared a salen-based organocobalt compound ((salen)CoCO$_2$CH$_3$ in Scheme 17B) and applied it to the photo-CRP of acrylates, acrylamides, and vinyl esters with CFL or Xe lamps (ca. Đ = 1.1−1.2).[140] The equilibrium between the carbon-centered radical (R$^\bullet$) and (salen)Co^{II} and the (salen)Co^{III}R species was determined to lie toward the dormant Co^{III} species (K_{eq} = 3.5 × 10^{10} M^{-1}), which explains the excellent control observed in this photo-CRP. The authors also found that introducing TPO as an additional photoinitiator in this system greatly enhanced the polymerization rate without a large influence on the dispersity. On the basis of kinetics studies, the authors suggested that the TPO-induced reaction is controlled by degenerative chain transfer of the organocobalt chain ends.[140]

3.5. Iodine Transfer Under Metal-Free Conditions

Alkyl iodides can often be photocleaved to provide a carbon-centered radical (R$^\bullet$) and an iodine radical (I$^\bullet$).[113] The iodine radical can rapidly combine with another iodine radical to form I$_2$, which is known to be a radical scavenger that can inhibit free radical polymerizations.[141,142] Hence, the generation of I$^\bullet$ is thought to be unfavorable in a photo-CRP process, and it can be difficult to obtain good control by directly employing alkyl iodides in photopolymerizations (i.e., in the absence of an additive like Mn$_2$(CO)$_{10}$).[113] Nonetheless, novel strategies for photo-CRP based on degenerative iodine transfer have emerged recently.

Lacroix-Desmazes and co-workers showed that photopolymerization from a photomacroiniferter (i.e., PDMS-I: iodo poly(dimethylsiloxane)) could be conducted in aqueous miniemulsion under UV irradiation.[143] In this system, the accumulation of I$_2$ in the organic phase is suppressed by reaction with I$^-$ in the aqueous medium to generate I$_3^-$. However, high dispersity values were obtained in this system (Đ > 2).

Scheme 19. UV−vis−NIR Spectra of Mixtures of CP-I and Catalysts[148] *a*
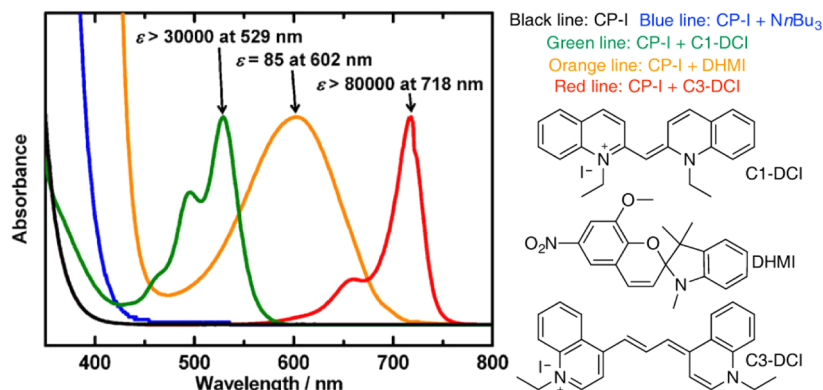
An alkyl radical can also be generated via the photolysis of a complex formed from an alkyl halide and a tertiary amine.[144−146] Exploiting this concept, Goto and colleagues developed an amine-catalyzed photo-CRP from an alkyl iodide (2-cyanopropyl iodide, CP-I) under visible light at 350−600 nm.[147] Using tributylamine as a catalyst, polymethacrylates with different side functional groups were produced with a narrow molar mass distribution (ca. $Đ$ = 1.1−1.4) and in moderate to high conversions. For example, using HEMA as a monomer affords up to 98% conversion in 2 h reaction time. In contrast, without an amine catalyst, the MMA monomer was not successfully polymerized, reaching only about 10% conversion and a large $Đ$ value of 1.6. Elemental analysis showed that a large percentage of chains were terminated with iodine. In addition, this photopolymerization followed pseudo-first-order kinetics and also could be readily controlled by switching the external light on and off. Two mechanistic possibilities for this process are presented in Scheme 18. As shown in Path A, an initially formed complex of the dormant species and amine is photocleaved to yield a propagating radical and an iodine-centered radical. Alternatively, in path B the C−I bond of the excited dormant species (R−P$_n$−I) is photocleaved to a polymeric carbon-centered radical and I•, which is subsequently captured by the amine. The authors observed a new peak in the UV−vis spectrum when CP-I and tributylamine were mixed together (as compared to the spectra for CP-I and amine alone), which supports the presence of a ground-state interaction between CP-I and the amine.[147]

Later, Goto and co-workers applied a variety of tertiary anilines as organic catalysts for photo-CRP from CP-I.[148] Enabled by the characteristic absorptions of the different catalysts, the polymerization could be regulated at desired wavelengths ranging from 350 to 750 nm by choice of catalyst (ca. $Đ$ = 1.1−1.4). The absorption spectra of different mixtures of CP-I and catalysts are illustrated in Scheme 19. The wavelength-controlled transformation also suggests that the C−I bond cleavage is realized through the photoexcitation of the complex of an alkyl iodide and an amine (Scheme 18, Path A). To demonstrate high end-group fidelity, chain extensions from poly(MMA)-I were employed to polymerize monomers at different wavelengths with corresponding catalysts. A block copolymer of MMA and δ-valerolactone (VL) was also successfully prepared in one pot by switching from a radical polymerization to a ring-opening polymerization with different wavelengths. In this process, starting from 2-hydroxyethyl 2-iodo-2-phenylacetate, MMA was polymerized

with 1′,3′-dihydro-8-methoxy-1′,3′,3′-trimethyl-6-nitrospiro-[2H-1-benzopyran-2,2′-(2H)-indole] (DHMI) as a catalyst (550−750 nm). Then VL was polymerized from the hydroxyl chain end by using triarylsulfonium hexafluorophosphate (350−380 nm) as a photo acid catalyst.

The Vana group reported the photo-CRP of n-butyl methacrylate (nBMA) from CP-I under UV irradiation (ca. $Đ$ = 1.2−1.6).[149] They claimed that homolysis of the C−I bond does not necessarily cause an accumulation of free iodine and inhibit the polymerization. Related kinetic simulations suggested that in addition to a degenerative chain-transfer process (iodine abstraction by a propagating radical), a reversible termination mechanism involving frequent C−I bond dissociation/formation and the formation of free iodine on a nanomolar scale is important to afford good control in this reaction. In addition, as demonstrated by experiments with on/off irradiation cycles, this polymerization is highly switchable.

Finally, though hypervalent iodine carboxylates, such as $(CX_3CO_2)_2I^{III}Ph$, have been predominantly used as oxidants, they can also generate $•CX_3$ radical species through decarboxylation under thermal or photochemical conditions.[150] By employing such hypervalent iodine derivatives as a $•CX_3$ radical source or a CX_3I precursor, Asandei and co-workers developed metal-free photo-CRP of VDF under visible light (Scheme 20).[151] In this method, polymerization of the low boiling point

Scheme 20. Proposed Mechanism of Photopolymerization of VDF with $(CX_3CO_2)_2I^{III}Ph$
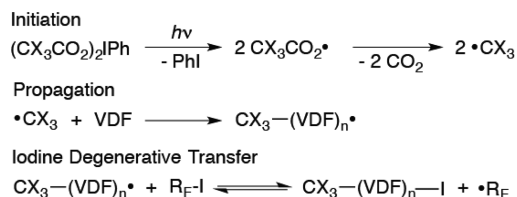
fluorinated alkene (VDF: −84 °C at 1 atm) was achieved in a glass tube at 40 °C using dimethyl carbonate as a solvent. Added $I(CF_2)_6I$ or in-situ-generated CF_3I (R_F−I) served as a chain-transfer reagent. The end-group fidelity of poly(VDF)-I was demonstrated by the synthesis of block copolymers with 2,2,2-trifluoroethyl methacrylate and methyl-2-(trifluoromethyl)-acrylate employing $Mn_2(CO)_{10}$ for the activation of the terminal C−I bond. The ease of generating $•CX_3$ radicals from hypervalent iodine carboxylates enables their usage as stable

and convenient $\bullet CX_3$ sources, especially compared to the inaccessible peroxide or azo analogues.

3.6. Organotellurium-Mediated Processes

Ditellurides can be employed as efficient trapping agents of carbon-centered radicals.[152] With the employment of dimethyl ditelluride $(MeTe)_2$ as an efficient deactivator in free radical polymerization of MMA with AIBN initiator, Yamago and co-workers synthesized poly(MMA) with a lower dispersity index ($Đ = 1.18$ vs 1.48) than the analogous reaction without $(MeTe)_2$.[153] In other work, the same group proved that carbon-centered radicals could be generated by homolytic substitution of tellurium-centered radicals with organotellurium compounds.[154] Since the MeTe$\bullet$ species can be generated via the photolysis of $(MeTe)_2$,[155,156] the authors realized that photo-generated tellurium radicals could activate dormant tellurium-capped polymer chains, as illustrated in Scheme 21A.[153] However, this polymerization was sluggish, and it was difficult to polymerize acrylates due to limited reactivation of dormant polyacrylate chains.

Scheme 21. Proposed Mechanism for Organotellurium-Mediated Photopolymerization
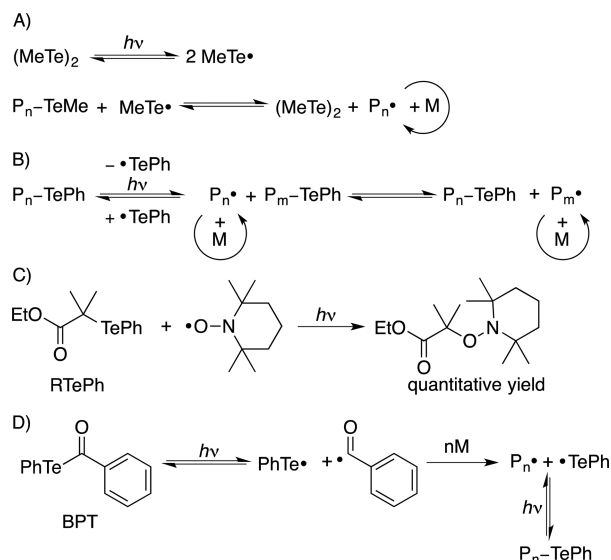
Yamago and co-workers applied an alternative organo-tellurium iniferter (R−TePh) to the photo-CRP of various monomers such as nBA, HEA, AA, NiPAAm, NVP, NVC, and N-vinylimidazole (NVI).[157,158] While the employment of a 500 W high-pressure mercury lamp produced poly(nBA) with a broad molar mass distribution ($Đ = 1.87$), long-wavelength irradiation (>470 nm) afforded the target polymers with excellent control over molar mass distribution (e.g., poly(nBA), $Đ = 1.09$) and very high conversions of monomers (conversions = 86−98%). When a very low amount of organotellurium compound (R−TeMe/nBA = 1/2000) was employed under their standard polymerization conditions, poly(nBA) was produced with a 223 kDa and 90% conversion in 5 h ($Đ = 1.18$). UV light and sunlight were also suitable light sources for this transformation. In addition, the chain growth could be instantly started or stopped by exposing the reaction vessel to light or dark, as demonstrated by three on/off cycles. The proposed mechanism for the tellurium-mediated photopolymerization is illustrated in Scheme 21B. Upon irradiation, the excited organotellurium dormant species (P_n−TePh) undergoes C−Te bond dissociation to

generate a tellurium-centered radical and a carbon-centered radical for propagation. The polymeric carbon radical can react with another tellurium dormant species via a degenerative chain-transfer process, which is the predominant mechanism under thermal conditions. The effective generation of a carbon-centered radical from RTePh was confirmed by reacting with TEMPO under irradiation, as shown in Scheme 21C.

Yamago and co-workers subsequently applied LED lights to their organotellurium-mediated polymerization.[159] They also developed a sequence of (1) organotellurium-mediated polymerization under thermal conditions and (2) photoinduced carbon−carbon bond formation of Te-terminated polymers in order to build well-defined symmetric block copolymers.[160]

Liska and co-workers showed that the organotellurium iniferter BPT (Scheme 22D) could be employed for polymer-

Scheme 22. Chemical Structures of Selected Selenium-Containing Iniferters Used in Photopolymerizations
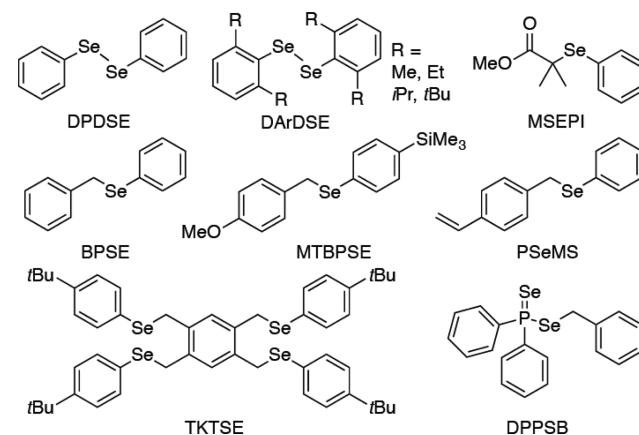
ization of acrylates and acrylamides (ca. $Đ = 1.2−1.3$) under visible-light irradiation (400−500 nm).[161] In this system, the photoexcited BPT undergoes homolysis to produce a Te-centered radical and a carbonyl radical, the latter of which initiates the polymerization reaction (Scheme 21D). The growing radical and the PhTe$\bullet$ species undergo reversible photoactivation/deactivation in the subsequent polymerization process, which may also compete with a degenerative chain-transfer mechanism. Related experiments to demonstrate the end-group fidelity of the polymers, such as chain extension studies, were not reported in this system.

3.7. Selenium-Mediated Processes

It is known that the photolysis of diphenyl diselenide or alkyl phenyl selenides can generate the stable phenylseleno radical, which has lower reactivity toward carbon−carbon double bonds than the corresponding sulfur radical.[156,162,163] Moreover, a diphenyl diselenide molecule can react with a carbon-centered radical via a bimolecular homolytic displacement process to generate a Se-centered radical. This process is ~160-fold faster than the corresponding diphenyl disulfide exchange.[152] The phenyl selenium group can be readily removed under mild conditions compared to many heteroatom-tethered substituents, for example, the arylthio group.[164] On the basis of these characteristics, selenium-based photoiniferters have been designed for free radical polymerizations.

Yuki and co-workers developed photopolymerization methods for St derivatives and MMA from iniferters such as diphenyl diselenide (DPDSE), methyl α-phenylseleno isobutylate

(MSEPI), benzyl phenyl selenide (BPSE), and *p*-methoxybenzyl *p*-trimethylsilylphenyl selenide (MTBPSE) (Scheme 22).[165−167] In these transformations, low to moderate conversions were normally obtained upon irradiation from a high-pressure mercury lamp. Although the molecular weights increased linearly with conversion, the molar mass distributions were usually broader than other photo-CRP techniques. For example, *Đ* values were frequently around 2.0.[167] Notably, high end-group fidelity of the SePh unit could be achieved, as demonstrated by subsequent chain extension reactions under the same photo-polymerization conditions and ^{77}Se NMR analysis.[168,169] Since the terminal phenyl selenium group can be efficiently converted into an alkene group on the chain end, graft copolymers composed of polystyrene branches could be prepared.[170] To further facilitate the synthesis of graft copolymers, the same authors developed a novel photoiniferter P-SeMS containing a St unit in the structure.[171] After a free radical polymerization initiated by AIBN under thermal conditions, a subsequent Se-mediated photopolymerization from the side chain enabled the preparation of a graft polymer composed of a poly(St) backbone and poly(MMA) sidechains. Considering the *p*-phenylseleno-methylstyrene (P-SeMS) molecule can act as both a monomer and an iniferter, the direct photopolymerization of this molecule allowed for the production of branched poly(St) materials containing a high percentage of selenide units.[172] In addition, Kwon et al. developed a tetrafunctional photoiniferter 1,2,4,5-tetrakis(*p-tert*-butylphenylselenomethyl)benzene (TKTSE) that they used to prepare star-sharped poly(St)-containing arylseleno units at polymer chain ends.[173]

By modifying the substituents on the phenyl rings of DPDSE, Zhu and co-workers prepared a variety of photoiniferters based on diaryl diselenide (DArDSE) as shown in Scheme 22.[174] Polymer products with *Đ* < 1.3 were obtained from an iniferter containing two methyl substituents on each phenyl ring. High end-group fidelity was confirmed by NMR and MALDI-TOF MS analysis. The same group also investigated photopolymerization with the iniferter *P,P*-diphenyl phosphinodiselenoic acid benzyl ester (DPPSB) under UV−vis irradiation.[175] Although linear reaction kinetics were observed and the molecular weights increased linearly with monomer conversions, only moderate control over molar mass distribution (ca. *Đ* = 1.5−2.0) was obtained with this method.

3.8. C−C Bond Dissociation/Combination Processes

Besides the commonly used motifs of CRP based on carbon−sulfur, carbon−oxygen, carbon−halogen, or carbon−metal bond cleavage, processes involving carbon−carbon bond dissociation/combination have also been investigated for many years. Since the 1980s, Otsu and co-workers[43,44,176] and Braun[177,178] and co-workers reported pioneering studies of the use of tetraphenyl-ethane derivatives to enable CRP. Compared to current CRP methods, broad molar mass distributions, poor end-group fidelity, and non-first-order kinetics at high conversions have limited the application of these methods in advanced material science. Furthermore, due to the generally high carbon−carbon bond dissociation energy, such systems frequently have low initiation efficiencies. In addition, the substituted diphenyl carbon-centered radicals produced by fragmentation, which are crucial species for initiating chain growth and deactivating polymeric radical chains to form dormant species, often undergo side reactions such as hydrogen abstraction and rearrangement, which leads to a decreased concentration of persistent radicals and undesired chain end groups.[43,44] Simultaneously maintaining

high activities in both activation and deactivation are challenging in these systems.

In perhaps the most promising case, Yang and co-workers reported cycloketyl radical-mediated living polymerization using BIXANDL under UV-light irradiation conditions (Scheme 23).[179] With this method a variety of (meth)acrylates could be

Scheme 23. Proposed Mechanism of Cycloketyl Radical-Mediated Photo-CRP
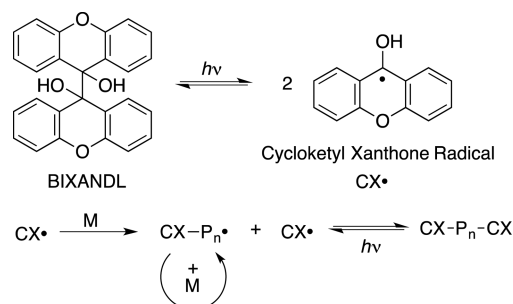
photopolymerized in THF with greater than 80% monomer conversions, producing products with dispersity indices ranging from 1.39 to 1.48 and up to 107 kDa molar mass. The experimental M_n showed a higher deviation from the theoretical value ($M_{n,th}$) at the beginning of the reaction and then gradually approached the theoretical number. The photoswitchable nature was verified with on/off experiments by periodically exposing a reaction solution to UV light (4 cycles), which resulted in a linear relationship between $\ln([M]_0/[M]_t)$ and exposure time. The presence of the CX group at the end of each polymer chain was quantitatively confirmed with a standard BIXANDL UV absorption curve. Furthermore, subsequent chain extensions starting from presynthesized poly(MMA)−CX were conducted under photo-CRP conditions. The authors suggested that the highly resonance-stabilized CX[•] species is critical for the observed high performance in the dissociation/combination process.

3.9. Photoinitiated ATRP

In this section and in section 4 of this review we summarize the development of photoinitiated and photoredox, respectively, CRP reactions that utilize Cu complexes. Since many of these reactions are related to classic thermal ATRP, we briefly summarize the current state-of-the-art for the latter here. In traditional ATRP, alkyl halides, e.g., alkyl bromides (R−Br) or alkyl chlorides (R−Cl), are often used as the initiators or dormant species; control is attained through a metal-catalyzed activation/deactivation cycle[180−183] wherein the alkyl halide is activated by a low oxidation state transition-metal catalyst, i.e., activator, to generate an alkyl radical and an oxidized form of the transition-metal complex, also referred to as deactivator. Several monomer units can be added to the alkyl radical before the high oxidation state metal complex deactivates it to reform the dormant alkyl halide and the activator. Repeating the activation/deactivation cycles for all dormant species allows the uniform growth of all polymer chains. Cu(I)/L and X−Cu(II)/L complexes, where L stands for the ligand, are the most common activators and deactivators, respectively. In contrast to conventional thermal ATRP, several new ATRP techniques that start from high oxidation state transition-metal complexes have been developed to overcome problems associated with fortuitous oxidation of activator. These techniques include reverse

ATRP,[184] simultaneous reverse and normal initiation (SR&NI) ATRP,[185] and activator generated by electron transfer (AGET) ATRP.[186]

One drawback of these ATRP techniques is the need for a high concentration of the metal complex to maintain the rate of polymerization throughout the reaction and overcome the effect of unavoidable biradical termination events that lead to irreversible formation of the deactivator complex according to the persistent radical effect.[78,187,188] To enable lowering the catalyst loading down to the sub-100 ppm level,[1,9,189] which is desirable for many applications, a continuous process of activator regeneration was introduced. Activator regeneration can be achieved simply by reducing the deactivator using various methods including addition of organic reducing agents such as tin^{II} 2-ethylhexanoate, ascorbic acid, glucose, and zerovalent metals, etc. (a technique referred to as activators for continuous activator regeneration by electron-transfer or "ARGET" ATRP),[190−192] introducing an external radical initiator (referred to as initiators for continuous activator regeneration or "ICAR" ATRP),[193] or applying a cathodic current (as occurs in electrochemically mediated ATRP).[13]

The activator (i.e., the low oxidation state transition-metal complex) in ATRP can also be regenerated via irradiation with light; this concept has been widely used to develop light-mediated ATRP reactions (i.e., "photo-ATRP"). There are two general photo-ATRP mechanisms that differ by the primary photochemical process: photoinitiated (discussed in this section) and photoredox (section 4.1.1) ATRP. In photoinitiated ATRP (Scheme 24A), the equilibrium between active and

Scheme 24. Simplified Mechanisms for Photoinitiated and Photoredox ATRP^a
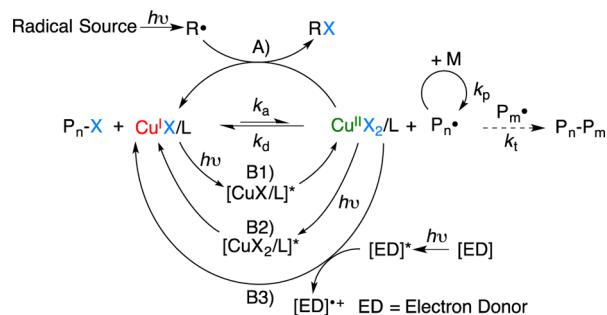
^{a}(A) Photoinitiated ATRP: reduction of Cu^{II} with a photogenerated radical. From B1 to B3 photoredox ATRP: (B1) Cu^{I}X/L is used as a photocatalyst; (B2) reduction of Cu^{II}X$_2$/L via photoexcitation; (B3) reduction of Cu^{II}X$_2$/L with an added photocatalyst.

dormant species is achieved by photochemical production of free radical species to (re)generate activator, similar to SR&NI/ICAR ATRP. As in the case of all of the examples in section 3 of this review, photoinitiated ATRP involves photocleavage of a photoinitiator. In photoredox ATRP (section 4.1.1, Scheme 24B), photoinduced electron transfer reactions are the key primary photochemical process that either (re)generate activator or establish the ATRP equilibrium.

It should also be noted that zerovalent metals such as Cu(0) are able to activate R−X species to generate radicals. Percec and co-workers proposed a mechanism called SET-LRP to describe CRP in the presence of zerovalent copper.[7,194] Haddleton and co-workers significantly broadened the application of this system to synthesize high molecular weight multiblock copolymers by

sequential monomer addition[6,195] and to prepare well-defined protein/peptide−polymer conjugates in aqueous solution.[196,197] There is an ongoing debate regarding the details of SET-LRP and ATRP for the description of thermal CRP in the presence of Cu(0).[198−207] In this review, and in particular section 4, it is most relevant to focus on one of the key proposed distinctions between ATRP and SET-LRP: inner- versus outer-sphere electron transfer, respectively, as the main mechanism for R−X activation. Though these details have not been elucidated in most photo-CRP systems, both inner- and outer-sphere SET (OSET) almost certainly occur in photoredox CRP depending on the system.

In photoinitiated ATRP, a number of strategies have been used to reduce Cu(II)/L deactivators to Cu(I)/L activators in the presence of light. For instance, Cu(II)/L can be reduced to Cu(I)/L by free radicals that are generated in situ from photoinitiators through photocleavage under UV or visible-light irradiation. Commercial photoinitiators including DMPA, benzophenone (BP), and (2,4,6-trimethylbenzoyl) diphenyl-phosphine oxide (TMDPO) have been used to conduct UV-initiated ATRP of MMA at room temperature.[208,209] In these reports, the polymerizations began with Cu(II)/L, where L was PMDETA. Unlike conventional ATRP, these systems did not require an alkyl halide initiator; radicals derived from photolysis of the photoinitiators served as initiators for the polymerization and also as reducing agents to reduce Cu(II)/L to Cu(I)/L (such initiating systems are also known as "reverse ATRP").[208,209] The degree of control over the polymerization process could be improved by introducing a fraction of alkyl halide initiators, thus establishing an SR&NI ATRP process.

Yagci and co-workers implemented this technique in the inverse microemulsion polymerization of oligo(ethylene glycol) methyl ether methacrylate (OEGMA).[210] In addition to SR&NI ATRP, a combination of AGET and ICAR ATRP was investigated using highly active tris(2-pyridylmethyl)amine (TPMA) ligand. As shown in Scheme 25, Cu^{II}Br$_2$, PMDETA or TPMA as a ligand, and poly(ethylene glycol) (PEG)-based alkyl halide macroinitiator were dissolved in a mixture of OEGMA, water, and PEG550 costabilizers to form an aqueous solution. The aqueous solution was then slowly added to a surfactant-containing organic solution, thereby generating a stable water-oil inverse microemulsion. UV irradiation of the water-soluble photoinitiator Irgacure 2959 produced benzoyl and α-substituted alkyl radicals that readily reduced Cu(II)/L into Cu(I)/L in the droplets. It should be noted that the photoreduction of Cu(II)/TPMA could undergo other path-ways, leading to a hybrid of ICAR ATRP and AGET ATRP mechanisms. This difference compared to the Cu(II)/PMDETA system will be discussed further below. Some of the droplets where Cu(II)/L was reduced served as the nuclei for the growth of polymer particles, while the remaining droplets functioned as monomer reservoirs. Therefore, polymer particles with larger size, compared to the size of the original monomer swollen micelles/droplets, formed due to the diffusion of monomer from the unactivated droplets to the growing polymer particles. It was also demonstrated that the particle size could be tuned by adjusting the UV exposure time, initial stoichiometry, and aqueous-phase fraction.

Photoinitiated SR&NI ATRP were extended to visible light using various dyes (e.g., eosin Y and erythrosin B) and Irgacure 819 photoinitiator.[211−213] Considerably higher values of experimental molecular weights compared to the theoretical ones and broad molar mass distribution ($Đ \approx 1.28−1.60$) were

Scheme 25. Photoinitiated SR&NI and AGET&ICAR ATRP in Inverse Microemulsion[210] [a]
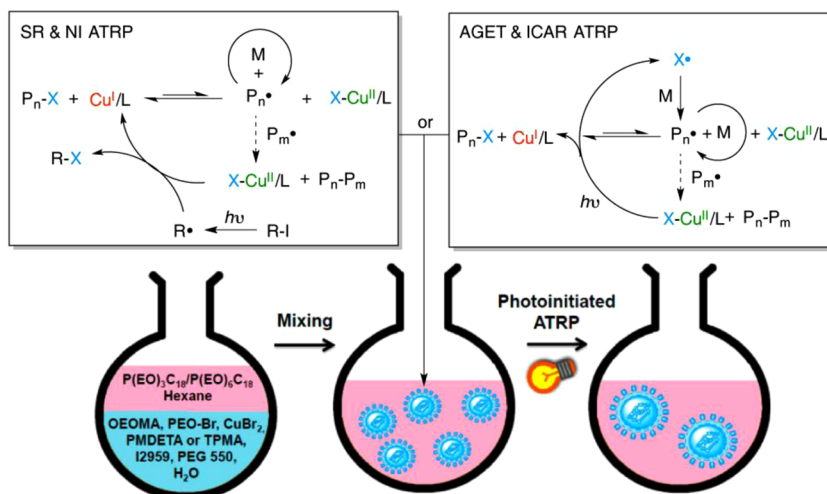
[a]Adapted from ref 210. Copyright 2013 American Chemical Society.

observed in the dye-sensitized SR&NI ATRP. However, the polymers obtained by the Irgacure 819 system provided molecular weight values consistent with the theoretical values and narrow molar mass distribution ($Đ ≈ 1.11–1.18$). Visible-light-induced electron transfer reactions of acylphosphine oxide-type photoinitiators, in conjunction with $Cu^{II}Cl_2$/PMDETA complex, were employed by the same group for both ATRP and copper-catalyzed azide–alkyne cycloaddition (CuAAC) processes.[214] Bowman and co-workers developed a novel copper(II) complex in which the counteranion, acylphosphinate (AP), served as a visible-light photoinitiator.[215] $Cu^{II}(AP)_2$/PMDETA was soluble in both aqueous and organic media and also exhibited the capability of catalyzing both CuAAC and ATRP upon visible-light exposure.

David and co-workers investigated in detail the photolysis of $Cu^{II}X_2$/L complexes in methanol at 350 nm and observed the formation of the corresponding $Cu^{I}X$/L complex and form-aldehyde as the products.[216,217] A reaction of homolytic cleavage of $Cu^{II}X_2$/L complexes upon UV exposure was proposed, and $Cu^{I}X$/L and halogen radical ($X^•$) formed as the primary photoproducts in this reaction. $X^•$ can be scavenged by methanol to form $^•CH_2OH$ and HX (Scheme 26). The Yagci group reported ATRP initiated by photolysis of CH_3OH/$Cu^{II}Br_2$/PMDETA/MMA solution where CH_3OH served as a solvent.[218]

Scheme 26. Photoinitiated ATRP and Related Reactions of CuX₂ in the Presence of Methanol
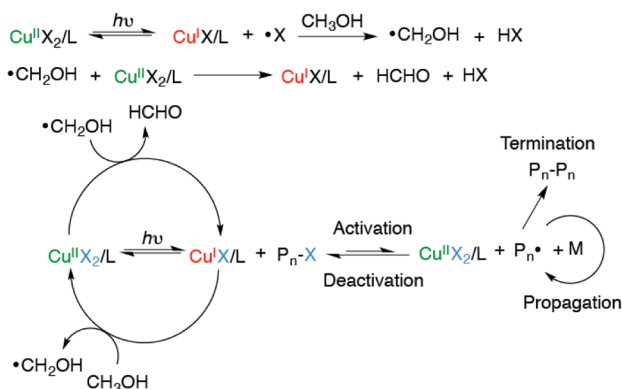
It was proposed that the photoproduct $^•CH_2OH$ could also reduce $Cu^{II}X_2$/L to $Cu^{I}X$/L and form formaldehyde. In the overall process, the excess $Cu^{II}X_2$/L deactivator is continuously reduced to the $Cu^{I}X$/L activator with the help of reactive solvent, i.e., CH_3OH. It is widely known that the solubility of $Cu^{II}X_2$/L complexes in organic media is limited, often resulting in heterogeneous ATRP. However, addition of CH_3OH into ATRP media promotes the solubility of $Cu^{II}X_2$/L complexes in the polymerization media, potentially enhancing the reversible deactivation process and maintaining a relatively high degree of control. Indeed, it was revealed that the presence of a small amount of CH_3OH led to better control over molecular weights and narrower molar mass distributions of polymers compared to the heterogeneous systems without CH_3OH.

In photoinitiated ATRP involving $Mn_2(CO)_{10}$, photogen-erated $^•Mn(CO)_5$ radicals are not only able to reduce the Cu(II)/L to Cu(I)/L directly but also to abstract halogen atoms from alkyl halides to generate alkyl radicals, as introduced previously in section 3.3[219] (Scheme 27).

Scheme 27. Proposed Mechanism of Photoinitiated ATRP with $Mn_2(CO)_{10}$
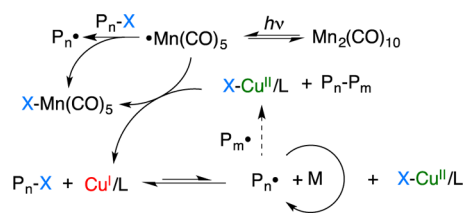
Recently, great interest has been placed on photoinitiated ATRP in the absence of conventional photoinitiators.[220−222] In 2000, Guan and Smart observed an acceleration of the polymerization rate of MMA using the combination of $Cu^{I}(bpy)Cl$ as catalyst and 2,2-dichloroacetophenone (DCAP) as initiator upon irradiation with visible light. This catalyst is generally poorly active in ATRP;[223] the authors proposed that direct photochemical activation of the initiator C−Cl bond through an inner-sphere complex [Cu^{I}, R−Cl] was critical for successful polymerization.

Scheme 28. (A) General Mechanism of Polymerization Catalyzed by Photolabile Cyclometalated Ru^{II} Complexes in Acetone; (B) Structures of the Cyclometalated Ruthenium(II) Complexes I and II
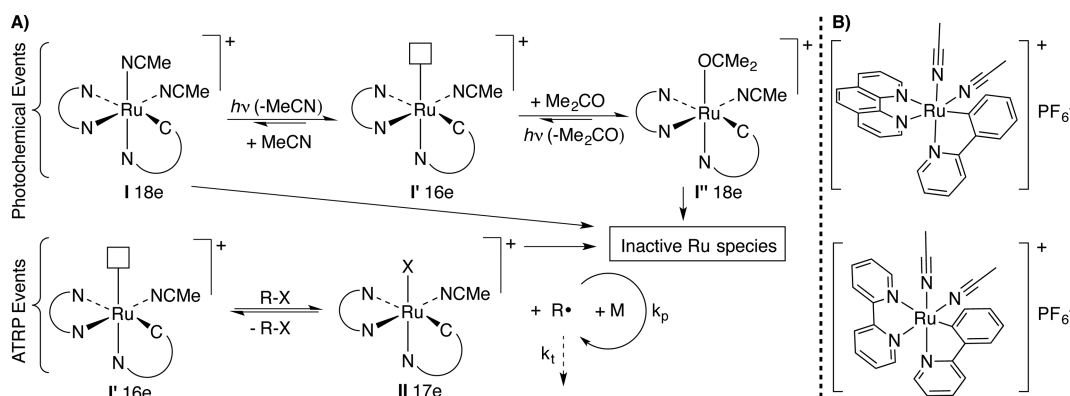
Ru(II) complexes have been extensively applied as catalysts in different polymerization reactions such as ATRP[3] and ring-opening metathesis polymerization (ROMP).[224] Furthermore, the well-known photosensitivity of Ru(II) complexes has led to their predominant role in photoredox catalysis.[225] Photo-activated ROMP reactions have been reported by various groups,[226−229] in most of which Ru(II) complexes were used as precatalysts, although the polymerizations have also been successfully performed with tungsten,[230] rhenium,[231] and molybdenum[232] complexes. Surprisingly, the number of Ru-mediated photo-CRPs is rather limited. Tris(1,10-phenanthroline)ruthenium(II) (Ru^{II}(phen)$_3$) and tris(2,2′-bipyridine)ruthenium(II) (Ru^{II}(bpy)$_3$) have been used to initiate a free radical polymerization, but no controlled/living feature was demonstrated in these systems.[233,234] Le Lagadec, Alexandrova, and co-workers developed a versatile photo-activated catalytic system for ATRP of MMA, St, and nBA based on cyclometalated ruthenium(II) complex.[235] This complex contains both strongly coordinating bidentate ligands as well as relatively labile ligands. As shown in Scheme 28, under irradiation with visible light, the solvento 18-electron species *cis*-[Ru(o-C$_6$H$_4$-2-py)(phen)(MeCN)(acetone)]$^+$ (compound I″) or *cis*-[Ru(o-C$_6$H$_4$-2-py)(phen)(MeCN)(MeCN)]$^+$ (compound I) can be activated with light to generate the 16-electron five-coordinated complex *cis*-[Ru(o-C$_6$H$_4$-2-py)(phen)-(MeCN)]$^+$ (compound I′), which is believed to be an active species for ATRP activation (see bottom of Scheme 28).

4. PHOTO-CRP ENABLED BY PHOTOREDOX CATALYSIS

4.1. Polymerization via C−Br Bond Cleavage

4.1.1. Copper-Mediated Processes. We now turn to photoredox CRP reactions wherein SET is the key primary photochemical process. Following the preceding section, which focused on photoinitiated ATRP, we begin here with ATRP reactions that are initiated by photoinduced SET, i.e., photo-redox ATRP. See section 3.9 for a detailed discussion of the differences between photoredox ATRP and photoinitiated ATRP.

Several groups continued a broad search for photosensitive additives that could generate electron donors under UV or visible irradiation to reduce Cu(II)/L deactivator to Cu(I)/L activator. These photosensitive reactants include semiconducting-doped ZnO nanoparticles,[236] graphitic carbon nitride,[237] alkyl dithio-carbamate,[238] and TiO$_2$ nanoparticles.[239,240] In these systems,

the reduction of Cu(II)/L involves OSET to Cu(II)/L from the excited additive (Scheme 29).

Scheme 29. Proposed Mechanism of Photoredox ATRP Catalyzed by ZnO Nanoparticles or mpg-C$_3$N$_4$
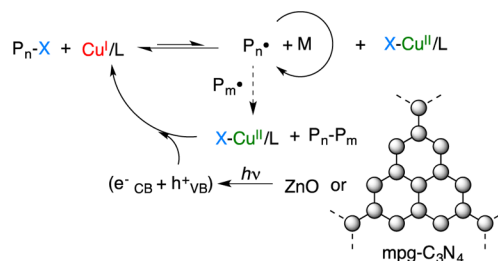
Mosnáček successfully polymerized MMA at 35 °C by irradiation ($\lambda > 350$ nm) of solutions containing copper concentrations as low as 50−100 ppm.[241] A mechanism of direct photoreduction of Cu(II)/L accompanied by the formation of Br$^{\bullet}$ radicals was proposed along with two possible photoredox processes: (1) Cu(I)/L could be excited to form [Cu(I)/L]*, which could then react with the dormant species; (2) Cu(II)/L could absorb light, and the resulting excited state [Cu(II)/L]* could react with the (macro)radical. In addition to the ATRP initiating pathway, Br$^{\bullet}$ radicals could also contribute to the initiation of a fraction of new polymer chains. A similar initiating system was extended by Jordan and co-workers to prepare (co)polymer brushes and patterned brushes on surfaces by surface-initiated ATRP.[242]

Matyjaszewski and co-workers also reported visible/sunlight-mediated ATRP using Cu^{II}Br$_2$/L; the photoreduction of Cu^{II}Br$_2$/L to Cu^{I}Br/L was proposed to proceed by ligand to metal charge transfer in the photoexcited state.[221] TPMA and tris((4-methoxy-3,5-dimethylpyridin-2-yl)amine) (TPMA*) were utilized as ligands for the controlled polymerization of methacrylates and acrylates, respectively.

Later, the aliphatic tertiary amine tris[2-(dimethylamino)-ethyl]amine (Me$_6$TREN) was used as a ligand for Cu-mediated photo-ATRP by Haddleton and co-workers.[243,244] Near-quantitative monomer conversion (>95%) was obtained, affording poly(acrylates) with dispersities as low as 1.05 and over 99% end-group fidelity. Moreover, well-defined α,ω-heterofunctional poly(acrylates) could be synthesized using this method thanks to good compatibility of hydroxyl- and *vic*-diol-functional initiators with the polymerization conditions.

One-pot diblock copolymerization by sequential addition of ethylene glycol acrylate to a poly(MA) macroinitiator was also successful (Figure 3). This approach was extended for the
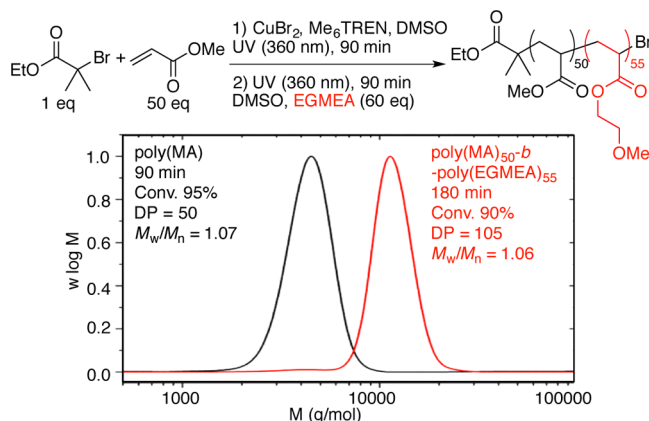
Figure 3. In-situ chain extension and block copolymerization from a poly(MA) macroinitiator with photoredox ATRP.[243] Adapted from ref 243. Copyright 2014 American Chemical Society.

preparation of high-order acrylic multiblock copolymers comprised of four different repeat units.[245] Various acrylates have been polymerized using this system in a variety of ionic liquids as solvents, including 1-ethyl-3-methylimidazolium ethyl sulfate $[emim^+][EtSO_4^-]$, 1-heptyl-3-methylimidazolium bromide $[C_7mim^+][Br^-]$, 1-hexyl-3-methylimidazoliumtetrafluoroborate $[C_6mim^+][BF_4^-]$, 1-hexyl-3-methylimidazoliumhexafluorophosphate $[C_6mim^+][PF_6^-]$, and 1-octyl-3-methylimidazoliumhexafluorophosphate $[C_8mim^+][PF_6^-]$.[246] A significant acceleration of the polymerization rate without compromising the chain-end fidelity was observed in polymerizations in ionic liquids, compared to the analogous system using dimethyl sulfoxide (DMSO) as solvent. An OSET mechanism, where an electron was transferred from photoexcited $[Me_6TREN]^*$ to the alkyl halide, resulting in homolysis of the C−Br bond, was proposed by the authors (Scheme 30), and this process has
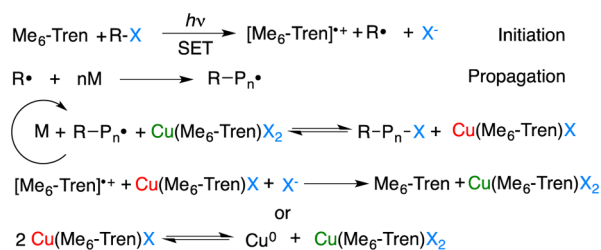
Scheme 30. Proposed Mechanism for Tertiary-Amine-Mediated, Photoredox OSET-Living Radical Polymerization[243] a

[a]Adapted from ref 243. Copyright 2014 American Chemical Society.

continued to garner interest as discussed below. For example, another possible mechanism for this reaction could involve light absorption by the Cu(II)/L complex followed by reduction of the excited state complex by Me_6TREN vide infra.

To further study this polymerization using Me_6TREN as ligand, the Matyjaszewski group performed a series of kinetic measurements to quantify the rates of multiple proposed photomediated processes for radical generation (Table 1, Scheme 31).[247,248] The simulation results obtained using

experimentally measured rate constants showed that the dominant reaction of activator regeneration is the photoreduction of Cu(II)/L by an excess of amine, i.e., Me_6TREN, similar to an ARGET ATRP (i.e., reaction 1, Scheme 31). The radical cation from oxidized Me_6TREN can initiate a new chain after proton transfer. The second most contributing reaction, 1 order of magnitude slower than the first one, is the photoinduced SET form the excited ligand to the alkyl halide (i.e., reaction 2, Scheme 31). Other photoinduced reactions such as homolytic cleavage of the alkyl halide (i.e., reaction 4, Scheme 31) or radical generation from the ligand or monomer (i.e., reaction 5, Scheme 31) were proposed to contribute negligibly.

Haddleton, Barner-Kowollik, and co-workers used pulsed-laser polymerization (PLP) and high-resolution electrospray-ionization mass spectrometry (ESI-MS) to investigate the mechanism of this reaction using the same ligand, i.e., Me_6TREN, and the alkyl halide initiator ethyl α-bromoisobutyrate (EBiB).[249] The chemical structures found by ESI-MS are listed in Scheme 32A. On the basis of these data, a more complicated process was proposed (Scheme 32B). Through this qualitative method, UV-light-induced C−Br bond scission of the initiator was observed, and the corresponding radicals propagated or reacted with Cu(II)/L. The authors again suggested that Cu(I)/L was generated via SET from excited Me_6TREN to Cu(II)/L. The excited Cu(II)/L can also be reductively quenched by free ligand, forming Cu(I)/L as well as an amine radical cation. Although there are many other pathways that could generate radicals, the contribution of Me_6TREN in the activator regeneration is predominant. We also note that very recently photoredox ATRP using TPMA ligand was developed by Matyjaszewski and co-workers for aqueous polymerization of OEGMA.[250]

The above examples describe processes where SET serves to generate an activator in ATRP. Photoinduced electron transfer can also directly participate into the ATRP equilibrium through either photocatalyzed activation of R−X or photocatalyzed deactivation of R•. (Scheme 33A).[251]

The mechanism in Scheme 33A (left) implies that the photoexcited deactivator is converted into the activator via reductive quenching with a propagating radical reductant. Although the number of ATRP reactions exclusively involving a reductive quenching mechanism is very limited, this process could occur concurrently in many photoinitiated ATRP reactions.

Conversely, the excited state activator could undergo oxidative quenching to produce a radical from a dormant species, i.e., R−X. ATRP involving an oxidative quenching mechanism has been achieved using photoredox catalysts containing different types of metals (Scheme 33A (right)). Poly and Lalevée and co-workers reported a copper-based catalyst, bis(1,10-phenanthroline)-copper(I) $(Cu(phen)_2^+)$, that was capable of photoredox ATRP using a simple household blue LED.[251] Using ethyl α-bromophenylacetate (EBPA) as the initiator and a low catalyst loading (80 ppm), good control over the polymerization of MMA in dimethylformamide (DMF) was observed. The excited state of the complex Cu(I)*/L can rapidly undergo oxidative quenching by the alkyl halide, resulting in the generation of Cu(II)−Br/L and a propagating radical. To achieve a fast enough regeneration of Cu(I)/L and to further reduce the catalyst loading down to 20 ppm, triethylamine (TEA) was added to accelerate the reduction of Cu(II)/L (Scheme 33B).

4.1.2. Iridium-Mediated Processes. Inspired by the recent interest in photoredox catalysis in organic chemistry,[225,252−254]

Table 1. List of Reactions Relevant to Photo-ATRP Processes Using Me$_6$TREN Ligand[248]

entry	reaction	rate coefficient at 298 K
	ATRP	
1	$RBr + Cu^{II}Br_2/L \rightarrow R^\bullet + Cu^{II}Br_2/L$	$k_{a1} = 2 \times 10^3 \ M^{-1} \ s^{-1}$
2	$R^\bullet + Cu^{II}Br_2/L \rightarrow RBr + Cu^{I}Br/L$	$k_{d1} = 5 \times 10^7 \ M^{-1} \ s^{-1}$
3	$P_jBr + Cu^{I}Br/L \rightarrow P_j^\bullet + Cu^{II}Br_2/L$	$k_a = 2 \times 10^2 \ M^{-1} \ s^{-1}$
4	$P_j^\bullet + Cu^{II}Br_2/L \rightarrow PBr + Cu^{I}Br/L$	$k_d = 2.8 \times 10^8 \ M^{-1} \ s^{-1}$
	radical propagation	
5	$R^\bullet + MA \rightarrow P_1^\bullet$	$k_{add,EBiB} = 7.3 \times 10^2 \ M^{-1} \ s^{-1}$
		$k_{add,other} = 1.6 \times 10^4 \ M^{-1} \ s^{-1}$
6	$P_j^\bullet + MA \rightarrow P_{j+1}^\bullet$	$k_p = 1.56 \times 10^4 \ M^{-1} \ s^{-1}$
	conventional radical termination	
7	$R^\bullet + R^\bullet \rightarrow D_0$	$k_{t0} = 2 \times 10^9 \ M^{-1} \ s^{-1}$
8	$R^\bullet + P_j^\bullet \rightarrow D_j$	$k_{t0} = 2 \times 10^9 \ M^{-1} \ s^{-1}$
9	$P_j^\bullet + P_j^\bullet \rightarrow D_{j+k}$	$k_t = 1 \times 10^8 \ M^{-1} \ s^{-1}$
	catalytic radical termination	
10	$R^\bullet + Cu^{I}Br/L \rightarrow D_0 + Cu^{I}Br/L$	$k_{tx0} = < 100 \ M^{-1} \ s^{-1}$
11	$P_j^\bullet + Cu^{I}Br/L \rightarrow D_j + Cu^{I}Br/L$	$k_{tx} = 4 \times 10^3 \ M^{-1} \ s^{-1}$
	radical transfer	
12	$P_j^\bullet + L \rightarrow D_j + R^\bullet$	$k_{tr,L} = 2.8 \times 10^3 \ M^{-1} \ s^{-1}$
13	$P_j^\bullet + RBr \rightarrow D_j + R^\bullet$	$k_{tr,EBiB} = 2.3 \times 10^2 \ M^{-1} \ s^{-1}$
	photochemical radical (re)generation	
14	$L + MA \rightarrow 2R^\bullet$	$k_{r2L,M} = 1.5 \times 10^{-9} \ M^{-1} \ s^{-1}$
15	$RBr \rightarrow 2R^\bullet$	$k_{r1EBiB} = 2.9 \times 10^{-9} \ s^{-1}$
16	$RBr + L \rightarrow 2R^\bullet$	$k_{r2EBiB,L} = 6.2 \times 10^{-6} \ M^{-1} \ s^{-1}$
17	$RBr + L \rightarrow 2R^\bullet$	$k_{r2MBP,L} = 1.4 \times 10^{-6} \ M^{-1} \ s^{-1}$
18	$Cu^{II}Br_2/L + L \rightarrow Cu^{I}Br/L + R^\bullet$	$k_{r2CuBr,L} = 1 \times 10^{-3} \ M^{-1} \ s^{-1}$
19	$Cu^{II}(OTf)_2/L + L \rightarrow Cu^{I}OTf/L + R^\bullet$	$k_{r2CuOTf,L} = 1 \times 10^{-2} \ M^{-1} \ s^{-1}$

Scheme 31. Proposed Activator (Re)Generation Pathways in Photoredox ATRP Using Me$_6$TREN Ligand[248] ^{a}

$$X\text{-}Cu^{II}/L + L \xrightarrow{h\nu} Cu^{I}/L + L^{\bullet +} + X^- \quad 1)$$
$$R\text{-}X + L \xrightarrow{h\nu} R\bullet + L^{\bullet +} + X^- \quad 2)$$
$$X\text{-}Cu^{II}/L \xrightarrow{h\nu} Cu^{I}/L + X\bullet \quad 3)$$
$$R\text{-}X \xrightarrow{h\nu} R\bullet + X\bullet \quad 4)$$
$$L + M \xrightarrow{h\nu} L^{\bullet +} + M^{\bullet -} \quad 5)$$
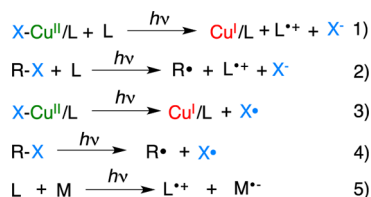
^{a}(1) Photochemical reduction of Cu^{II} by an electron donor; (2, 4, and 5) generation of radicals by reactions of an alkyl halide and/or a ligand; (3) direct reduction of X−Cu^{II}/L. Adapted from ref 248. Copyright 2014 American Chemical Society.

various metal complexes have been developed and studied for photoredox-catalyzed CRP. In 2012, Fors and Hawker reported the first example of using the Ir-based photoredox catalyst tris(2-phenylpyridinato)iridium(III) (fac-[Ir(ppy)$_3$]) to conduct photo-CRP of methacrylates[222] (Scheme 34). Similar to the Cu-mediated reaction involving an oxidative quenching as introduced above (Scheme 33), the photoexcited Ir(III)* species can reduce an R−Br initiator to produce an alkyl radical, thereby initiating polymerization. This activation is most likely an OSET process. Importantly, the highly oxidizing Ir(IV) complex, which serves as a deactivator, is able to react with the propagating

radical to regenerate the ground state Ir(III) PC and a dormant chain end. The living nature of this photoredox CRP was further demonstrated by an on/off experiment and chain extension from a poly(MMA) macroinitiator using benzyl methacrylate (BnMA) monomer. A random copolymerization of MAA and BnMA with 10% MAA resulted in a relatively narrow molar mass distribution (Đ = 1.24), which suggested some tolerance to the acidic monomer. Controlled polymerization of acrylates under the same conditions was more challenging due to the increased propagation rate of these monomers and the difficulty in chain-end reduction compared to methacrylates.[255] Hawker and co-workers then optimized conditions for the polymerization of acrylates by increasing the concentrations of monomer and catalyst.[256] For example, 0.05 mol % of Ir(ppy)$_3$, which is 10 times higher than what is typically used in the polymerization of methacrylates, resulted in a polymerization of 3.5 M MA with an improved molar mass distribution (Đ = 1.25 vs 1.45) in media containing benzyl α-bromoisobutyrate as initiator under irradiation by either 380 nm LEDs or a 50 W fluorescent lamp.

Using fac-[Ir(ppy)$_3$] as a PC and the bifunctional initiator dimethyl 2,6-dibromoheptanedioate, Yang and co-workers performed a one-pot process with sequential monomer addition of MMA and 1,1,1-trifluoroethyl methacrylate (TFEMA) to prepare poly(TFEMA)-$block$-poly(MMA)-$block$-poly(TFEMA) triblock copolymers.[257] A solvent effect study revealed that the

Scheme 32. (A) All Species Detected by ESI-MS That Formed in Different Combinations of Reagents under PLP Conditions for MMA Polymerization; (B) Proposed Mechanism of Photo-RDRP, Based on Structures Found in ESI-MS[249] [a]
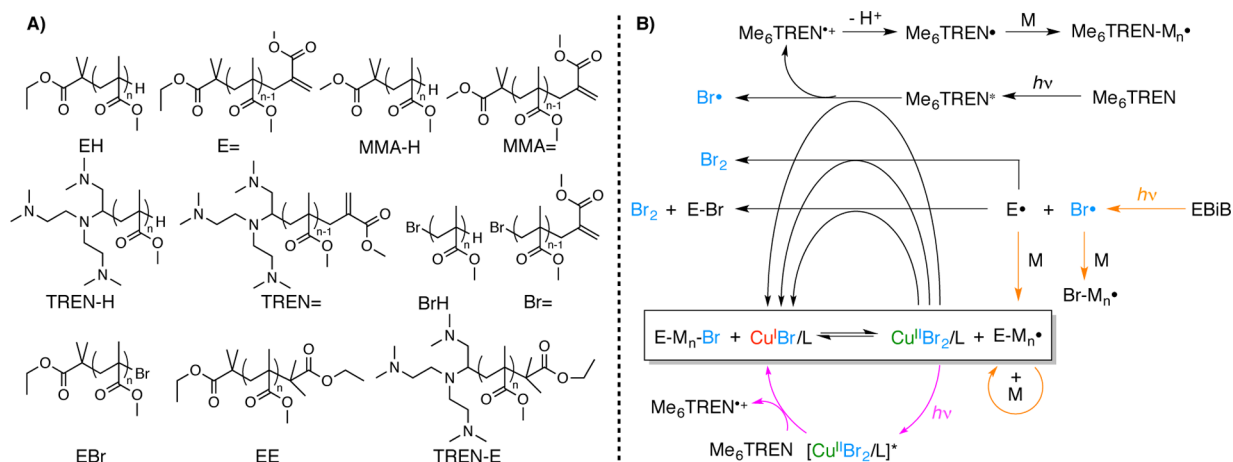
[a]Adapted from ref 249. Copyright 2015 American Chemical Society.

Scheme 33. (A) Photoredox ATRP via Either Reductive or Oxidative Quenching of the Excited State Derived from the Deactivator or the Activator; (B) Catalytic Cycle Proposed for the ATRP Involving Cu(phen)$_2^+$[251] [a]
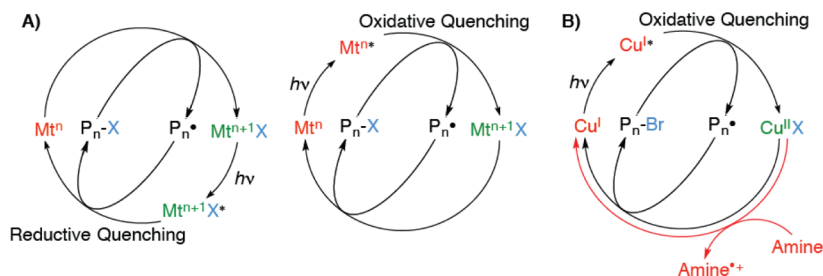
[a]Adapted from ref 251. Copyright 2015 American Chemical Society.

Scheme 34. Proposed Mechanism of Visible-Light-Mediated Living Radical Polymerization Using the PC fac-[Ir(ppy)$_3$]
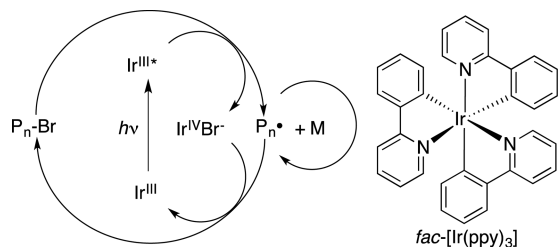
polymerization in anisole gave a higher degree of control compared to the same polymerization in DMF or acetonitrile (MeCN).[258] Furthermore, Yang and co-workers reported that an alkyl iodide, perfluoro-1-iodohexane (CF$_3$(CF$_2$)$_5$I), could also be activated by photoexcited fac-[Ir(ppy)$_3$] for photoredox CRP of MMA.[259]

In addition to fac-[Ir(ppy)$_3$], multiple Ir complexes were developed by the Lalevée group and used as photoredox catalysts.[260−262] Although little focus was placed on a controlled/living process in these studies, it was demonstrated that these complexes could initiate a free radical polymerization or a free radical-promoted cationic photopolymerization.

4.1.3. Photoredox Catalysis Mediated by Other Transition Metals.
Iron (Fe) has also been extensively studied as a catalyst in ATRP.[263] Polymerization of methacrylates using EBiB as initiator and [Fe^{II}(bpy)$_3$](PF$_6$)$_2$ as photocatalyst

resulted in relatively low levels of control and livingness.[224] During the writing of this review, Matyjaszewski and co-workers reported Fe-based photoredox ATRP of methacrylic monomers in the absence of additional ligands.[264] Molecular weight increased linearly with the conversion of monomer, and the dispersity index of polymer was as low as 1.15. Earlier work had already demonstrated that no additional ligands are required in ATRP of MMA using the Fe^{II}Br$_2$/Fe^{III}Br$_3$ catalytic system due to the use of MeCN or DMF as polar solvents, which serve as solubilizing/stabilizing ligands.[265] In this Fe-based system, it was found that alkyl halides could be activated by FeBr$_2$ not only under thermal conditions but also by photoactivation at ambient temperature, i.e., an oxidative quenching process. In addition, photoreduction of FeBr$_3$ by MMA was also proved by NMR spectroscopy, which suggests that a photoredox process continuously regenerates FeBr$_2$ activator.

Digold bis(diphenylphosphino)methane dichloride ([Au$_2$(μ-dppm)$_2$]Cl$_2$) has been shown to be able to catalyze photo-CRP of various (meth)acrylates.[266] However, poor control was observed in this system, which could be ascribed to an inefficient deactivation of propagating radicals by Au$_2$(III) complexes that originated from the activation of alkyl halides by photoexcited Au$_2$(II). Niobium (Nb) nanoparticles made from the suspension of NbCl$_5$ in anhydrous benzyl alcohol have also been introduced into photo-CRP of NiPAAm as a recyclable photocatalyst.[267] The carbon-centered radical on the benzyl alcohol-coated Nb nanoparticle, through a photopromoted electron transfer from surface to metal, has been proposed to be able to activate alkyl

halides to form a propagating radical and Br$^\bullet$ coupled to the Nb nanoparticle surface, although the deactivation mechanism has not been further explored and livingness has not been evaluated in this system.

4.1.4. Metal-Free Photoredox Catalysis. As noted in section 3, metal-free CRP reactions, including photo-CRP, have been known for decades. These reactions, however, typically require stoichiometric amounts of organic reagents (i.e., initiators or iniferters) to produce polymers. Building from the broad application of organocatalysis in organic synthesis,[268−272] researchers have recently begun to employ organic PCs in the context of polymerization. For example, facile access to radical cation intermediates via SET to organic PCs has enabled the development of metal-free variants of ROMP[273,274] and cationic polymerization.[275] Hawker, Fors, and co-workers reported the first example of what they termed "metal-free ATRP" (note that OSET is likely operative in R−X activation in this case, as in all of the cases discussed in this section), which was catalyzed by an organic PC under 380 nm irradiation at room temperature.[276] A commercially available 10-methylphenothiazine (Me−PTH) PC was first tested; poor control over dispersity was observed, which the authors attributed to catalyst decomposition. To stabilize the catalyst, the nitrogen substituent on the phenothiazine ring was adjusted, and ultimately 10-phenylphenothiazine (PTH) was used (Scheme 35). Using PTH, photo-CRP of MMA was

Scheme 35. Proposed Mechanism of Metal-Free Photocatalyzed ATRP with PTH as the PC
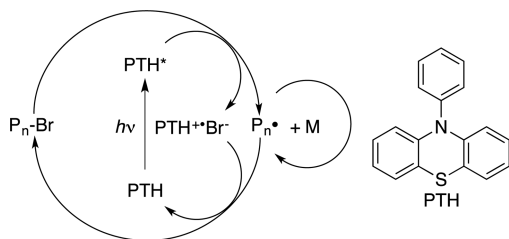
achieved with low dispersity and excellent chain-end fidelity. It was postulated that the higher reduction potential of excited PTH compared to Ir(ppy)$_3$ as well as the stability of the corresponding PTH radical cation are keys to the success of this reaction. An additional advantage of this system is its potential compatibility with a broad range of functional groups. Indeed, the polymerization of DMAEMA using 0.1 mol % PTH provided a much narrower molar mass distribution compared to the system with 0.005 mol % Ir(ppy)$_3$ ($Đ$ = 1.11 vs 3.69). PTH and its derivatives have also been successfully used by Matyjaszewski and co-workers in the photo-CRP of AN.[277] Similarly, Miyake and Theriot reported another example of metal-free photo-CRP of MMA involving perylene as a photoredox catalyst.[278] Very recently, Matyjaszewski, Liu, Gennaro, and co-workers performed a series of kinetic, electrochemical, and density functional theory (DFT) calculation studies on the mechanism of this system using several phenothiazine derivatives and other photoredox catalysts. Both experimental and calculated results suggest that the deactivation involves an associative electron transfer involving a termolecular complex, which is the exact reverse of the dissociative electron transfer occurring in the activation process.[279]

4.2. Polymerization from Thiocarbonylthio and Trithiocarbonate Compounds

Although thiocarbonylthio and trithiocarbonate iniferters have been successfully used in controlled radical polymerization via a direct photochemical mechanism (see section 3), UV irradiation is generally required to achieve excitation. In an effort to conduct analogous polymerizations using visible light, chemists have employed PCs that absorb strongly in the visible region[225,280,281] and undergo SET to thiocarbonylthio or trithiocarbonates to initiate photoredox-catalyzed iniferter processes. Note that these polymerizations are frequently referred to as photo-RAFT or photoinduced electron transfer RAFT (PET-REFT). Though the RAFT equilibrium is almost certainly involved, given the currently proposed mechanism (which admittedly has not been studied in great detail), and following the mechanistic distinctions presented above, we suggest that the term photoiniferter polymerization is more appropriate to describe the examples described throughout section 4.2. Regardless of the terminology used, these reactions are extremely versatile and useful for polymer synthesis.

A simplified mechanism for these reactions is provided in Scheme 36. Activated by electron transfer from an excited

Scheme 36. Proposed Mechanism for Photo-CRP of Thiocarbonylthio and Trithiocarbonate Iniferters Using a Photoredox Catalyst
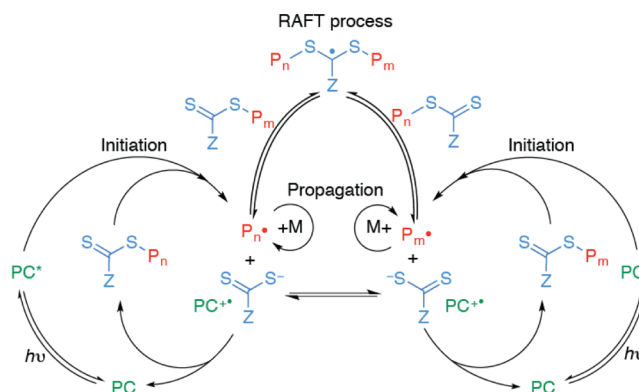
photoredox catalyst (PC*), the iniferter radical anion can produce a radical (P$_n^\bullet$ or P$_m^\bullet$) that can undergo either propagation or reversible chain transfer (RAFT process). The sulfur fragment of the iniferter agent (ZCS$_2^-$) and PC$^{+\bullet}$ can deactivate the growing radical chain by generating a dormant macroiniferter and a ground state PC. These compounds can re-enter the catalytic cycle through further photoinduced SET events.[282]

4.2.1. Iridium-Catalyzed Processes. In 2014, Boyer, Xu, and colleagues established a robust fac-[Ir(ppy)$_3$]-catalyzed photo-CRP of conjugated and unconjugated monomers from thiocarbonylthio and trithiocarbonate compounds using low-energy visible LED light (λ_{max} = 435 nm).[283] For example, 4-cyanopentanoic acid dithiobenzoate (CPADB), 3-benzylsulfa-nylthiocarbonylsulfanyl propionic acid (BSTP), and 2-(n-butyltrithiocarbonate)-propionic acid (BTPA) (Scheme 37) iniferters have been successfully applied to photo-CRP of acrylamides N-(2-hydroxypropyl) methacrylamide (HPMA), NiPAAm and N,N-dimethylacrylamide (DMA)), (meth)-acrylates (e.g., MMA, MA, and OEGMA), and St. Furthermore, xanthates enabled the efficient polymerization of vinyl esters (e.g., VAc, vinyl pivalate (VP), and vinyl benzoate (VBz)) and

Scheme 37. Chemical Structures of Selected Thiocarbonylthio Iniferters Used in PET-Iniferter-Mediated CRPs Enabled by Photoredox Catalysis
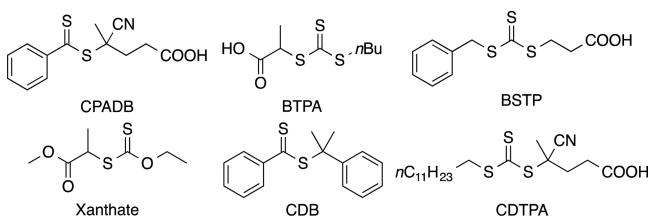
amides (e.g., NVP). Collectively, PET-iniferter-mediated CRP offers a versatile protocol to prepare polymers with molar masses ranging from 10^3 to 2×10^6 g/mol and narrow molar mass distributions (ca. Đ = 1.1–1.4). High end-group fidelity was shown by chain extensions to yield multiblock copolymers with low dispersity values. Moreover, photocontrol was demonstrated by exposing the reaction solution to on/off cycles. Importantly, this method also allows for the synthesis of polymers under nonrigorously degassed conditions, as the iridium PC is able to consume some oxygen within the system. To demonstrate the end-group integrity of polymers obtained under air, chain extension experiments were further conducted by directly adding nondegassed solutions of monomers into the reaction, which afforded block copolymers with precise control over molecular weight.

Combining this Ir-catalyzed photo-CRP method with an enzymatic monomer transformation, the Boyer group also developed a facile technique to prepare multiblock copolymers (e.g., poly(MA)-*block*-poly(EA)-*block*-poly(PA)-*block*-poly-(*n*BA)-*block*-poly(P′A)) (PA = *n*-propyl acrylate and P′A = *n*-pentyl acrylate) with high conversions of each monomer.[284] This protocol provides an alternative way to synthesize complex polymeric materials with multiple functionalities and sophisticated structures.

Isotactic and syndiotactic polymers often possess distinct physical and chemical properties compared to atactic ones. Although metal-catalyzed and living ionic polymerization strategies can provide good control over tacticity in some cases, it is still challenging to obtain polymers with high stereoselectivity via radical processes. Inspired by the seminal works from the Matyjaszewski[285] and Okamoto[286] groups, Boyer and Shanmugam applied rare earth metal triflates to the *fac*-[Ir(ppy)$_3$]-catalyzed photo-CRP reaction from BTPA to control its tacticity.[287] By complexation of Y(OTf)$_3$ with monomers and growing radical chains, a strategy that has also been previously

used by Li to improve stereoselectivity in photo-CRP from DBTTC,[62] the isotacticity of the polymer chains increased (*m/r* tacticity changed from 0.48/0.52 to 0.84/0.16). Since DMSO can coordinate to Y(OTf)$_3$ and poison this Lewis acid, the isotacticity of polymers can be gradually changed by the portionwise addition of DMSO into the reaction system. On the basis of this strategy, pseudogradient pentablock polymers containing five segments of varying degrees of isotacticity were successfully synthesized. This work facilitates further investigations into the physical and chemical properties of novel stereoblock and gradient copolymers.

4.2.2. Ruthenium-Catalyzed Process. While Lalevée and others demonstrated that Ru(bpy)$_3$Cl$_2$ can be utilized as a photoredox catalyst to perform free radical polymerizations,[234,288−290] Boyer and co-workers made important contributions to photo-CRP from thiocarbonylthio (e.g., CPADB) and trithiocarbonate (e.g., BTPA) iniferters with the same catalyst.[291] As exemplified in their work, methyl acrylates, acrylates, and acrylamides are all successful monomers that can be transformed into corresponding polymers with very narrow molar mass distributions (ca. Đ = 1.1) and excellent end-group fidelity. Successive chain extensions with the same photo-CRP method yielded decablock copolymers. Similar to the related Ir(ppy)$_3$-catalyzed photo-CRP, this reaction is also tolerant to limited amounts of oxygen and it can be regulated by on/off cycles, even starting from nondegassed reaction mixtures. To understand whether Ru(bpy)$_3$Cl$_2$ is decomposed during the photopolymerization under air, the authors prepared a preirradiated catalyst solution under air without monomers and iniferter and used it for subsequent air-free polymerization of MMA from CPADB under irradiation. By comparing the obtained kinetic study results to that of control experiments, they found no clear difference as shown in Figure 4A, suggesting the absence of significant decomposition of catalyst under air. Furthermore, the oxygen tolerance investigation was conducted at different catalyst concentrations. Interestingly, as illustrated in Figure 4B, although much longer induction times are required for cases in the presence of oxygen, linear kinetic plots are afforded with a similar but lower slope for both catalyst concentrations tested, implying a constant radical concentration during the polymerizations. The authors suggested that the retarded polymerization under air is due to a slow consumption of oxygen in the system. Nevertheless, precise control over molar mass distribution was observed for experiments conducted both in the absence and in the presence of oxygen.

With the Ru(bpy)$_3$Cl$_2$ PC, Boyer, Xu, and co-workers also developed photo-CRP with visible LED lights in water.[292]

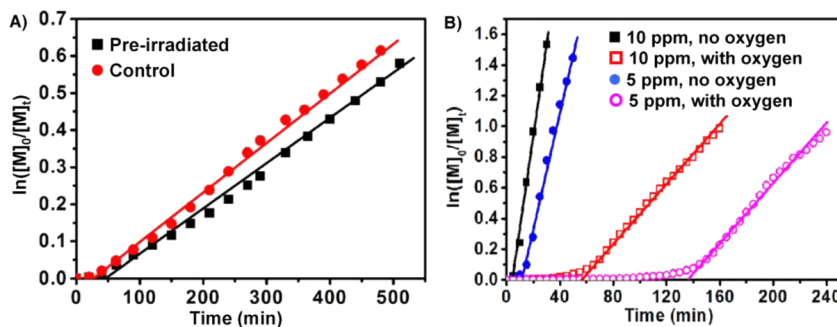**Figure 4.** Online Fourier transform near-infrared (FTNIR) measurement for kinetic studies.[291] (A) Degradation test of Ru(bpy)$_3$Cl$_2$ catalyst for photo-CRP of MMA from CPADB; (B) photo-CRP of MA from BTPA with different concentrations of Ru(bpy)$_3$Cl$_2$, ln([M]$_0$/[M]$_t$) vs exposure time in the absence and presence of oxygen. Reproduced from ref 291. Copyright 2014 American Chemical Society.

Although this technique only uses very low concentrations of the catalyst (typically 1 ppm to monomers), well-defined polymers with narrow molar mass distributions ($Đ < 1.3$) are produced at moderate to high conversions of monomers. In addition, biological media has also been successfully employed in this photopolymerization, affording polymers with good dispersities ($Đ < 1.4$). Employing a "graft from" approach, protein–polymer bioconjugates were synthesized using bovine serum albumin as a model, for which the enzymatic bioactivity of the protein is successfully maintained using a standard assay.

4.2.3. Chlorophyll A Enabled Photo-CRP. Chlorophyll is the most abundant natural visible-light catalyst on earth.[293] Chlorophyll A (Scheme 38), which features a substituted chlorin

Scheme 38. Employing Chlorophyll A as a Catalyst for Photo-CRP
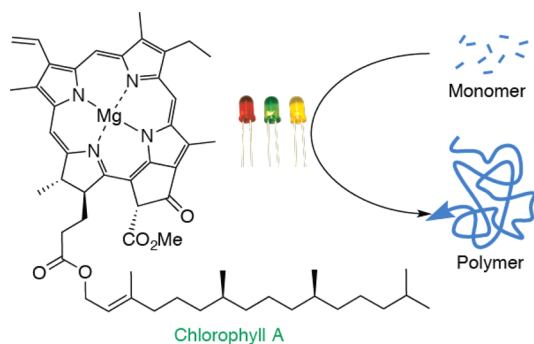
Chlorophyll A

ring, a central magnesium atom, and a hydrocarbon tail, is a specific form of chlorophyll[293] that is used by all oxygenic photosynthetic organisms. It serves as an electron donor in the electron transport chain (ETC) that drives adenosine triphosphate (ATP) synthesis. The electron transfer step from the photoexcited Chlorophyll A to a ground state acceptor is similar to the initiation of many recently reported photoredox reactions.[294] In light of the photochemistry of Chlorophyll A, this molecule has been employed in photo-CRP from thiocarbonylthio (CPADB, CDB, and CTP) and trithiocarbonate (BTPA, BSTP, and CDTPA) iniferters under irradiation with blue ($\lambda_{max} = 461$ nm) and red ($\lambda_{max} = 635$ nm) LED lights.[295] This process enables the polymerization of various acrylates and acrylamides to yield polymers with narrow molar mass distributions (ca. $Đ = 1.1–1.2$). The end-group fidelities were confirmed by NMR and UV–vis spectroscopic analysis as well as with chain extension studies. Light-controlled polymerization using on/off cycles has also been successfully demonstrated. Very recently, Boyer and

co-workers also reported the employment of a biocatalyst, Bacteriochlorophyll A, to promote photo-CRP of MMA in DMSO using near-infrared/far red light irradiation as an external trigger. Utilizing the ability of near-infrared light to penetrate through a translucent barrier the authors conducted the photo-CRP by irradiation of reaction mixtures through paper sheets of various thicknesses (0.05–0.2 mm).[296]

4.2.4. Zinc Porphyrin-Enabled Photo-CRP. In past decades porphyrin compounds have garnered interest due to their numerous applications in fields such as energy conversion, medicine, electronics, organic synthesis, and so on.[297,298] In the 1990s, metalloporphyrin catalysts were utilized to promote living anionic polymerization.[299,300] Later, the Matyjaszewski[301] and Bruns[302] groups applied iron–porphyrin complexes (based on heme) to mediate ATRP reactions. In 2015, Boyer and co-workers reported that zinc porphyrins (ZnTPP, Figure 5A) were able to promote photo-CRP from trithiocarbonate iniferters with different (methyl)acrylates and (methyl)acrylamides monomers (ca. $Đ = 1.1–1.2$).[303] Interestingly, according to the redox potential of the thiocarbonylthio (e.g., CPADB, −0.4 V versus SCE) and trithiocarbonate (e.g., BTPA, −0.6 V versus SCE) compounds tested within this study, the former should be easier to initiate via a singe-electron reduction. However, the ZnTPP-catalyzed photopolymerization with dithiobenzoate CPADB was sluggish; the photo-CRP with the trithiocarbonate BTPA was much faster. The authors suggested that this unique selectivity can be attributed to an unusual interaction between ZnTPP and the trithiocarbonate that generates a redox-active coordination environment for the redox-inert zinc center. The authors demonstrate that due to the different absorption intensities of ZnTPP within the visible-light spectrum (Figure 5B), the polymerization rates show a wavelength dependence as one would expect. As shown in Figure 5C, these reaction rates follow an order of yellow > green > orange > red and blue. In addition, this photo-CRP method can afford temporal control by switching the light on or off.

4.2.5. Photo-CRP under Metal-Free Conditions. Organic PCs have also been used as alternative options to metal-centered complexes in photo-CRP reactions of thiocarbonylthio and trithiocarbonate iniferters.

Eosin Y (Scheme 39) is a common organic dye that is usually applied in fluorescence studies. It has also been successfully utilized to mediate free radical polymerization under photochemical conditions by Bowman,[304] Pérez-Luna,[305] and others.[306] Using Eosin Y as a putative photoredox catalyst, the Boyer group realized photo-CRP of various functional monomers of glycidyl methacrylate (GMA), HEMA, OEGMA,
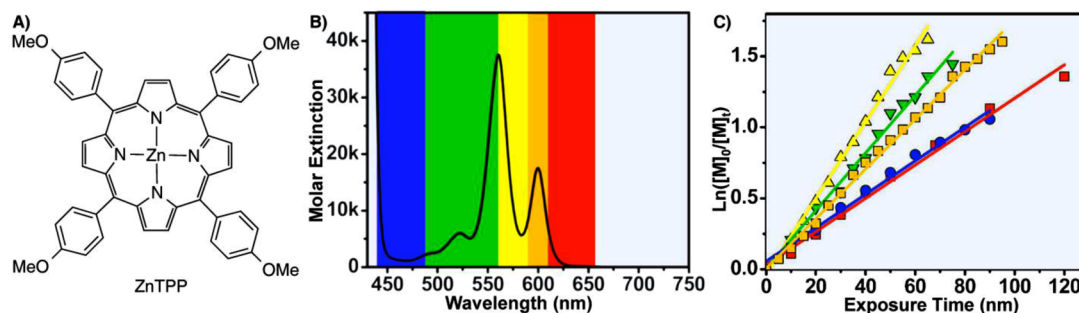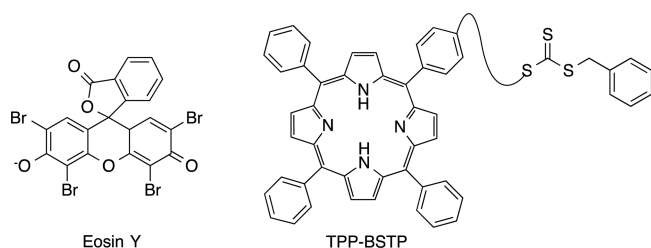

Figure 5. (A) Structure of zinc porphyrin (ZnTPP). (B) Overlap of wavelength ranges of LED lights used on the absorption spectrum of ZnTPP. (C) Plot of $\ln([M]_0/[M]_t)$ vs exposure time for polymerization under blue, green, yellow, orange, and red light using ZnTPP as the photoredox catalyst.[303] Adapted from ref 303. Copyright 2015 American Chemical Society.

Scheme 39. Structures of Photocatalysts Eosin Y and TPP-BSTP

Eosin Y   TPP-BSTP

Scheme 40. Proposed Mechanism of the Photopolymerization with DMA and Selenium Reagents

DMAEMA, pentafluorophenyl methacrylate (PFPMA), MAA, and HPMA, which yielded corresponding polymers with narrow molar mass distributions.[307] MeCN, water, DMSO, and DMF were compatible solvents with this method. Importantly, the addition of triethylamine as a sacrificing agent to reduce oxygen enables the polymerization to be conducted under an aerobic atmosphere. Moreover, the additional amine also provides a shorter induction period as demonstrated by kinetic studies.

Later, the same group designed a novel porphyrin-trithiocarbonate TPP-BSTP (Scheme 39), which acted as a light-harvesting antenna that facilitated the electron transfer process from the porphyrin to the trithiocarbonate unit under LED irradiation (green or red light sources).[308] In contrast to the reaction with both TPP and BTPA (TPP/BTPA = 2/98), the combination of TPP-BSTP and BTPA (TPP-BSTP/BTPA = 2/98) provides a much faster reaction rate (in 6 h reaction time, 3% conversion versus 56% conversion) under otherwise identical reaction conditions. Beside the target products with BTPA in their structure, unsurprisingly, polymers terminated with the TPP catalyst are also produced in this method as observed by ^{1}H NMR analysis. The authors also found that extending the connecting chain between TTP and BSTP by adding a $-CH_2CH_2-$ group resulted in a decreased reaction rate and less control over the molar mass distribution.

The Johnson group found that the organic photocatalyst PTH was also capable of promoting photo-CRP from a symmetric trithiocarbonate using a CFL bulb as a light source to yield telechelic polymers.[282] In this method, the polymerization could be efficiently switched between on and off in response to irradiation. The molar masses of the polymers increased linearly with conversion and narrow molar mass distributions were obtained ($Đ$ < 1.2). Enabled by the high fidelity of the trithiocarbonate units incorporated in the center of these polymers, chain extension reactions with different methods including the visible-light-mediated protocol using a PTH catalyst, the UV photoiniferter method, and traditional RAFT polymerization were successfully employed to prepare triblock copolymers.

4.3. Polymerization from Organoselenium Compounds

Organoselenium compounds are interesting in materials science, organic synthesis, pharmaceuticals, and photochemistry.[164] In 2004, Singh and colleagues developed a novel method to produce seleno-terminated polystyrene under visible-light photoredox conditions making use of DMA as a photocatalyst (Scheme 40).[309,310] Although the molar mass distributions for the obtained polymers were normally between 1.23 and 1.60, pseudo-first-order kinetics in monomer conversion were observed in these transformations. The seleno group on the polymeric chain end was proven by a successful chain extension under the same photopolymerization conditions (before: M_n =
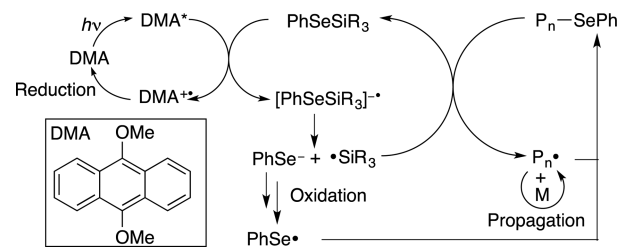
5600 g/mol, $Đ$ = 1.35; after: M_n = 17 100 g/mol, $Đ$ = 1.60). Results of on/off experiments have not been reported for this system. A tentative mechanism is illustrated in Scheme 40, the excited DMA* molecule first donates an electron to PhSeSiR$_3$, generating a radical cation species (DMA$^{+•}$) and an unstable [PhSeSiR$_3$]$^{-•}$ species, which further cleaves into a Se-centered anion and a Si-centered radical. The $^•$SiR$_3$ radical reacts with the dormant polymeric chain (P$_n$−SePh) and reinitiates the polymerization. During this process, extra ascorbic acid was added to reduce the oxidized photocatalyst; the mechanism for oxidizing a PhSe$^-$ species to a radical has not been proposed.[310]

5. APPLICATIONS

5.1. Surface Fabrication

Surface modification is a powerful approach to generate materials with novel properties.[311−313] Photopolymerization on a surface of a material is pervasively employed to achieve desired surface properties such as adhesiveness, wettability, biocompatibility, etc.[23,314,315] Additionally, photopolymerization is a versatile tool for spatially controlled surface modification. Since there have been prominent reviews on surface fabrication with photopolymerizations,[314−317] this section primarily focuses on surface fabrication with the emerging photo-CRP methods, which allow for the fabrication of surface-bound polymers with controlled structure and morphology as well as complex patterns and functionalities, all in a living fashion.

5.1.1. Surface Fabrication of Flat Materials. *5.1.1.1. Surface Grafting with a Layer/Layers of Polymer Chains. 5.1.1.1.1. Fabrication with Semipinacol-Functionalized Surfaces.* The photoreduction of aromatic ketones generates carbon-centered ketyl radicals in the presence of hydrogen donor substrates. The ketyl radicals are capable of transforming growing radical chains into dormant species, which can be reversibly activated under UV conditions, as shown in Scheme 41. Taking advantage of this process, semibenzopinacol derivatives have been connected to the surface of materials to initiate the growth of polymer brushes. Notably, the semibenzopinacol free radical can add to monomers or undergo termination via homocoupling, which usually results in limited control.

Rånby and Yang designed a surface grafting polymerization with benzophenone derivatives as photoinitiators on the surface of low-density polyethylene (LDPE) films and proposed the reinitiating ability of the semibenzopinacol end groups.[318] Samulski and co-workers also discovered that benzophenone is very effective for the grafting of styrene onto polypropylene substrates.[319]

Later, Bowman and co-workers developed a two-step sequential living graft photopolymerization method to produce hydrophilic polypropylene membranes with negatively charged

Scheme 41. Proposed Mechanism of Photografting Polymerization on a Surface Derived from Benzophenone

Photoexcitation

Photoreduction and Initiation

Propagation

Reversible Termination

Scheme 42. Proposed Mechanism of Photografting Polymerization from an Iniferter-Modified Surface

Initiation

Propagation

Reversible Termination
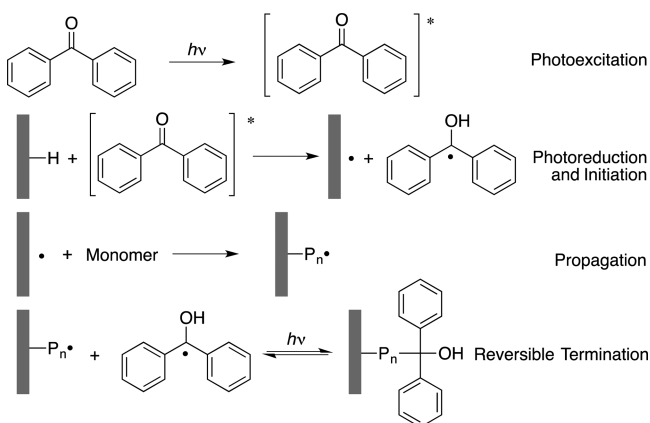
surfaces by grafting acrylic acid.[320] In the first step, a surface initiator was formed via C−H bond functionalization on a substrate under UV irradiation in the presence of benzophenone solutions. In the second step, monomers were grafted to the substrate by photopolymerization from the pretreated surface. The grafting density and graft polymer chain length could be controlled by alternating the reaction parameters. As demonstrated by kinetics studies, there was a linear relationship between the graft polymerization rate and the monomer concentration. This two-step method also showed a reaction rate 4-fold greater than the one-step method of directly grafting acrylic acid onto polypropylene membranes with benzophenone. Fréchet and co-workers evaluated the effect of both methods on the performance of photografting hydrophilic monomers on macroporous polymer monoliths.[321]

Yang and co-workers developed a surface grafting polymerization induced by visible-light irradiation at room temperature.[322] In this approach, isopropyl thioxanthone is first reduced under UV light and subsequently coupled onto low-density polyethylene films. Both the surface grafting chain length versus conversion of monomer and the grafting polymerization rate versus concentration of monomer showed a linear dependence, which are in accord with the characteristics of a photo-CRP. They also introduced different graft compositions with desired functions such as thermosensitive or pH-switching properties onto polymeric membranes.

5.1.1.1.2. Fabrication with Thiocarbonylthio-Functionalized Surfaces. On the basis of the photoiniferter strategy developed by Otsu and co-workers, Hadziioannou and co-workers explored photografting polymerization from monolayers of thiocarbonylthio inferters on the surface of silicon wafers or glass slides[323] as shown in Scheme 42. This method can not only change the hydrophilicity of the surface by polymerizing different monomers but it can also regulate the layer thickness (up to ∼100 nm) by managing reaction parameters. Importantly, single-layer grafted block copolymers are easily achieved by subsequent photopolymerizations of different monomers. The combination of the photoiniferter with surface grafting opens new ways to modify the properties of substrates and provides useful access to various functional surfaces.

Bowman and colleagues investigated the grafting efficiency and graft conversion of EGMA on the surface of dithiocarbamate-containing polymer substrates.[324] A novel methylacrylic monomer iniferter was chemically tethered to the growing polymeric backbone, enabling the production of photopattern-

able grafted polymer networks.[325,326] Nishida, Endo, and co-workers investigated a graft polymerization of vinyl monomers on a photoiniferter precoated solid material under UV irra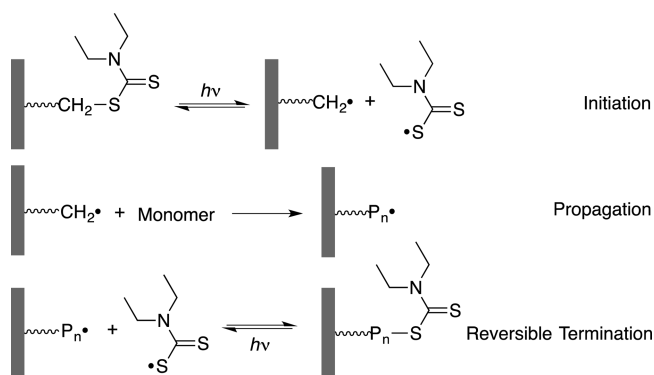diation; controlled radical polymerization of vaporized monomers on the solid surface was achieved.[327] By immobilizing photoiniferters on polypropylene microfiltration membranes, the Ulbricht group achieved surface-selective graft functionalization,[328] promoting the preparation of advanced macroporous membranes with a wide range of functional properties.

Metters and colleagues systematically studied the kinetics of photopolymerization from a solid surface precoated with photoiniferers.[329,330] While the initial rate of the polymerization approximately followed a first-order dependence on monomer concentration, the reaction rate decreased with reaction time, indicating the presence of termination reactions at high conversions of monomers.[329] By comparing model predictions with experimental data, they suggested that bimolecular termination is the dominant termination mechanism. Moreover, they evaluated the effect of incident light intensity and concentration of an added deactivating compound (tetraethylthiuram disulfide (TED)) on the polymerization kinetics.[330] In accord with the model predictions, the experimental results indicate that the maximum thickness of the poly(MMA) layers improved as the concentration of TED increased and as the irradiation intensity decreased. Kilbey and co-workers revealed that the polymer layers prepared in the presence of TED more readily formed surface-tethered block copolymers upon reinitiation under light compared with polymer layers produced without TED.[331]

With photoiniferter-immobilized Si/SiO₂ substrates, Spencer and co-workers developed aqueous-phase fabrication of surface-bonded poly(MMA) brushes with a UV-LED as a light source at room temperature.[332] The poly(MMA) layer could lubricate the solid surface and reduce sliding friction in an aqueous environment. Facilitated by a similar strategy, these authors also tethered poly(acrylamide) brushes onto solid surfaces with up to 1 μm thickness in water.[333] Adding trace amounts of the cross-linker bis(acrylamide) in the presence of monomers afforded covalently cross-linked hydrogel brushes, which strongly influenced both bulk and interfacial properties of the polymer films. In agreement with theoretical studies, the incorporation of cross-linked networks resulted in a substantial increase of film wettability with water as the polymer-brush conformational freedom decreased. Recently, Spencer, Benetti, and co-workers reported the synthesis of surface-grafted polymeric films featuring graded physical properties.[334] As illustrated in Scheme 43, two-layer films comprising either a

Scheme 43. Synthetic Route to Stratified PAAm Films through Sequential Iniferter-Mediated Photopolymerization[334] [a]
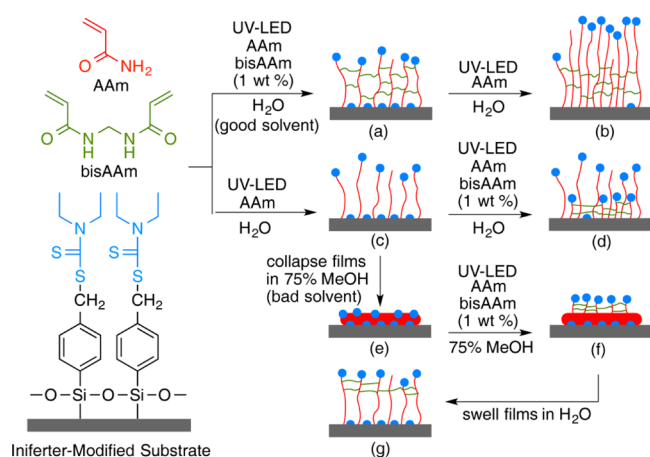
[a]Adapted from ref 334. Copyright 2014 Wiley-VCH.

"free" polymer brush supporting a cross-linked brush-hydrogel or a gel supporting a "free" polymer brush were prepared by employing different sequences of photoiniferter-mediated photografting polymerization. This method enabled the incorporation of a predetermined amount of cross-linked brush-hydrogel at specific depths within the grafted layers, offering novel access to films with adjustable and gradable bulk physical and interfacial properties.

In light of the strong interaction between gold and sulfur, Vancso and co-workers tethered dithiocarbamate photoiniferters on a gold surface via thiolate anchors.[335] With a stepwise process involving (1) grafting of poly(MMA) brush layers from the iniferters, (2) functionalization with the cell-adhesive arginine-glycine-aspartic acid (RGD) motif, and (3) extension of the brush by reinitiating the polymerization to obtain an additional layer of polymers, the peptide-functionalized segments were successfully buried inside the brush structure. Immunofluorescence studies indicated that there is a direct correlation between the vertical position of the RGD motif and the cell morphology.[336] Also on a gold surface, Jiang and co-workers photografted zwitterionic carboxybetaine polymer thin films with uniform and controlled thickness at high surface packing densities.[337] Related evaluation with a surface plasmon resonance biosensor demonstrated the protein-resistant properties of grafted films; they displayed ultralow fouling to undiluted human blood plasma. Antibody immobilization enabled the detection of the corresponding antigen directly from undiluted human plasma down to ~1 ng/mL. Employing amino acid (e.g., aspartic acid and glutamic acid) derivatives as vinyl monomers, Liu and co-workers synthesized a variety of zwitterionic polymers grafted on gold surfaces, providing films with ultralow adsorptions from undiluted human serum and plasma.[338−340]

Qiao and colleagues developed a thin film (ca. 5 nm) fabrication technology based on the continuous assembly of polymers from dithiocarbamates on the surface of Si wafers.[341] In this method, macromolecules substituted with acrylates were used as both monomers and cross-linkers, allowing the production of cross-linked and surface-confined films in one step.

Finally, Yin and co-workers prepared two-layer polymer brushes possessing dual functions on photoiniferter-modified cycloolefin polymer (COP) surfaces.[342] By combining a nonfouling poly(EGMEA) bottom layer with a poly(AA) top layer for antibody loading on a COP surface, this technique improved the antigen detection efficiency and suppressed fibrinogen interference on antigen recognition.

5.1.1.1.3. Fabrication with Metal- or Metalloid-Mediated Photopolymerization. From a bromo-isobutyryl bromide-functionalized cellulose surface, photo-ATRP has been employed by Carlmark and co-workers to fabricate brushes from MA and DEGA monomers.[343] They observed that the polymerization on the surface proceeded with different kinetics and resulted in broader molar mass distribution compared to polymerization with a free initiator.

Inspired by recent studies of Hawker and Fors, PCs have been applied to surface grafting.[222] Yang and colleagues combined $Ir(ppy)_3$-catalyzed surface-grafting polymerization and thiol–yne click reactions under visible-light irradiation and synthesized poly(propargyl methacrylate) films on LDPE substrates containing reactive thiol groups.[344] Meng and co-workers applied visible-light-controlled photoredox catalysis to polymerize a series of hydrophilic and polar methyl acrylates on a microporous polypropylene membrane surface.[345] The dormant chain ends of grafted polymers could be reactivated to produce diblock copolymer brushes.

Wu and co-workers demonstrated the use of $Mn_2(CO)_{10}$ for surface grafting polymerization on Au surfaces with a visible-light source.[346,347] Ellipsometry analysis indicated that the formation of poly(NiPAAm) films of up to 200 nm in thickness could be achieved in about 10 min at room temperature. Later, they applied the same method to modify the surface of PDMS, which is usually not trivial due to the chemical inertness of the substrate. With a two-step procedure, the PDMS surface could be functionalized with a variety of polymers, such as poly(TFEMA), poly(NiPAAm), poly(AA), and poly(VAc).

Tsujii and co-workers synthesized brushes of water-soluble polymers (poly(HEA) and poly(PEGA)) on silicon wafers by organotellurium-mediated photopolymerization.[158] Since the graft polymers have no charged groups, adding extra salt had little effect on their swollen structures and frictional properties. In addition, good lubrication was realized for the concentrated polymer brushes of poly(PEGA) without the help of electrostatic interactions.

5.1.1.2. Fabrication with Designed Patterns. The generation of patterned polymer films with controlled nano/microstructure has witnessed rapid development in the past decade.[348−350] Patterning polymer films on solid surfaces is critical for many important applications such as the manufacturing of microchips and microelectromechanical devices as well as the preparation of substrates for cell growth and adhesion.[348−350] CRP methods are typically able to produce polymer patterns with high fidelity, high grafting densities, diverse functionalities, and good mechanical properties, and they are often compatible with other patterning techniques.[349,351,352] The recent advances in photo-CRP have provided considerable advantages for preparing complex chemical patterns in a spatially and/or temporally controlled fashion, which is of paramount importance for developing new applications.

With preprepared semibenzopinacol-functionalized macroporous polymer monoliths, the Fréchet group developed a patternable photografting technique by first grafting a hydrophilic surface within the monolith that was subsequently patterned with a layer of reactive polymer chains and immobilized with green fluorescent protein, which enabled microanalytical devices.[321]

Metters and colleagues reported the creation of surfaces exhibiting position-dependent chain density of a functional anionic monomer in a continuous manner.[353] These surfaces were functionalized with cell-adhesive RGD peptide gradients, providing specific cell adhesion in a spatially defined manner across a macroscopic surface. Cell adhesion increased in the direction of increasing RGD density.

Anseth and co-workers demonstrated the application of photografting of polyacrylates from polymer substrates to produce chemically and biologically active surfaces that are responsive to cells (Figure 6).[354] While grafting poly(ethylene
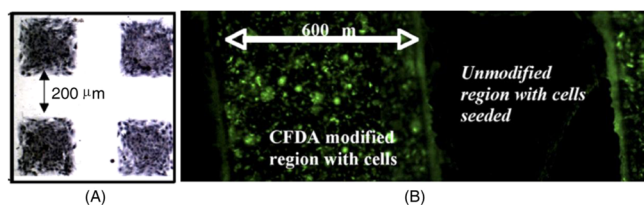

Figure 6. (A) 3T3 fibroblasts seed at 20 000 cells/cm² onto PEG-grafted polymer substrate surfaces to demonstrate spatial control over cell adhesion. Hematoxylin staining is used in this image where white areas represent PEG-modified regions and purple areas are regions with stained, adherent cells. (B) 3T3 fibroblasts seed at 20 000 cells/cm² onto CFDA-modified surfaces. Fluorescence only occurs in the cells that are seeded on the 400 µm CFDA-modified stripes. Unmodified regions with seeded cells remain nonfluorescent.[354] Adapted from ref 354. Copyright 2007 Elsevier.

glycol) acrylate can inhibit cell adhesion thanks to its inherent hydrophilic properties, NIH 3T3 fibroblast (American Type Tissue Collection) adhesion selectively takes place in spatially grafted regions, offering a cell differentiation technique. In addition, methacrylated carboxyfluorescein diacetate (CFDA) functionalities were photografted onto cell-adhesive substrates to demonstrate cellular sensing in specific patterned regions on polymer surfaces.

Vancso and co-workers reported the efficient synthesis of tunable temperature-responsive poly(NiPAAm) brushes.[355] The temperature-induced morphology and adherence changes of the microscale-patterned gold surfaces were measured with in-situ atomic force microscopy (AFM) near the lower critical solution temperature (LCST) of poly(NiPAAm) in aqueous environments, affording a "smart" thermoresponsive polymeric surface.

Recently, Hawker, Poelma, and co-workers demonstrated an excellent example of temporally and spatially controlled brush formation with their Ir(ppy)₃-catalyzed photo-CRP.[356] This surface fabrication technique has advantages that include the following: (1) initiating species remain intact in unexposed regions and thus they can be utilized in further transformations; (2) neutral density filters can be used to regulate the intensity of incident light, which is directly correlated with the polymerization kinetics on a surface, thus allowing for the preparation of gradient brushes and arbitrary three-dimensional (3D) structures in one simple step over a large area; (3) the initiating activity can be kept after the initial polymerization step, enabling patterning of block copolymer brushes with different chemical functionalities and surface topographies. The micrograph in Figure 7A shows clear patterning of the poly(MMA) brushes obtained under irradiation through a photomask containing rectangular patterns. The authors suggest that the short excited state lifetime of the Ir(ppy)₃ catalyst (ca. 50 ns) is the key to minimizing the influence of diffusion on the resolution for this system. Enabled
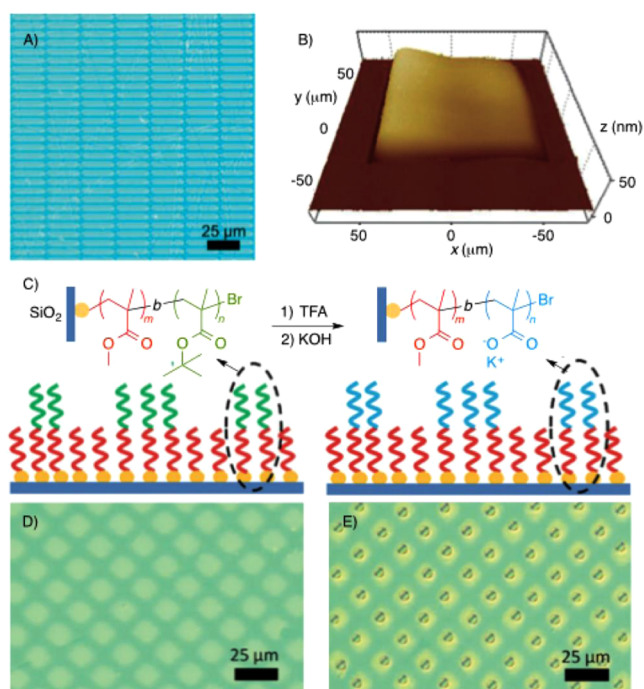
Figure 7. (A) Optical microscopy image of patterned poly(MMA) brushes obtained using a negative photomask with 2.5 mm by 25 mm rectangles. (B) 3D AFM image of nanoscale-inclined plane. (C) Schematic of patterned block copolymer brushes and conversion of poly(MMA)-*block*-poly(tBMA) to poly(MMA)-*block*-ploy(MAA). (D) Optical micrograph of poly(MMA)-*block*-poly(tBMA) brushes patterned from a uniform poly(MMA) initiating layer. (E) Selective wetting of poly(MMA)-*block*-poly(MAA) regions in D after exposure to water vapor.[356] Adapted from ref 356. Copyright 2013 Wiley-VCH.

by the outstanding three-dimensional spatial control of this method, a variety of surface features including inclined planes, microprisms, gradients, and arrays of microlenses were readily prepared with a grayscale lithography mask. Figure 7B shows a 3D AFM image of an inclined plane prepared from a uniform initiating layer in a single step. In addition, spatially defined block copolymer brushes were prepared by efficient reinitiation of the active alkyl bromide chain ends on the first poly(MMA) layer. As shown in Figure 7C−E, patterned block copolymer brushes are selectively converted from hydrophobic to hydrophilic, demonstrating that variations of surface properties can be efficiently achieved. Hawker, Fors, and co-workers also applied this photoredox catalysis system to manufacture well-defined chemically differentiated monolayers and complex nonlinear chemical gradients with multiple functionalities.[357]

With a newly designed iridium complex, Lalevée, Gigmes, and co-workers developed radical and cationic polymerizations from surfaces. In this system, surface modification was conducted by direct writing using a visible-light laser. As shown in Figure 8A, with a green Nd:YAg laser emitting at 532 nm, micropatterns with controlled heights were obtained by varying the laser power in a constant irradiation time. A main advantage of laser writing is the ability to arbitrarily generate microstructures over the sample surface. To demonstrate this potential, a logo (Figure 8B) and regular grids were produced by polymerization on the polymer surface. In these studies, the height of the structures is constantly maintained, demonstrating excellent control.[262]

Zhou and co-workers reported the application of photo-ATRP with Cu to produce various patterned surfaces of brushes in the
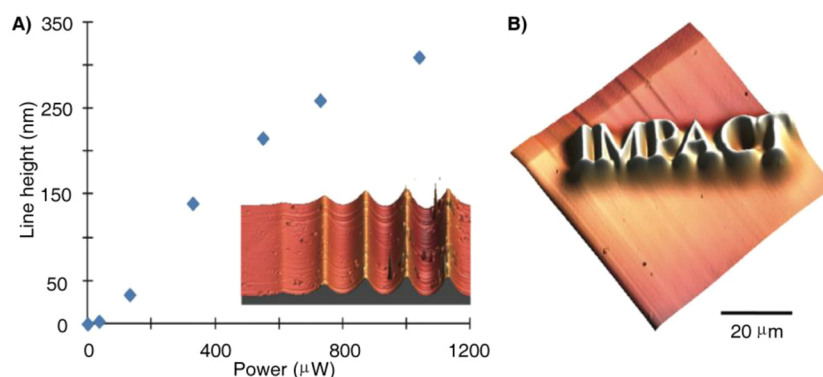
Figure 8. Laser direct-write using a Nd:Yag microlaser (532 nm, 0.6 ns) with ×40 microscope objective: (A) Control of line height with laser power for 5 ms irradiation (3D image in inset); (B) AFM images of complex microstructures, e.g., logo created with 130 μW, 10 ms.[262] Reproduced from ref 262. Copyright 2015 Royal Society of Chemistry.

presence of ruthenium-complex-sensitized titanium oxide nano-particles.[239] Patterns with sub-50 nm resolution were obtained with a simulated sunlight source in their study.

The Yang group prepared poly(TFEMA) grafted layers with different surface morphologies on semibenzopinacol-modified LDPE surfaces.[358] Their results indicated that the incorporation of micro- and nanoscale hierarchical structures altered the surface roughness, resulting in improved hydrophobicity of the material. On the basis of similar photochemistry, Yang and others developed a strategy to prepare 3D protein micropatterns with an antifouling background and a high protein capacity.[359] A two-step grafting process that involves growth of poly(EGMMA) and a mixture of GMA and poly(ethylene glycol) diacrylate (PEGDA) was employed to afford height-controllable cylinder microarrays, which provided a larger protein loading to enhance the signal intensity. The patterns were used to test the immunoglobulin G concentration in human serum, suggesting potential applications in biomedical diagnosis.

Soppera and colleagues employed photopolymerization from an alkoxyamine (see section 3.2) to fabricate functional micropatterns by UV mask lithography.[360] Taking advantage of the active chain ends that remained in polymers from the first grafting step, vertical spatial control from tens of nanometers to a few micrometers was achieved to generate covalently bonded hydrophilic/hydrophobic micropatterns and luminescent surfaces.

5.1.1.3. Surface Grafting with Particles. On the basis of the success of the two-step surface photografting polymerization from benzophenone derivatives, the Yang group investigated the use of conventional emulsions and microemulsions as grafting media.[361−363] Solid polymer nanoparticles with uniform particle size distributions were successfully immobilized on the surface of polypropylene films, as confirmed by AFM and scanning electron microscopy (SEM) images. The dormant semibenzopinacol functionalities on the surface of these particles provided opportunities to graft multilayer nanoparticles.[361] With the development of a novel technique they called "in-situ polymerization stringed assembly", microscale spherical particles were grown on the surfaces of organic substrates with microemulsion as the photografting medium.[363]

5.1.2. Surface Fabrication of Particles. From dithiocarbamate photoiniferter coated polymer particles, Kawaguchi and Tsuji prepared different types of temperature-sensitive hairy particles using NiPAAm and AA monomers.[364] When block polymers are used as hairy brushes, the sequence of each block is found to be a key factor for controlling the temperature

responsiveness of the particles. These particles showed responses to pH and ionic strength. Meanwhile, interesting properties such as electrophoretic mobility, adsorption of dye molecules, as well as swelling/deswelling were also investigated in this work. The same photochemistry has also been used by Liu and co-workers to fabricate polyacrylamide-grafted cross-linked poly(vinyl chloride) beads, which are good adsorbents for Hg(II) ion removal from aqueous solutions.[365] Derouet and Thuc developed a procedure to prepare poly(MMA)-grafted silica microparticles.[366] On the basis of a combination of diazonium salt chemistry and the iniferter protocol, Sicard and colleagues obtained aluminum nanoparticles with strongly anchored polymer shells.[367] The thickness of the polymer shell reached 3−4 nm, which provided an organic coating that protected the metallic core from oxidation. With spherical colloidal core particles prepared in different sizes, Ishizu and co-workers applied copper-mediated photopolymerization from dithiocarbamates to graft polymer brushes.[368,369]

Using TiO$_2$ nanoparticles as photoactive materials to generate Cu(I) species from a Cu(II) precursor, Zhou and co-workers reported a UV-light-promoted photo-ATRP reaction from Cu^{II}/ L and applied this polymerization to yield polymer brushes on the surface of TiO$_2$ particles with controllable thickness, composition, and architecture.[240] Jain and others performed polymerizations from the surface of titania/reduced graphene oxide (TiO$_2$/rGO) nanocomposites using a visible-light controlled photo-ATRP reaction.[370]

With monomers of acrylamide, acrylic acid, and maleic anhydride, the Albertsson group developed a surface grafting from technique to prepare polylactide particle substrates modified with different chemical layers from semibenzopinacol-functionalized surfaces.[371] Although polylactide particles are directly used in the two-step fabrication, their 3D shape and molecular weights are not changed after grafting, indicating the nondestructive nature of this technique.

5.2. Particle Preparation

Three-dimensional micro- and nanoparticles with good mechanical properties, high water content, biocompatibility, or other interesting characteristics are of fundamental and practical importance for applications in many fields, such as drug delivery, biotechnology, electronics, nonlinear-optical devices, biomedical implants, catalysis, etc.[372−376] Photo-CRP provides another promising approach to prepare these small particles with complex chemical structures and uniform sizes.

On the basis of the properties of semibenzopinacol free radicals, Yang and colleagues reported the synthesis of various unique particles including hollow supramolecular polymer particles assembled by nanounits and linkers,[377] core—shell nanoparticles based on vulcanized acrylonitrile butadiene rubber latex,[378] microscale Janus particles facilitated by selective surface grafting polymerizations and couplings,[379] soft hydrogel nano-particles with poly(NiPAAm) hairs,[380] as well as anisotropic particles with tunable morphology, dimensions, and surface roughness.[381]

Yoshida applied the photochemistry of nitroxide compounds (see section 3.2) to synthesize micrometer-scale spherical vesicles by adjusting the ratio of alkyl methacrylates and MAA.[382−384] When the hydrophobic—hydrophilic balance of the copolymer is manipulated through the polymerization, materials with different morphologies are obtained.

Winnik and co-workers synthesized poly(MMA) micro-particles with a narrow size distribution by dispersion photo-polymerization with trithiocarbonate DDMAT as a photo-iniferter.[385] Under UV irradiation conditions, poly(MMA) microspheres were obtained with variation in the particle diameter less than 3% using a macromonomer PEGMA as the stabilizer. Functional microspheres with carboxy-functional groups were prepared via a two-stage (seeded) polymerization with MAA as a comonomer in the second stage. These functionalized particles were effective substrates for attaching proteins such as bovine serum albumin (BSA) and IgG immunoglobulins. They also demonstrated that nearly 10^4 IgGs could be detected per PMMA microbead with the dye-labeled secondary antibody.

With the employment of Ru(bpy)$_3$Cl$_2$-catalyzed dispersion polymerization under visible-light photoredox conditions, the Boyer group reported the chain extension of poly(OEGMA) with benzyl methacrylate to afford in-situ self-assembled polymeric nanoparticles with various morphologies, including spherical micelles, worm-like micelles, and vesicles.[386] They also demonstrated temporal control over the polymerization process by modulating the light on and off as measured with online FTNIR spectroscopy.

The Qiao group demonstrated the one-pot synthesis of core cross-linked star polymer nanoparticles under visible-light irradiation using a trithiocarbonate iniferter.[387] This reaction system achieves the simple synthesis of star polymers with high end-group fidelity at high monomer conversions. The integrity of the chain ends kept in the star structures was evidenced by the efficient reinitiation from core-localized trithiocarbonate moi-eties to produce pseudomiktoarm star polymers with increased molecular weights.

5.3. Photoresponsive Gels

Self-healing materials that can repair internal and external damage are attractive for numerous applications.[388−391] Typical approaches to access mechanically robust yet self-healing gel materials rely on introducing bonds that become dynamic in response to external stimuli, such as photo, thermal, and chemical stimulation.[388−391] Taking advantage of the photochemical properties of trithiocarbonates, Matyjaszewski and co-workers demonstrated an elegant example of repeatable photoinduced self-healing of covalently cross-linked polymers (Scheme 44).[392] As described in section 3, under UV irradiation the carbon—sulfur bond of suitable trithiocarbonate groups can undergo homolytic cleavage to generate sulfur-centered radicals and carbon-centered radicals that can further react with other

Scheme 44. Model Self-Healing Reactions by UV Irradiation[392] ^{a}
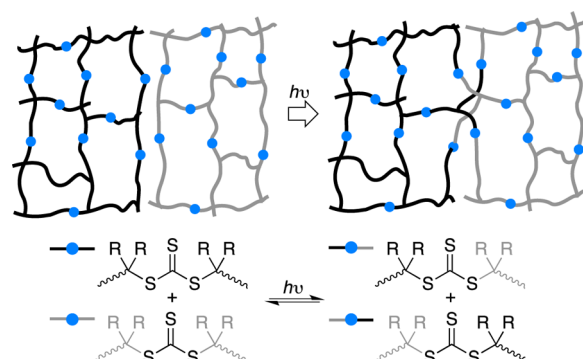
^{a}Adapted from ref 392. Copyright 2011 Wiley-VCH.

trithiocarbonate functionalities via degenerative chain transfer to produce new carbon—sulfur covalent bonds. Self-healing is achieved by exchange of such functionalities at the interface where two cut pieces are placed in contact. The tensile modulus obtained after healing was almost the same as that of an original sample under solution conditions, indicating an efficient photostimulated macroscopic self-healing. Additionally, self-healing in the bulk state and for completely separated fragments were all successfully demonstrated. The photoresponsive reshuffling capacity of trithiocarbonate units was confirmed with model reactions between different trithiocarbonates under UV irradiation conditions.

Later, the same group applied this strategy to produce self-healing materials linked via thiuram disulfide units.[393] This modification allowed for the transformation to be stimulated by visible-light irradiation at ambient conditions in the presence of air. Self-healing of the polymeric networks was achieved through the reorganization of thiuram disulfide units initiated by sulfur-centered radicals formed from photolysis. The authors also disclosed that the healing efficiency depends on the ratio of reactive to permanent units in the networks. While incorporating more thiuram disulfide units in the network accelerates the self-healing process, decreased mechanical strength of the resulting material is observed.

The swelling nature of cross-linked polymers in different solvents is a unique feature of polymeric gels and is directly affected by the network composition and structure.[394,395] Investigation of efficient methods to modify network structure can benefit the development of functional materials including self-healing and shape-memory polymers.[391,396] Taking advant-age of trithiocarbonate units again, Matyjaszewski and co-workers achieved variation of the network mesh size of chemical gels by reshuffling reactions under UV irradiation.[397] In these experiments, the gels were treated with either good solvent or nonsolvent and subsequently exposed to external light stimulus to trigger the reconstruction of networks. As a result, the degree of swelling and network size increased in the presence of good solvents and decreased in the presence of nonsolvents, respectively. Since the networks do not degrade upon irradiation, such changes to the network properties are likely the result of formation or loss of elastically inactive "loop" defects.[398−400]

Light has also been employed as a trigger for the growth of polymer chains within chemical gels, thus leading to a direct increase in mesh size.[401] After developing a photo-CRP from a bis-norbornene-substituted trithiocarbonate iniferter (see sec-

tion 3.1.1 for details), Johnson and colleagues synthesized norbornene-telechelic NiPAAm polymers and connected them with tris-tetrazine cross-linkers via inverse-electron demand Diels−Alder cycloaddition to provide gels that possessed trithiocarbonate moieties in the center of each network chain, as illustrated in Scheme 45.[66] Exposing the gels to sunlight in the

Scheme 45. End-Linking PNiPAAm with a Tris-Tetrazine To Give a Gel Network[66] [a]
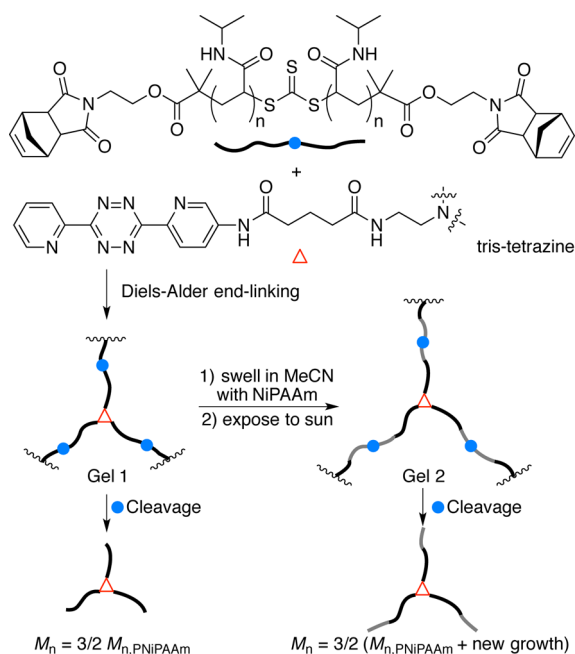
[a]Adapted from ref 66. Copyright 2013 Wiley-VCH.

presence of monomer solutions led to an increase in the average molecular weight between cross-links via direct extension of the network chains. The trithiocarbonate groups were cleaved by aminolysis, and the extent of photogrowth was quantified by GPC. This "photo-growth" process represents a novel strategy to prepare photoresponsive polymeric networks by photo-CRP. It also provides access to soft materials with both mechanical and chemical 3D gradients.

5.4. Novel Techniques Applied To Perform Photo-CRP

In many photopolymerization processes, although stronger light intensity increases the reaction rate, deleterious effects on molar mass distribution are observed when conversions reach higher levels.[45,54,65,71,72] To afford excellent control of well-defined

polymers with narrow molar mass distribution, low light intensity and long reaction times are normally required. However, when large-scale synthesis of polymers via photo-CRP is desired, it is difficult to achieve uniform irradiation.[402,403] Therefore, in contrast to thermal polymerizations, photopolymerizations typically require new equipment for different reaction scales to ensure uniform and sufficient irradiations. Therefore, a simple, scalable photopolymerization technique that could provide precise control over molecular weight would be a significant advance in the utility of photopolymerizations.

Recently, continuous-flow processes have increasingly received significant attention from both academia and industry.[404−408] This technique has been recognized as a practical and robust way to produce small molecules[404−408] as well as polymers[409−413] due to its advantages of easy scale up, excellent mass and heat transfer, automated-manufacturing prospects, and enhanced safety. Notably, compared to photochemical reactions conducted under batch conditions, flow techniques are capable of enabling much more uniform irradiation of the reaction solution due to their high surface-to-volume ratios of microchannels within continuous-flow reactors (Figure 9).[414,415]

Junkers and co-workers reported a photoredox copper-mediated radical polymerization of MA using $CuBr_2$ and Me_6TREN as a catalyst/ligand pair in 2014 (see section 4.1.1 for details of this polymerization in batch processes).[416] In their experiments, a tubular milliscale reactor made with PFA tubings and a glass-chip microreactor were investigated under flow conditions. Excellent control over the polymerization was observed under both flow conditions. Reactions followed pseudo-first-order kinetics. In contrast with reactions carried out under batch conditions, the flow techniques allowed much faster conversions for this photo-ATRP reaction, enabling nearly 90% conversion within 20 min of reaction residence time. The highest molecular weight of poly(MA) synthesized by this method was 9800 Da. Starting from poly(MA) (M_n = 3100 g/mol, Đ = 1.10), poly(MA)-*block*-poly(*n*BA) polymers (M_n = 4990 g/mol, Đ = 1.16, 51% conversion of *n*BA) were prepared in the microflow reactor.

Later, Detrembleur, Junkers, and co-workers applied microflow techniques to conduct cobalt-mediated radical polymerization under UV irradiation conditions (see section 3.4 of this review for details of this polymerization in batch processes).[417] In comparison to the related cobalt-mediated transformation under batch conditions, a faster reaction rate for the polymerization of vinyl acetate is achieved with the flow method. However, when the conversion of VAc reached up to 53%, poly(VAc) was produced in a molar mass of 17.5 kDa with an increased
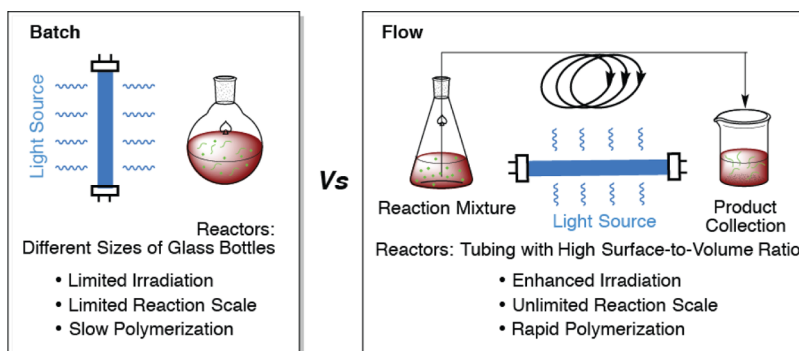

Figure 9. Photopolymerization under batch or flow conditions.

dispersity ($Đ = 1.50$), and slight shoulder peaks were observed in the GPC traces. The copolymerization of VAc and α-olefins is usually slow due to the formation of a more stable C–Co bond at the polymer chain end when the α-olefin unit is last incorporated. Facilitated by the flow technique, they also developed a rapid copolymerization of VAC and α-olefin, containing up to 50 mol % of the 1-octene monomer.

In 2015, Johnson and Chen developed a simple, scalable, and efficient continuous-flow technique for photo-CRP from a trithiocarbonate iniferter (see section 3.1.1 for details of this polymerization in batch processes), representing the first example of metal-free and switchable photopolymerization accomplished under flow conditions.[418] This new method enabled the accelerated preparation of high molecular weight polymers (up to 109k) that had not been achieved before with this photo-CRP. Notably, as shown in Figure 10, to access
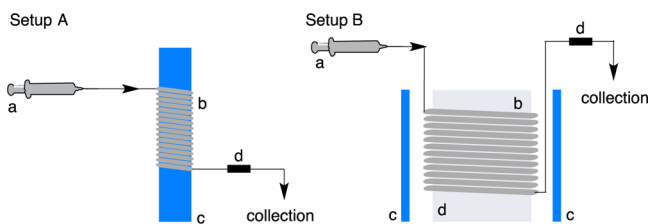

Figure 10. Continuous-flow setup for photo-CRP. For both setups: (a) injection syringe; (b) Halar tubing reactor; (c) UV lamp light source; (d) back pressure regulator.[418] Adapted from ref 418. Copyright 2015 The Royal Society of Chemistry.

control over the molar mass distribution, two flow setups were designed to achieve photo-CRPs with different monomer/iniferter ratios. In setup A, the reaction solution was injected into a reactor made of Halar tubing, which was wrapped around a UV lamp (352 nm). In setup B, the tubing reactor was wrapped around a glass bottle, which was placed in the middle of a chamber surrounded by a cycle of UV lambs. A longer distance from the light sources to the reactor, compared with that of setup A, afforded a decreased light intensity in setup B. With these designs, photopolymerizations with a wide ratio range of iniferter/monomer (from 1/250 to 1/2000) were investigated, enabling the efficient synthesis of polyacrylates and polyacrylamides with precise control (e.g., poly(DMA), isolated in 2.95 g, M_n = 24 900 g/mol, $Đ$ = 1.11, 87% conversion in 40 min residence time). In addition, on/off experiments were conducted to verify that the polymer produced via photo-CRP could be reactivated through external light activation with new designed setups as shown in Figure 11A. In this setup, sections of the reactor tubing were covered to simulate the light being off. Furthermore, collection valves were installed at various points along the reactor tubing to allow for sample isolation. When the flow reaction started, only one outlet from "a" to "g" was kept open for sample collection. Cycles of on/off experiments confirmed the capability of controlling the photopolymerization with light as an external stimulus. Importantly, this design also potentially streamlines the synthesis of high-quality polymers with a variety of molecular weights by collecting at different outlets of the same continuous-flow setup.

Recently, Hawker, Poelma, and coworkers reported the continuous-flow synthesis of poly(MMA) using their Ir-catalyzed photoredox CRP (see section 4.1.2 for details of this polymerization in batch processes).[419] During these studies, they tested different tubing materials and found that Halar, with its
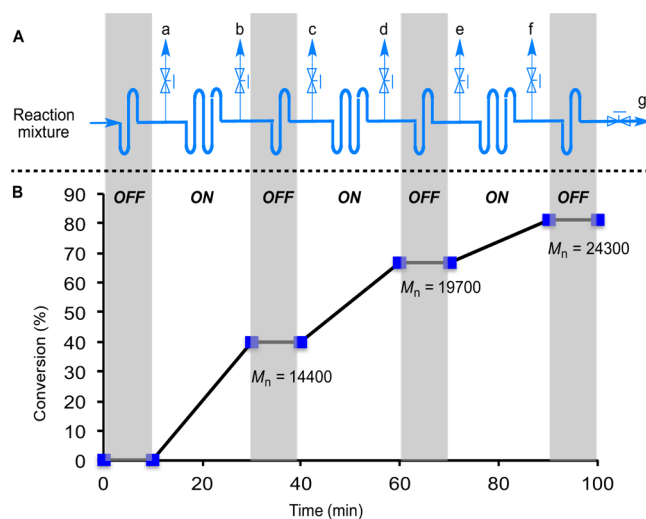
Figure 11. On/off experiments for photo-CRP under switchable flow conditions. Adapted from ref 415. Copyright 2015 The Royal Society of Chemistry.

low permeability to oxygen, was critical for the success of the photopolymerization. First-order kinetics were observed under both batch and flow conditions. Compared with the polymerization of the same monomer in batch, a rate increase of at least 50% was observed under continuous-flow conditions.

6. CONCLUSIONS

Although photo-CRP has been developed for more than 30 years, the recent explosion of interest in this topic has led to exciting advances. Now, photo-CRP methods exist for the synthesis of polymers and materials with spatiotemporal control and unprecedented levels of functionality. Light is an attractive and practical external stimulus to achieve precise control in photo-CRP systems. The continually improved understanding of photopolymerization mechanisms facilitates these rapid advancements, and inspiration from photosynthesis, small-molecule photoredox catalysis, and organometallic chemistry continues to impact this field. Thus, it is reasonable to anticipate more progress in the field of photo-CRP in upcoming years.

Looking toward the future, light-controlled synthesis of complex polymers with precise molar mass, well-defined primary structure (sequence and tacticity[420−422]), and diverse composition will continue to be a major goal in polymer science. These endeavors will inspire new synthetic tactics and strategies and also guide the development of novel materials for modern applications. Furthermore, the development of transformations that are mediated by external stimuli will continue to increase in sophistication. For example, many existing processes involve either on or off states, but one can imagine systems that could be switched in more sophisticated ways, e.g., between types of polymerization mechanism, between which monomer is incorporated into a growing chain, between distinct polymer architectures, etc.[423] Some challenges cannot be underestimated. For example, as discussed above, scaling up photopolymerization is often limited by irradiation efficiency and cost, and although continuous-flow technology has been developed to address the former issue, it is only applicable to monomers and polymers with suitable solubility. We anticipate significant engineering advances in continuous flow methods that will facilitate scalable photo-CRP. As is the general case with all radical addition reactions, new approaches to achieve stereoselective olefin

addition in photo-CRP reactions will be sought. Also, photo-CRP reactions that make use of longer wavelength light sources (i.e., infrared light) will continue to be pursued.[296] Finally, while current photo-CRP methods rely on the direct photoexcitation of an iniferter or an initiator (intramolecular photochemical process) or an electron transfer from/to a photoactivated catalyst (photoredox process), proton-coupled electron transfer and/or intermolecular energy transfer processes have not yet been harnessed to induce/catalyze photo-CRP. In the latter case, one can imagine the development of photo-CRP reactions based on Förster or Dexter energy transfer (using dyes or sensitizers as photocatalysts) or even more complex singlet fission or triplet−triplet annihilation processes.

Given the numerous commercial applications of traditional photopolymerization and the resulting infrastructure for conducting such reactions, the barrier to adoption of novel photo-CRP methods in applications should be low. With rational design, researchers will be able to design advanced polymers with well-defined and unprecedented complexities at reasonable costs. As described in this review, photo-CRP has already proven useful for surface processing, particle fabrication, and photo-responsive gel formation, etc. Such accomplishments represent only a starting point from which numerous potential applications can be envisioned. Advanced materials with "smart" properties powered by photo-CRP could impact countless areas of materials science including controlled surface transformation, tunable self-healing, and switchable patterning to name a few.

AUTHOR INFORMATION

Corresponding Author
*E-mail: jaj2109@mit.edu.

Author Contributions
§M.C. and M.Z. contributed equally to this work.

Notes
The authors declare no competing financial interest.

Biographies

Mao Chen grew up in Chongqing, a city famous for hot pot in China. After receiving his B.S. degree at Wuhan University, he undertook his Ph.D. research focused on transition-metal-catalyzed reactions at the same place under the supervision of Prof. Aiwen Lei and Prof. Xumu Zhang. Later, he joined Prof. Stephen L. Buchwald's group at MIT for the postdoctoral study of continuous-flow technology promoted transition-metal catalysis from 2012 to 2014. In Oct 2014, he joined Prof. Jeremiah A. Johnson's group in the same institute as a postdoctoral scientist, where he explores polymerization and organic materials science. His research interests include novel catalysis and technology, which can promote the synthesis of small organic molecules, macromolecules, as well as "smart" materials.

Mingjiang Zhong performed undergraduate research with Prof. Yun-Dong Wu at Peking University, where he received his B.S. degree in double majors of Chemistry and Mathematics in 2008. He received his Ph.D. degree at Carnegie Mellon University under the direction of Professors Krzysztof Matyjaszewski and Tomasz Kowalewski in 2013. He is currently a postdoctoral fellow at the Massachusetts Institute of Technology coadvised by Professors Jeremiah A. Johnson and Bradley D. Olsen. He will join the Department of Chemical and Environmental Engineering at Yale University as an assistant professor in July 2016. His primary research interests span the subjects of mechanistic study of controlled/living polymerization, rational design and understanding of complex macromolecular structures, and nanocarbon and soft materials

for energy applications. He received a variety of honors for his research achievements, including the Astrid and Bruce McWilliams Fellowship, the Chinese Government Award for Outstanding Self-Financed Students Abroad, Guy C. Berry Graduate Research Award, and the Excellent Graduate Student Award, ACS Polymer Division.

Jeremiah A. Johnson conducted undergraduate research with Prof. Karen L. Wooley at Washington University, where he received his B.S. degree in Biomedical Engineering and Chemistry in 2004. He then moved to Columbia University, where he received his Ph.D. degree in Chemistry under the mentorship Prof. Nicholas J. Turro in 2009. After a Beckman Postdoctoral Fellowship at California Institute of Technology under the guidance of Professors David A. Tirrell and Robert H. Grubbs, he moved to MIT, where he is now a Firmenich Career Development Assistant Professor of Chemistry. He is also a member of the MIT Program in Polymers and Soft Matter (PPSM). He has received a Sloan Research Fellowship, the Air Force Young Investigator Award, the Thieme Journal Award for Young Faculty, the DuPont Young Professor Award, the 3M Nontenured Faculty Award, and an NSF CAREER award. His research group is focused on the development of new concepts and methods for macromolecular synthesis and surface functionalization.

ACKNOWLEDGMENTS

ABBREVIATIONS

AA	acrylic acid
AADC	acetic acid 2-(*N,N*-diethyldithiocarbamyl)-ethyl ether
AEAM	*N*-(2-aminoethyl) acrylamide hydrochloride
AFM	atomic force microscopy
AGET	activator generation by electron transfer
AIBN	2,2′-azobis(2-methylpropionitrile)
AN	acrylonitrile
ARGET	activator regeneration by electron transfer
ATRP	atom transfer radical polymerization
$[Au_2(\mu\text{-dppm})_2]Cl_2$	digold bis(diphenylphosphino)methane dichloride
BDT	*S*-benzyl *N,N*-diethyldithiocarbamate
BIXANDL	9,9′-bixanthene-9,9′-diol
BnMA	benzyl methacrylate
BP	benzophenone
bpy	2,2′-bipyridine
BPSE	benzyl phenyl selenide
BTPA	2-(*n*-butyltrithiocarbonate)-propionic acid
BSA	bovine serum albumin
BSTP	3-benzylsulfanylthiocarbonylsulfanyl propionic acid
CDB	2-phenyl-2-propyl benzodithioate
CDPA	(4-cyano-4-diethyldithiocarbamyl)-pentanoic acid
CDTPA	4-cyano-4-[(dodecylsulfanylthiocarbonyl)-sulfanyl] pentanoic acid
CETP	4-cyano-4-ethyl-trithiopentanoic acid
CFDA	methacrylated carboxyfluorescein diacetate
CFL	compact fluorescent lamp
CH_3OH	methanol
CHO	cyclohexene oxide

$[C_6mim^+][BF_4^-]$	1-hexyl-3-methylimidazoliumtetrafluoroborate
$[C_6mim^+][PF_6^-]$	1-hexyl-3-methylimidazoliumhexafluorophosphate
$[C_7mim^+][Br^-]$	1-heptyl-3-methylimidazolium bromide
$[C_8mim^+][PF_6^-]$	1-octyl-3-methylimidazolium hexafluorophosphate
$Co(acac)_2$	bis-acetylacetonatocobalt
COP	cycloolefin polymer
CPADB	4-cyanopentanoic acid dithiobenzoate
CPDN	2-cyanoprop-2-yl-1-dithionaphthalate
CPEC	S-2-cyano-2-propyl-O-ethyl xanthate
CRP	controlled radical polymerization
CTP	cyanopentanoic acid dithiobenzoate
DArDSE	diaryl diselenide
DBDS	dibenzoyl disulfide
DBTTC	dibenzyl trithiocarbonate
DCAP	2,2-dichloroacetophenone
DCIA	2-(N,N-diethyldithiocarbamyl)isobutyric acid ethyl ester
DDMAT	S-dodecyl-S′-(α,α′-dimethyl-α″-acetic acid) trithiocarbonate
DEGA	di(ethylene glycol) ethyl ether acrylate
DFT	density functional theory
DMA	N,N-dimethylacrylamide
DMAEMA	2-(dimethylamino)ethyl methacrylate
DMF	dimethylformamide
DMPA	2,2-dimethoxy-2-phenylacetophenone
DMSO	dimethyl sulfoxide
DPDSE	diphenyl diselenide
DPPSB	P,P-diphenyl phosphinodiselenoic acid benzyl ester
DTCA	2-(N,N-diethyldithiocarbamyl)isobutyric acid
DTEM	2-(N,N-diethyldithiocarbamyl)ethyl methacrylate
EA	ethyl acrylate
EBiB	α-bromoisobutyrate
EBPA	ethyl α-bromophenylacetate
EDMAT	S-ethyl-S′-(α,α′-dimethyl-α″-acetic acid) trithiocarbonate
EPDTB	1-(ethoxycarbonyl)prop-1-yl dithiobenzoate
$[emim^+][EtSO_4^-]$	1-ethyl-3-methylimidazolium ethyl sulfate
ESI-MS	electrospray ionization mass spectrometry
fac-[Ir(ppy)$_3$]	tris(2-phenylpyridinato)iridium(III)
FTNIR	Fourier transform near-infrared
GMA	glycidyl methacrylate
GPC	gel permeation chromatography
HEA	2-hydroxyethyl acrylate
HEMA	2-hydroxyethyl methacrylate
1-Hex	1-hexene
HPMA	N-(2-hydroxypropyl) methacrylamide
ICAR	initiators for continuous activator regeneration
Irgacure 819	phenyl bis(2,4,6-trimethylbenzoyl)phosphine oxide
LCST	lower critical solution temperature
LDPE	low-density polyethylene
LED	light-emitting diode
M_w	weight-average molar mass
M_n	number-average molar mass
MA	methyl acrylate
MAh	maleic anhydride
MALDI-TOF	matrix-assisted laser desorption/ionization time-of-flight
MAX	S-methacryloyl O-ethyl xanthate
Me$_6$TREN	tris[2-(dimethylamino)ethyl]amine
MeCN	acetonitrile
Me-PTH	10-methylphenothiazine
MMA	methyl methacrylate
mpg-C_3N_4	graphitic carbon nitride
MS	mass spectroscopy
MSEPI	methyl α-phenylseleno isobutylate
MTBPSE	p-methoxybenzyl p-trimethylsilyphenyl selenide
MTEMPO	4-methoxy-2,2,6,6-tetramethylpiperidine-1-oxyl
nBA	n-butyl acrylate
nBMA	n-butyl methacrylate
NiPAAm	N-isopropylacrylamide
NMP	nitroxide-mediated radical polymerization
NMR	nuclear magnetic resonance
NVP	N-vinylpyrrolidone
NVC	N-vinylcarbazole
NVI	N-vinylimidazole
NVCL	N-vinylcaprolactam
OEGMA	oligo(ethylene glycol) methyl ether methacrylate
OSET	outer-sphere electron transfer
PA	n-propyl acrylate
P′A	n-pentyl acrylate
PDMS	polydimethylsiloxane
PEG	poly(ethylene glycol)
PEGA	poly(oxyethylene glycol)methyl ether acrylate
PEGDA	poly(ethylene glycol) diacrylate
PEGMA	poly(ethylene glycol) methyl ether methacrylate
PEPDTA	1-phenylethyl phenyldithioacetate
PE-QTEMPO	1-phenylethyl 2-methyl-3-hydroxy quinoline
PE-XTEMPO	1-phenyl-1-[4′-(2″-xanthon-3‴-yloxyacetoxyl)-2′,2′,6′,6′-tetramethyl-1′-piperidinyloxy]ethane
PFPMA	pentafluorophenyl methacrylate
PLP	pulsed laser polymerization
PMDC	phenacyl morpholine-4-dithiocarbamate
PMDETA	N,N,N′,N″,N″-pentamethyldiethylenetriamine
PSeMS	p-phenylselenomethylstyrene
PTH	10-phenylphenothiazine
RAFT	reversible addition−fragmentation chain transfer
RGD	arginine-glycine-aspartic acid
rGO	reduced graphene oxide
ROMP	ring-opening metathesis polymerization
Ru^{II}(bpy)$_3$	tris(2,2′-bipyridine)ruthenium(II)
Ru^{II}(phen)$_3$	tris(1,10-phenanthroline)ruthenium(II)
SARA	supplemental activator and reducing agent
SCE	standard calomel electrode
SEM	scanning electron microscopy
SET	single-electron transfer
SET-LRP	single-electron transfer living radical polymerization
SR&NI	simultaneous reverse and normal initiation

St	styrene
tBA	tert-butyl acrylate
tBMA	tert-butyl methacrylate
TEA	triethylamine
TED	tetrathylthiuram disulfide
TEMPO	2,2,6,6-tetramethyl-1-piperidinyloxy
TFEMA	2,2,2-trifluoroethyl methacrylate
TKTSE	1,2,4,5-tetrakis(p-tert-butylphenylselenomethyl)benzene
TMDPO	(2,4,6-trimethylbenzoyl) diphenylphosphine oxide
TOF-SIMS	time-of-flight secondary ion mass spectroscopy
TPMA	tris(2-pyridylmethyl)amine
TPMA*	tris((4-methoxy-3,5-dimethylpyridin-2-yl)amine)
TPO	(2,4,6-trimethylbenzoyl) diphenylphosphine oxide
TTCA	S,S-bis(α,α'-dimethyl-α''-acetic acid) trithiocarbonate
TTDS	tetraethylthiuram disulfide
UV	ultraviolet
VA-086	2,2′-azobis[2-methyl-N-(2-hydroxyethyl)-propionamide]
VAc	vinyl acetate
VBA	vinylbenzyl alcohol
VBz	vinyl benzoate
VDF	vinylidene fluoride
VL	δ-valerolactone
VP	vinyl pivalate
xanthate	2-[(ethoxycarbonothioyl)sulfanyl]-propanoate
XDT	p-xylylene bis(N,N-diethyldithiocarbamate)
ZnTPP	zinc porphyrins
Đ	dispersity index, $Đ = M_w/M_n$

REFERENCES

(1) Tsarevsky, N. V.; Matyjaszewski, K. "Green" Atom Transfer Radical Polymerization: From Process Design to Preparation of Well-Defined Environmentally Friendly Polymeric Materials. *Chem. Rev.* **2007**, *107*, 2270−2299.

(2) Moad, G.; Rizzardo, E.; Thang, S. H. Living Radical Polymerization by the RAFT Process. *Aust. J. Chem.* **2005**, *58*, 379−410.

(3) Ouchi, M.; Terashima, T.; Sawamoto, M. Transition Metal-Catalyzed Living Radical Polymerization: Toward Perfection in Catalysis and Precision Polymer Synthesis. *Chem. Rev.* **2009**, *109*, 4963−5050.

(4) Braunecker, W. A.; Matyjaszewski, K. Controlled/Living Radical Polymerization: Features, Developments, and Perspectives. *Prog. Polym. Sci.* **2007**, *32*, 93−146.

(5) Hawker, C. J.; Bosman, A. W.; Harth, E. New Polymer Synthesis by Nitroxide Mediated Living Radical Polymerizations. *Chem. Rev.* **2001**, *101*, 3661−3688.

(6) Anastasaki, A.; Nikolaou, V.; Nurumbetov, G.; Wilson, P.; Kempe, K.; Quinn, J. F.; Davis, T. P.; Whittaker, M. R.; Haddleton, D. M. Cu(0)-Mediated Living Radical Polymerization: A Versatile Tool for Materials Synthesis. *Chem. Rev.* **2016**, *116*, 835.

(7) Rosen, B. M.; Percec, V. Single-Electron Transfer and Single-Electron Transfer Degenerative Chain Transfer Living Radical Polymerization. *Chem. Rev.* **2009**, *109*, 5069−5119.

(8) Yamago, S. Precision Polymer Synthesis by Degenerative Transfer Controlled/Living Radical Polymerization Using Organotellurium, Organostibine, and Organobismuthine Chain-Transfer Agents. *Chem. Rev.* **2009**, *109*, 5051−5068.

(9) Matyjaszewski, K.; Tsarevsky, N. V. Macromolecular Engineering by Atom Transfer Radical Polymerization. *J. Am. Chem. Soc.* **2014**, *136*, 6513−6533.

(10) Leibfarth, F. A.; Mattson, K. M.; Fors, B. P.; Collins, H. A.; Hawker, C. J. External Regulation of Controlled Polymerizations. *Angew. Chem., Int. Ed.* **2013**, *52*, 199−210.

(11) Otsu, T.; Yoshida, M. Role of Initiator-Transfer Agent-Terminator (Iniferter) in Radical Polymerizations: Polymer Design by Organic Disulfides as Iniferters. *Makromol. Chem., Rapid Commun.* **1982**, *3*, 127−132.

(12) Otsu, T.; Yoshida, M.; Tazaki, T. A Model for Living Radical Polymerization. *Makromol. Chem., Rapid Commun.* **1982**, *3*, 133−140.

(13) Magenau, A. J. D.; Strandwitz, N. C.; Gennaro, A.; Matyjaszewski, K. Electrochemically Mediated Atom Transfer Radical Polymerization. *Science* **2011**, *332*, 81−84.

(14) Bortolamei, N.; Isse, A. A.; Magenau, A. J. D.; Gennaro, A.; Matyjaszewski, K. Controlled Aqueous Atom Transfer Radical Polymerization with Electrochemical Generation of the Active Catalyst. *Angew. Chem., Int. Ed.* **2011**, *50*, 11391−11394.

(15) Park, S.; Chmielarz, P.; Gennaro, A.; Matyjaszewski, K. Simplified Electrochemically Mediated Atom Transfer Radical Polymerization Using a Sacrificial Anode. *Angew. Chem., Int. Ed.* **2015**, *54*, 2388−2392.

(16) Gregson, C. K. A.; Gibson, V. C.; Long, N. J.; Marshall, E. L.; Oxford, P. J.; White, A. J. P. Redox Control within Single-Site Polymerization Catalysts. *J. Am. Chem. Soc.* **2006**, *128*, 7410−7411.

(17) Broderick, E. M.; Guo, N.; Vogel, C. S.; Xu, C.; Sutter, J.; Miller, J. T.; Meyer, K.; Mehrkhodavandi, P.; Diaconescu, P. L. Redox Control of a Ring-Opening Polymerization Catalyst. *J. Am. Chem. Soc.* **2011**, *133*, 9278−9281.

(18) Prager, L.; Wennrich, L.; Heller, R.; Knolle, W.; Naumovll, S.; Prager, A.; Decker, D.; Liebe, H.; Buchmeiser, M. R. Vacuum-UV Irradiation-Based Formation of Methyl-Si-O-Si Networks from Poly-(1,1-Dimethylsilazane-*co*-1-Methylsilazane). *Chem. - Eur. J.* **2009**, *15*, 675−683.

(19) Caruso, M. M.; Davis, D. A.; Shen, Q.; Odom, S. A.; Sottos, N. R.; White, S. R.; Moore, J. S. Mechanically-Induced Chemical Changes in Polymeric Materials. *Chem. Rev.* **2009**, *109*, 5755−5798.

(20) Piermattei, A.; Karthikeyan, S.; Sijbesma, R. P. Activating Catalysts with Mechanical Force. *Nat. Chem.* **2009**, *1*, 133−137.

(21) Teator, A. J.; Lastovickova, D. N.; Bielawski, C. W. Switchable Polymerization Catalysts. *Chem. Rev.* **2016**, *116*, 1969−1992.

(22) Kelly, G. J.; Latzko, E. *Thirty Years of Photosynthesis*; Springer: Heidelberg, 2006.

(23) Yagci, Y.; Jockusch, S.; Turro, N. J. Photoinitiated Polymerization: Advances, Challenges, and Opportunities. *Macromolecules* **2010**, *43*, 6245−6260.

(24) Tehfe, M. A.; Louradour, F.; Lalevee, J.; Fouassier, J.-P. Photopolymerization Reactions: On the Way to a Green and Sustainable Chemistry. *Appl. Sci.* **2013**, *3*, 490−514.

(25) Yamago, S.; Nakamura, Y. Recent Progress in the Use of Photoirradiation in Living Radical Polymerization. *Polymer* **2013**, *54*, 981−994.

(26) Dadashi-Silab, S.; Atilla Tasdelen, M.; Yagci, Y. Photoinitiated Atom Transfer Radical Polymerization: Current Status and Future Perspectives. *J. Polym. Sci., Part A: Polym. Chem.* **2014**, *52*, 2878−2888.

(27) Decker, C. Photopolymerization and Ultraviolet Curing of Multifunctional Monomers. *Mater. Sci. Technol.* **1997**, *18*, 615−657.

(28) Fouassier, J. P.; Allonas, X.; Burget, D. Photopolymerization Reactions under Visible Lights: Principle, Mechanisms and Examples of Applications. *Prog. Org. Coat.* **2003**, *47*, 16−36.

(29) Andrzejewska, E. Photopolymerization Kinetics of Multifunctional Monomers. *Prog. Polym. Sci.* **2001**, *26*, 605−665.

(30) Xiao, P.; Zhang, J.; Dumur, F.; Tehfe, M. A.; Morlet-Savary, F.; Graff, B.; Gigmes, D.; Fouassier, J. P.; Lalevee, J. Visible Light Sensitive Photoinitiating Systems: Recent Progress in Cationic and Radical Photopolymerization Reactions under Soft Conditions. *Prog. Polym. Sci.* **2015**, *41*, 32−66.

(31) Dietlin, C.; Schweizer, S.; Xiao, P.; Zhang, J.; Morlet-Savary, F.; Graff, B.; Fouassier, J.-P.; Lalevee, J. Photopolymerization Upon LEDs:

New Photoinitiating Systems and Strategies. *Polym. Chem.* **2015**, *6*, 3895−3912.

(32) Turro, N. J.; Ramamurthy, V.; Scaiano, J. C. *Modern Molecular Photochemistry of Organic Molecules*; University Science Books: Sausalito, 2010.

(33) Dadashi-Silab, S.; Doran, S.; Yagci, Y.; Yagci, Y. Photoinduced Electron Transfer Reactions for Macromolecular Syntheses. *Chem. Rev.* **2016**, DOI: 10.1021/acs.chemrev.5b00586.

(34) Bandari, R.; Prager-Duschke, A.; Kuhnel, C.; Decker, U.; Schlemmer, B.; Buchmeiser, M. R. Tailored Ring-Opening Metathesis Polymerization Derived Monolithic Media Prepared from Cyclooctene-Based Monomers and Cross-Linkers. *Macromolecules* **2006**, *39*, 5222−5229.

(35) Flamigni, L.; Barbieri, A.; Sabatini, C.; Ventura, B.; Barigelletti, F. Photochemistry and Photophysics of Coordination Compounds: Iridium. *Top. Curr. Chem.* **2007**, *281*, 143−203.

(36) Kalyanasundaram, K. Photophysics, Photochemistry and Solar Energy Conversion with Tris(Bipyridyl)Ruthenium(II) and Its Analogs. *Coord. Chem. Rev.* **1982**, *46*, 159−244.

(37) Moad, G.; Rizzardo, E.; Thang, S. H. Radical Addition-Fragmentation Chemistry in Polymer Synthesis. *Polymer* **2008**, *49*, 1079−1131.

(38) Moad, G.; Chong, Y. K.; Postma, A.; Rizzardo, E.; Thang, S. H. Advances in RAFT Polymerization: The Synthesis of Polymers with Defined End-Groups. *Polymer* **2005**, *46*, 8458−8468.

(39) Keddie, D. J. A Guide to the Synthesis of Block Copolymers Using Reversible-Addition Fragmentation Chain Transfer (RAFT) Polymerization. *Chem. Soc. Rev.* **2014**, *43*, 496−505.

(40) Hill, M. R.; Carmean, R. N.; Sumerlin, B. S. Expanding the Scope of RAFT Polymerization: Recent Advances and New Horizons. *Macromolecules* **2015**, *48*, 5459−5469.

(41) Gregory, A.; Stenzel, M. H. Complex Polymer Architectures Via RAFT Polymerization: From Fundamental Process to Extending the Scope Using Click Chemistry and Nature's Building Blocks. *Prog. Polym. Sci.* **2012**, *37*, 38−105.

(42) Moad, G.; Rizzardo, E.; Thang, S. H. Toward Living Radical Polymerization. *Acc. Chem. Res.* **2008**, *41*, 1133−1142.

(43) Otsu, T.; Matsumoto, A. Controlled Synthesis of Polymers Using the Iniferter Technique: Developments in Living Radical Polymerization. *Adv. Polym. Sci.* **1998**, *136*, 75−137.

(44) Otsu, T. Iniferter Concept and Living Radical Polymerization. *J. Polym. Sci., Part A: Polym. Chem.* **2000**, *38*, 2121−2136.

(45) Lambrinos, P.; Tardi, M.; Polton, A.; Sigwalt, P. The Mechanism of the Polymerization of n-Butyl Acrylate Initiated with N,N-Diethyldithiocarbamate Derivatives. *Eur. Polym. J.* **1990**, *26*, 1125−1135.

(46) Kannurpatti, A. R.; Lu, S.; Bunker, G. M.; Bowman, C. N. Kinetic and Mechanistic Studies of Iniferter Photopolymerizations. *Macromolecules* **1996**, *29*, 7310−7315.

(47) Ishizu, K.; Khan, R. A.; Ohta, Y.; Furo, M. Controlled Radical Polymerization of 2-Hydroxyethyl Methacrylate Initiated by Photofunctional 2-(N,N-Diethyldithiocarbamyl)Isobutyric Acid. *J. Polym. Sci., Part A: Polym. Chem.* **2004**, *42*, 76−82.

(48) Ishizu, K.; Khan, R. A.; Furukawa, T.; Furo, M. Controlled Radical Polymerization of N-Isopropylacrylamide Initiated by Photofunctional 2-(N,N-Diethyldithiocarbamyl)Isobutyric Acid Sodium Salt in Aqueous Medium. *J. Appl. Polym. Sci.* **2004**, *91*, 3233−3238.

(49) Ishizu, K.; Katsuhara, H.; Itoya, K. Controlled Radical Polymerization of Methacrylic Acid Initiated by Diethyldithio-Carbamate-Mediated Iniferter. *J. Polym. Sci., Part A: Polym. Chem.* **2005**, *43*, 230−233.

(50) Ishizu, K.; Katsuhara, H.; Kawauchi, S.; Furo, M. Controlled Radical Polymerization of Styrene Initiated by Diethyldithiocarbamate-Mediated Iniferters. *J. Appl. Polym. Sci.* **2005**, *95*, 413−418.

(51) Wu, D.-C.; Hong, C.-Y.; Pan, C.-Y.; He, W.-D. Study on Controlled Radical Alternating Copolymerization of Styrene with Maleic Anhydride under UV Irradiation. *Polym. Int.* **2003**, *52*, 98−103.

(52) Tasdelen, M. A.; Durmaz, Y. Y.; Karagoz, B.; Bicak, N.; Yagci, Y. A New Photoiniferter/RAFT Agent for Ambient Temperature Rapid and Well-Controlled Radical Polymerization. *J. Polym. Sci., Part A: Polym. Chem.* **2008**, *46*, 3387−3395.

(53) Khan, M. Y.; Cho, M.-S.; Kwark, Y.-J. Dual Roles of a Xanthate as a Radical Source and Chain Transfer Agent in the Photoinitiated RAFT Polymerization of Vinyl Acetate. *Macromolecules* **2014**, *47*, 1929−1934.

(54) Quinn, J. F.; Barner, L.; Barner-Kowollik, C.; Rizzardo, E.; Davis, T. P. Reversible Addition-Fragmentation Chain Transfer Polymerization Initiated with Ultraviolet Radiation. *Macromolecules* **2002**, *35*, 7620−7627.

(55) Francis, R.; Ajayaghosh, A. Minimization of Homopolymer Formation and Control of Dispersity in Free Radical Induced Graft Polymerization Using Xanthate Derived Macro-Photoinitiators. *Macromolecules* **2000**, *33*, 4699−4704.

(56) Ajayaghosh, A.; Francis, R. Narrow Polydispersed Reactive Polymers by a Photoinitiated Free Radical Polymerization Approach. Controlled Polymerization of Methyl Methacrylate. *Macromolecules* **1998**, *31*, 1436−1438.

(57) Ajayaghosh, A.; Francis, R. A Xanthate-Derived Photoinitiator That Recognizes and Controls the Free Radical Polymerization Pathways of Methyl Methacrylate and Styrene. *J. Am. Chem. Soc.* **1999**, *121*, 6599−6606.

(58) Ishizu, K.; Shibuya, T.; Kawauchi, S. Kinetics on Formation of Hyperbranched Poly(Ethyl Methacrylate) Via a Controlled Radical Mechanism of Photofunctional Inimer. *Macromolecules* **2003**, *36*, 3505−3510.

(59) Ishizu, K.; Takashimizu, C.; Shibuya, T.; Uchida, S. Synthesis and Solution Properties of Alternating Maleimide/Styrene Hyperbranched Copolymers Via Controlled Radical Mechanism. *Polym. Int.* **2003**, *52*, 1010−1015.

(60) Ishizu, K.; Ohta, Y.; Kawauchi, S. Degree of Branching of Hyperbranched Polystyrenes Via a Controlled Radical Mechanism of an Inimer: Determination by a Kinetic Approach. *J. Appl. Polym. Sci.* **2005**, *96*, 1810−1815.

(61) You, Y.-Z.; Hong, C.-Y.; Bai, R.-K.; Pan, C.-Y.; Wang, J. Photo-Initiated Living Free Radical Polymerization in the Presence of Dibenzyl Trithiocarbonate. *Macromol. Chem. Phys.* **2002**, *203*, 477−483.

(62) Su, X.; Zhao, Z.; Li, H.; Li, X.; Wu, P.; Han, Z. Stereocontrol During Photo-Initiated Controlled/Living Radical Polymerization of Acrylamide in the Presence of Lewis Acids. *Eur. Polym. J.* **2008**, *44*, 1849−1856.

(63) Muthukrishnan, S.; Pan, E. H.; Stenzel, M. H.; Barner-Kowollik, C.; Davis, T. P.; Lewis, D.; Barner, L. Ambient Temperature RAFT Polymerization of Acrylic Acid Initiated with Ultraviolet Radiation in Aqueous Solution. *Macromolecules* **2007**, *40*, 2978−2980.

(64) Ran, R.; Yu, Y.; Wan, T. Photoinitiated RAFT Polymerization in the Presence of Trithiocarbonate. *J. Appl. Polym. Sci.* **2007**, *105*, 398−404.

(65) Wang, H.; Li, Q.; Dai, J.; Du, F.; Zheng, H.; Bai, R. Real-Time and in Situ Investigation of "Living"/Controlled Photopolymerization in the Presence of a Trithiocarbonate. *Macromolecules* **2013**, *46*, 2576−2582.

(66) Zhou, H.; Johnson, J. A. Photo-Controlled Growth of Telechelic Polymers and End-Linked Polymer Gels. *Angew. Chem., Int. Ed.* **2013**, *52*, 2235−2238.

(67) Liu, G.; Shi, H.; Cui, Y.; Tong, J.; Zhao, Y.; Wang, D.; Cai, Y. Toward Rapid Aqueous RAFT Polymerization of Primary Amine Functional Monomer under Visible Light Irradiation at 25 °C. *Polym. Chem.* **2013**, *4*, 1176−1182.

(68) Zhang, H.; Deng, J.; Lu, L.; Cai, Y. Ambient-Temperature RAFT Polymerization of Styrene and Its Functional Derivatives under Mild Long-Wave UV-Vis Radiation. *Macromolecules* **2007**, *40*, 9252−9261.

(69) Shi, Y.; Liu, G.; Gao, H.; Lu, L.; Cai, Y. Effect of Mild Visible Light on Rapid Aqueous RAFT Polymerization of Water-Soluble Acrylic Monomers at Ambient Temperature: Initiation and Activation. *Macromolecules* **2009**, *42*, 3917−3926.

(70) Tong, J.; Shi, Y.; Liu, G.; Huang, T.; Xu, N.; Zhu, Z.; Cai, Y. Visible Light Mediated Fast Iterative RAFT Synthesis of Amino-Based Reactive Copolymers in Water at 20°. *Macromol. Rapid Commun.* **2013**, *34*, 1827−1832.

(71) Lu, L.; Zhang, H.; Yang, N.; Cai, Y. Toward Rapid and Well-Controlled Ambient Temperature RAFT Polymerization under UV-Vis Radiation: Effect of Radiation Wave Range. *Macromolecules* **2006**, *39*, 3770−3776.

(72) Lu, L.; Yang, N.; Cai, Y. Well-Controlled Reversible Addition-Fragmentation Chain Transfer Radical Polymerization under Ultraviolet Radiation at Ambient Temperature. *Chem. Commun.* **2005**, 5287−5288.

(73) Zhang, J.; Li, A.; Liu, H.; Yang, D.; Liu, J. Well-Controlled RAFT Polymerization Initiated by Recyclable Surface-Modified Nb(OH)5 Nanoparticles under Visible Light Irradiation. *J. Polym. Sci., Part A: Polym. Chem.* **2014**, *52*, 2715−2724.

(74) Nicolas, J.; Guillaneuf, Y.; Lefay, C.; Bertin, D.; Gigmes, D.; Charleux, B. Nitroxide-Mediated Polymerization. *Prog. Polym. Sci.* **2013**, *38*, 63−235.

(75) Sciannamea, V.; Jerome, R.; Detrembleur, C. In-Situ Nitroxide-Mediated Radical Polymerization (NMP) Processes: Their Understanding and Optimization. *Chem. Rev.* **2008**, *108*, 1104−1126.

(76) Georges, M. K.; Veregin, R. P. N.; Kazmaier, P. M.; Hamer, G. K. Narrow Molecular Weight Resins by a Free-Radical Polymerization Process. *Macromolecules* **1993**, *26*, 2987−2988.

(77) Hawker, C. J. "Living" Free Radical Polymerization: A Unique Technique for the Preparation of Controlled Macromolecular Architectures. *Acc. Chem. Res.* **1997**, *30*, 373−382.

(78) Fischer, H. The Persistent Radical Effect: A Principle for Selective Radical Reactions and Living Radical Polymerizations. *Chem. Rev.* **2001**, *101*, 3581−3610.

(79) Scaiano, J. C.; Connolly, T. J.; Mohtat, N.; Pliva, C. N. Exploratory Study of the Quenching of Photosensitizers by Initiators of Free Radical "Living" Polymerization. *Can. J. Chem.* **1997**, *75*, 92−97.

(80) Hu, S.; Malpert, J. H.; Yang, X.; Neckers, D. C. Exploring Chromophore Tethered Aminoethers as Potential Photoinitiators for Controlled Radical Polymerization. *Polymer* **2000**, *41*, 445−452.

(81) Goto, A.; Scaiano, J. C.; Maretti, L. Photolysis of an Alkoxyamine Using Intramolecular Energy Transfer from a Quinoline Antenna - Towards Photo-Induced Living Radical Polymerization. *Photochem. Photobiol. Sci.* **2007**, *6*, 833−835.

(82) Guillaneuf, Y.; Bertin, D.; Gigmes, D.; Versace, D.-L.; Lalevee, J.; Fouassier, J.-P. Toward Nitroxide-Mediated Photopolymerization. *Macromolecules* **2010**, *43*, 2204−2212.

(83) Versace, D.-L.; Guillaneuf, Y.; Bertin, D.; Fouassier, J. P.; Lalevee, J.; Gigmes, D. Structural Effects on the Photodissociation of Alkoxyamines. *Org. Biomol. Chem.* **2011**, *9*, 2892−2898.

(84) Guillaneuf, Y.; Versace, D.-L.; Bertin, D.; Lalevee, J.; Fouassier, J.-P.; Gigmes, D. Light Sensitive Alkoxyamines: Applications in Nitroxide Mediated Photopolymerization. *Polym. Prepr.* **2011**, *52*, 527−528.

(85) Su, J.; Liu, X.; Hu, J.; You, Q.; Cui, Y.; Chen, Y. Photo-Induced Controlled Radical Polymerization of Methyl Methacrylate Mediated by Photosensitive Nitroxides. *Polym. Int.* **2015**, *64*, 867−874.

(86) Yoshida, E. Photo-Living Radical Polymerization of Methyl Methacrylate by a Nitroxide Mediator. *Colloid Polym. Sci.* **2008**, *286*, 1663−1666.

(87) Yoshida, E. Nitroxide-Mediated Photo-Living Radical Polymerization of Vinyl Acetate. *Colloid Polym. Sci.* **2010**, *288*, 73−78.

(88) Yoshida, E. Nitroxide-Mediated Photo-Living Radical Polymerization of Methyl Methacrylate in Solution. *Colloid Polym. Sci.* **2010**, *288*, 1639−1643.

(89) Yoshida, E. Nitroxide-Mediated Photo-Controlled/Living Radical Polymerization of Ethyl Acrylate. *Colloid Polym. Sci.* **2011**, *289*, 1127−1132.

(90) Yoshida, E. Controlled Photoradical Polymerization Mediated by 2,2,6,6-Tetramethylpiperidine-1-Oxyl. *Polymers* **2012**, *4*, 1125−1156.

(91) Yoshida, E. Photo-Controlled/Living Radical Polymerization Mediated by 2,2,6,6-Tetramethylpiperidine-1-Oxyl in Inert Atmospheres. *Colloid Polym. Sci.* **2012**, *290*, 1087−1091.

(92) Yoshida, E. Photo-Controlled/Living Radical Polymerization of 2-(Dimethylamino)Ethyl Methacrylate Using 4-Methoxy-2,2,6,6-Tetramethylpiperidine-1-Oxyl as a Mediator. *Colloid Polym. Sci.* **2012**, *290*, 965−969.

(93) Yoshida, E. Nitroxide-Mediated Photo-Living Radical Polymerization of Methyl Methacrylate in the Presence of (η6-Benzene)(η5-Cyclopentadienyl)Fe^{II} Hexafluorophosphate. *Colloid Polym. Sci.* **2010**, *288*, 1745−1749.

(94) Yoshida, E. Photo-Living Radical Polymerization of Methyl Methacrylate by 2,2,6,6-Tetramethylpiperidine-1-Oxyl in the Presence of a Photo-Acid Generator. *Colloid Polym. Sci.* **2009**, *287*, 767−772.

(95) Yoshida, E. Photo-Controlled/Living Radical Polymerization of Tert-Butyl Methacrylate in the Presence of a Photo-Acid Generator Using a Nitroxide Mediator. *Colloid Polym. Sci.* **2012**, *290*, 661−665.

(96) Yoshida, E. Selective Controlled/Living Photoradical Polymerization of Glycidyl Methacrylate, Using a Nitroxide Mediator in the Presence of a Photosensitive Triarylsulfonium Salt. *Polymers* **2012**, *4*, 1580−1589.

(97) Yoshida, E. Elucidation of Acceleration Mechanisms by a Photosensitive Onium Salt for Nitroxide-Mediated Photocontrolled/Living Radical Polymerization. *Open J. Polym. Chem.* **2014**, *4*, 47−55.

(98) Brimm, E. O.; Lynch, M. A., Jr.; Sesny, J. W. Preparation and Properties of Manganese Carbonyl. *J. Am. Chem. Soc.* **1954**, *76*, 3831−3835.

(99) Haines, L. I. B.; Poe, A. J. Initiation of Vinyl Polymerization by Manganese Carbonyl and Carbon Tetrachloride. *Nature* **1967**, *215*, 699−701.

(100) Meyer, T. J.; Caspar, J. V. Photochemistry of Metal-Metal Bonds. *Chem. Rev.* **1985**, *85*, 187−218.

(101) Goodman, J. L.; Peters, K. S.; Vaida, V. The Determination of the Manganese-Manganese Bond Strength in Mn$_2$(Co)$_{10}$ Using Pulsed Time-Resolved Photoacoustic Calorimetry. *Organometallics* **1986**, *5*, 815−816.

(102) Sarakha, M.; Ferraudi, G. Photophysical Features of the M$_2$(Co)$_{10}$, M = Mn and Re, Solution Photochemistry. *Inorg. Chem.* **1999**, *38*, 4605−4607.

(103) Hughey, J. L. I. V.; Anderson, C. P.; Meyer, T. J. Photochemistry of Decacarbonyldimanganese. *J. Organomet. Chem.* **1977**, *125*, C49−C52.

(104) Fukuyama, T.; Nishitani, S.; Inouye, T.; Morimoto, K.; Ryu, I. Effective Acceleration of Atom Transfer Carbonylation of Alkyl Iodides by Metal Complexes. Application to the Synthesis of the Hinokinin Precursor and Dihydrocapsaicin. *Org. Lett.* **2006**, *8*, 1383−1386.

(105) Friestad, G. K.; Ji, A. Mn-Mediated Coupling of Alkyl Iodides and Ketimines: A Radical Addition Route to A,A-Disubstituted A-Aminoesters. *Org. Lett.* **2008**, *10*, 2311−2313.

(106) Friestad, G. K.; Ji, A.; Baltrusaitis, J.; Korapala, C. S.; Qin, J. Scope of Stereoselective Mn-Mediated Radical Addition to Chiral Hydrazones and Application in a Formal Synthesis of Quinine. *J. Org. Chem.* **2012**, *77*, 3159−3180.

(107) Yagci, Y.; Hepuzer, Y. A Novel Visible Light Initiating System for Cationic Polymerization. *Macromolecules* **1999**, *32*, 6367−6370.

(108) Koumura, K.; Satoh, K.; Kamigaito, M. Manganese-Based Controlled/Living Radical Polymerization of Vinyl Acetate, Methyl Acrylate, and Styrene: Highly Active, Versatile, and Photoresponsive Systems. *Macromolecules* **2008**, *41*, 7359−7367.

(109) Gilbert, B. C.; Harrison, R. J.; Lindsay, C. I.; McGrail, P. T.; Parsons, A. F.; Southward, R.; Irvine, D. J. Polymerization of Methyl Methacrylate Using Dimanganese Decacarbonyl in the Presence of Organohalides. *Macromolecules* **2003**, *36*, 9020−9023.

(110) Jenkins, D. W.; Hudson, S. M. Heterogeneous Graft Copolymerization of Chitosan Powder with Methyl Acrylate Using Trichloroacetyl-Manganese Carbonyl Co-Initiation. *Macromolecules* **2002**, *35*, 3413−3419.

(111) Koumura, K.; Satoh, K.; Kamigaito, M. Mn$_2$(Co)$_{10}$-Induced Controlled/Living Radical Copolymerization of Methyl Acrylate and 1-Hexene in Fluoroalcohol: High A-Olefin Content Copolymers with Controlled Molecular Weights. *Macromolecules* **2009**, *42*, 2497−2504.

(112) Koumura, K.; Satoh, K.; Kamigaito, M. Mn$_2$(Co)$_{10}$-Induced Controlled/Living Radical Copolymerization of Vinyl Acetate and Methyl Acrylate: Spontaneous Formation of Block Copolymers Consisting of Gradient and Homopolymer Segments. *J. Polym. Sci., Part A: Polym. Chem.* **2009**, *47*, 1343−1353.

AK

(113) David, G.; Boyer, C.; Tonnar, J.; Ameduri, B.; Lacroix-Desmazes, P.; Boutevin, B. Use of Iodocompounds in Radical Polymerization. *Chem. Rev.* **2006**, *106*, 3936−3962.

(114) Acik, G.; Kahveci, M. U.; Yagci, Y. Synthesis of Block Copolymers by Combination of Atom Transfer Radical Polymerization and Visible Light Radical Photopolymerization Methods. *Macromolecules* **2010**, *43*, 9198−9201.

(115) Kahveci, M. U.; Acik, G.; Yagci, Y. Synthesis of Block Copolymers by Combination of Atom Transfer Radical Polymerization and Visible Light-Induced Free Radical Promoted Cationic Polymerization. *Macromol. Rapid Commun.* **2012**, *33*, 309−313.

(116) Bektas, S.; Ciftci, M.; Yagci, Y. Hyperbranched Polymers by Visible Light Induced Self-Condensing Vinyl Polymerization and Their Modifications. *Macromolecules* **2013**, *46*, 6751−6757.

(117) Ciftci, M.; Batat, P.; Demirel, A. L.; Xu, G.; Buchmeiser, M.; Yagci, Y. Visible Light-Induced Grafting from Polyolefins. *Macromolecules* **2013**, *46*, 6395−6401.

(118) Imae, T. Fluorinated Polymers. *Curr. Opin. Colloid Interface Sci.* **2003**, *8*, 307−314.

(119) Lacroix-Desmazes, P.; Ameduri, B.; Boutevin, B. Use of Fluorinated Organic Compounds in Living Radical Polymerizations. *Collect. Czech. Chem. Commun.* **2002**, *67*, 1383−1415.

(120) Asandei, A. D.; Adebolu, O.; Simpson, C.; Chen, Y. Towards Transition Metal Mediated Radical Polymerization of Main Chain Fluorinated Monomers. *Polym. Prepr.* **2011**, *52*, 759−760.

(121) Asandei, A. D.; Adebolu, O. I.; Simpson, C. P. Mild-Temperature Mn2(Co)10-Photomediated Controlled Radical Polymerization of Vinylidene Fluoride and Synthesis of Well-Defined Poly(Vinylidene Fluoride) Block Copolymers. *J. Am. Chem. Soc.* **2012**, *134*, 6080−6083.

(122) Asandei, A. D.; Adebolu, O. I.; Simpson, C. P. Mn$_2$(Co)$_{10}$-Visible Light Photomediated, Controlled Radical Polymerization of Main Chain Fluorinated Monomers and Synthesis of Block Copolymers Thereof. *Handb. Fluoropolym. Sci. Technol.* **2014**, 21−42.

(123) Simpson, C. P.; Adebolu, O. I.; Kim, J.-S.; Vasu, V.; Asandei, A. D. Metal and Ligand Effects of Photoactive Transition Metal Carbonyls in the Iodine Degenerative Transfer Controlled Radical Polymerization and Block Copolymerization of Vinylidene Fluoride. *Macromolecules* **2015**, *48*, 6404−6420.

(124) Miao, X.; Li, J.; Zhang, Z.; Cheng, Z.; Zhang, W.; Zhu, J.; Zhu, X. Dimanganese Decacarbonyl/2-Cyanoprop-2-yl-1-Dithionaphthalate: Toward Sunlight Induced RAFT Polymerization of MMA. *Polym. Chem.* **2014**, *5*, 4641−4648.

(125) Kendrick, M. J.; Al-Akhdar, W. Preparation and Characterization of (Alkylperoxo)Cobalt(III) Porphyrins: First Direct Evidence for Metal-Carbon Bond Homolysis in Dioxygen Insertion Reactions. *Inorg. Chem.* **1987**, *26*, 3971−3972.

(126) Watanabe, J.-y.; Setsune, J.-i. Facile Alkylation of Cobalt(III) Porphyrins by Organosilicon Compounds. *Organometallics* **1997**, *16*, 3679−3683.

(127) Wayland, B. B.; Poszmik, G.; Mukerjee, S. L.; Fryd, M. Living Radical Polymerization of Acrylates by Organocobalt Porphyrin Complexes. *J. Am. Chem. Soc.* **1994**, *116*, 7943−7944.

(128) Li, S.; Bruin, B. d.; Peng, C.-H.; Fryd, M.; Wayland, B. B. Exchange of Organic Radicals with Organo-Cobalt Complexes Formed in the Living Radical Polymerization of Vinyl Acetate. *J. Am. Chem. Soc.* **2008**, *130*, 13373−13381.

(129) Debuigne, A.; Poli, R.; Jerome, C.; Jerome, R.; Detrembleur, C. Overview of Cobalt-Mediated Radical Polymerization: Roots, State of the Art and Future Prospects. *Prog. Polym. Sci.* **2009**, *34*, 211−239.

(130) Debuigne, A.; Caille, J.-R.; Detrembleur, C.; Jerome, R. Effective Cobalt Mediation of the Radical Polymerization of Vinyl Acetate in Suspension. *Angew. Chem., Int. Ed.* **2005**, *44*, 3439−3442.

(131) Hurtgen, M.; Debuigne, A.; Jerome, C.; Detrembleur, C. Solving the Problem of Bis(Acetylacetonato)Cobalt(II)-Mediated Radical Polymerization (CMRP) of Acrylic Esters. *Macromolecules* **2010**, *43*, 886−894.

(132) Hurtgen, M.; Detrembleur, C.; Jerome, C.; Debuigne, A. Insight into Organometallic-Mediated Radical Polymerization. *Polym. Rev.* **2011**, *51*, 188−213.

(133) Arvanitopoulos, L. D.; Gruel, M. P.; Harwood, H. J. "Living" Free Radical Polymerization Using Alkyl Cobaloximes as Photoinitiators. *Polym. Prepr.* **1994**, *35*, 549−550.

(134) Arvanitopoulos, L. D.; Greuel, M. P.; King, B. M.; Shim, A. K.; Harwood, H. J. Photochemical Polymerizations Initiated and Mediated by Soluble Organocobalt Compounds. *ACS Symp. Ser.* **1998**, *685*, 316−331.

(135) Debuigne, A.; Schoumacher, M.; Willet, N.; Riva, R.; Zhu, X.; Ruetten, S.; Jerome, C.; Detrembleur, C. New Functional Poly(N-Vinylpyrrolidone) Based (Co)Polymers Via Photoinitiated Cobalt-Mediated Radical Polymerization. *Chem. Commun.* **2011**, *47*, 12703−12705.

(136) Detrembleur, C.; Versace, D.-L.; Piette, Y.; Hurtgen, M.; Jerome, C.; Lalevee, J.; Debuigne, A. Synthetic and Mechanistic Inputs of Photochemistry into the Bis-Acetylacetonatocobalt-Mediated Radical Polymerization of n-Butyl Acrylate and Vinyl Acetate. *Polym. Chem.* **2012**, *3*, 1856−1866.

(137) Miao, X.; Zhu, W.; Zhang, Z.; Zhang, W.; Zhu, X.; Zhu, J. Photo-Induced Cobalt-Mediated Radical Polymerization of Vinyl Acetate. *Polym. Chem.* **2014**, *5*, 551−557.

(138) Zhao, Y.; Yu, M.; Zhang, S.; Liu, Y.; Fu, X. Visible Light Induced Living/Controlled Radical Polymerization of Acrylates Catalyzed by Cobalt Porphyrins. *Macromolecules* **2014**, *47*, 6238−6245.

(139) Zhao, Y.; Yu, M.; Fu, X. Photo-Cleavage of the Cobalt-Carbon Bond: Visible Light-Induced Living Radical Polymerization Mediated by Organo-Cobalt Porphyrins. *Chem. Commun.* **2013**, *49*, 5186−5188.

(140) Zhao, Y.; Yu, M.; Zhang, S.; Wu, Z.; Liu, Y.; Peng, C.-H.; Fu, X. A Well-Defined, Versatile Photoinitiator (Salen)Co-CO$_2$CH$_3$ for Visible Light-Initiated Living/Controlled Radical Polymerization. *Chem. Sci.* **2015**, *6*, 2979−2988.

(141) Bartlett, P. D.; Kwart, H. Dilatometric Studies of the Behavior of Some Inhibitors and Retarders in the Polymerization of Liquid Vinyl Acetate. I. *J. Am. Chem. Soc.* **1950**, *72*, 1051−1059.

(142) Lacroix-Desmazes, P.; Severac, R.; Boutevin, B. Reverse Iodine Transfer Polymerization of Methyl Acrylate and n-Butyl Acrylate. *Macromolecules* **2005**, *38*, 6299−6309.

(143) Tonnar, J.; Pouget, E.; Lacroix-Desmazes, P.; Boutevin, B. Synthesis of Poly(Vinyl Acetate)-B-Poly(Dimethylsiloxane)-B-Poly-(Vinyl Acetate) Triblock Copolymers by Iodine Transfer Polymerization. *Macromol. Symp.* **2009**, *281*, 20−30.

(144) Stevenson, D. P.; Coppinger, G. M. Solvent Effects on N-σ* Transitions: Complex Formation between Amines and Halomethanes. *J. Am. Chem. Soc.* **1962**, *84*, 149−152.

(145) Lautenberger, W. J.; Jones, E. N.; Miller, J. G. Reaction of Amines with Halo Alkanes. I. Photochemical Reaction of Butylamine with Carbon Tetrachloride. *J. Am. Chem. Soc.* **1968**, *90*, 1110−1115.

(146) Goto, A.; Suzuki, T.; Ohfuji, H.; Tanishima, M.; Fukuda, T.; Tsujii, Y.; Kaji, H. Reversible Complexation Mediated Living Radical Polymerization (RCMP) Using Organic Catalysts. *Macromolecules* **2011**, *44*, 8709−8715.

(147) Ohtsuki, A.; Goto, A.; Kaji, H. Visible-Light-Induced Reversible Complexation Mediated Living Radical Polymerization of Methacrylates with Organic Catalysts. *Macromolecules* **2013**, *46*, 96−102.

(148) Ohtsuki, A.; Lei, L.; Tanishima, M.; Goto, A.; Kaji, H. Photocontrolled Organocatalyzed Living Radical Polymerization Feasible over a Wide Range of Wavelengths. *J. Am. Chem. Soc.* **2015**, *137*, 5610−5617.

(149) Wolpers, A.; Vana, P. UV Light as External Switch and Boost of Molar-Mass Control in Iodine-Mediated Polymerization. *Macromolecules* **2014**, *47*, 954−963.

(150) Zhdankin, V. V.; Stang, P. J. Chemistry of Polyvalent Iodine. *Chem. Rev.* **2008**, *108*, 5299−5358.

(151) Asandei, A. D.; Adebolu, O. I.; Simpson, C. P.; Kim, J.-S. Visible-Light Hypervalent Iodide Carboxylate Photo(Trifluoro)Methylations and Controlled Radical Polymerization of Fluorinated Alkenes. *Angew. Chem., Int. Ed.* **2013**, *52*, 10027−10030.

(152) Russell, G. A.; Tashtoush, H. Free-Radical Chain-Substitution Reactions of Alkylmercury Halides. *J. Am. Chem. Soc.* **1983**, *105*, 1398−1399.

(153) Kwak, Y.; Tezuka, M.; Goto, A.; Fukuda, T.; Yamago, S. Kinetic Study on Role of Ditelluride in Organotellurium-Mediated Living Radical Polymerization (TERP). *Macromolecules* **2007**, *40*, 1881−1885.

(154) Yamago, S.; Miyazoe, H.; Goto, R.; Hashidume, M.; Sawazaki, T.; Yoshida, J.-i. Synthetic and Theoretical Studies on Group-Transfer Imidoylation of Organotellurium Compounds. Remarkable Reactivity of Isonitriles in Comparison with Carbon Monoxide in Radical-Mediated Reactions. *J. Am. Chem. Soc.* **2001**, *123*, 3697−3705.

(155) Ogawa, A.; Yokoyama, K.; Obayashi, R.; Han, L. B.; Kambe, N.; Sonoda, N. Photoinduced Ditelluration of Acetylenes with Diphenyl Ditelluride. *Tetrahedron* **1993**, *49*, 1177−1188.

(156) Ouchi, A.; Ando, W.; Oba, M. Advances in the Photochemistry of Organoselenium and Organotellurium Compounds. *Chem. Org. Selenium Tellurium Compd.* **2013**, *4*, 447−541.

(157) Yamago, S.; Ukai, Y.; Matsumoto, A.; Nakamura, Y. Organotellurium-Mediated Controlled/Living Radical Polymerization Initiated by Direct C-Te Bond Photolysis. *J. Am. Chem. Soc.* **2009**, *131*, 2100−2101.

(158) Nomura, A.; Goto, A.; Ohno, K.; Kayahara, E.; Yamago, S.; Tsujii, Y. Controlled Synthesis of Hydrophilic Concentrated Polymer Brushes and Their Friction/Lubrication Properties in Aqueous Solutions. *J. Polym. Sci., Part A: Polym. Chem.* **2011**, *49*, 5284−5292.

(159) Nakamura, Y.; Yamago, S. Organotellurium-Mediated Living Radical Polymerization under Photoirradiation by a Low-Intensity Light-Emitting Diode. *Beilstein J. Org. Chem.* **2013**, *9*, 1607−1612.

(160) Nakamura, Y.; Arima, T.; Tomita, S.; Yamago, S. Photoinduced Switching from Living Radical Polymerization to a Radical Coupling Reaction Mediated by Organotellurium Compounds. *J. Am. Chem. Soc.* **2012**, *134*, 5536−5539.

(161) Benedikt, S.; Moszner, N.; Liska, R. Benzoyl Phenyltelluride as Highly Reactive Visible-Light TERP-Reagent for Controlled Radical Polymerization. *Macromolecules* **2014**, *47*, 5526−5531.

(162) Ogawa, A.; Hirao, T. Highly Selective Thioselenation of Carbon-Carbon Unsaturated Bonds with a Disulfide-Diselenide Binary System. *Rev. Heteroat. Chem.* **1998**, *18*, 1−10.

(163) Ogawa, A.; Tanaka, H.; Yokoyama, H.; Obayashi, R.; Yokoyama, K.; Sonoda, N. A Highly Selective Thioselenation of Olefins Using Disulfide-Diselenide Mixed System. *J. Org. Chem.* **1992**, *57*, 111−115.

(164) Pataiand, S.; Rappoport, Z. *The Chemistry of Organic Selenium and Tellurium Compounds*; Wiley& Sons: New York, 1986.

(165) Kwon, T. S.; Kondo, S.; Kunisada, H.; Yuki, Y. Synthesis of Polystyrene and Poly(Methyl Methacrylate) Each with a Phenylseleno Group at Terminal Chain End by Radical Polymerization in the Presence of Benzyl Phenyl Selenide as a Photoiniferter. *Polym. J.* **1998**, *30*, 559−565.

(166) Kwon, T. S.; Kumazawa, S.; Yokoi, T.; Kondo, S.; Kunisada, H.; Yuki, Y. Living Radical Polymerization of Styrene with Diphenyl Diselenide as a Photoiniferter. Synthesis of Polystyrene with Carbon-Carbon Double Bonds at Both Chain Ends. *J. Macromol. Sci., Part A: Pure Appl.Chem.* **1997**, *34*, 1553−1567.

(167) Kwon, T. S.; Ochiai, H.; Kondo, S.; Takagi, K.; Kunisada, H.; Yuki, Y. Radical Polymerization of P-Substituted Styrenes with Benzyl Phenyl Selenide as Photoiniferter. *Polym. J.* **1999**, *31*, 411−417.

(168) Kwon, T. S.; Suzuki, K.; Takagi, K.; Kunisada, H.; Yuki, Y. Radical Polymerization of Methyl Methacrylate with Diphenyl Diselenide under Thermal or Photoirradiational Conditions. *J. Macromol. Sci., Part A: Pure Appl.Chem.* **2001**, *38*, 591−604.

(169) Kwon, T. S.; Takagi, K.; Kunisada, H.; Yuki, Y. Synthesis of Diblock Copolymers by End Functional Polystyrene Containing Phenylseleno Groups as Polymeric Photoiniferter. *J. Macromol. Sci., Part A: Pure Appl.Chem.* **2002**, *39*, 991−1006.

(170) Kwon, T. S.; Takagi, K.; Kunisada, H.; Yuki, Y. Synthesis of Macromonomer Using End Functional Polystyrene Prepared from P-Methoxybenzyl P-Trimethylsilylphenyl Selenide as a Photoiniferter. *J. Macromol. Sci., Part A: Pure Appl.Chem.* **2000**, *37*, 1461−1473.

(171) Kwon, T. S.; Kondo, S.; Takagi, K.; Kunisada, H.; Yuki, Y. Synthesis and Radical Polymerization of P-Phenylselenomethylstyrene and Applications to Graft Copolymers. *Polym. J.* **1999**, *31*, 483−487.

(172) Takagi, K.; Nishikawa, Y.; Kwon, T. S.; Kunisada, H.; Yuki, Y. Synthesis of Branched Polystyrene by Photopolymerization of Selenium-Containing Styrene Monomer. *Polym. J.* **2000**, *32*, 970−973.

(173) Kwon, T. S.; Takagi, K.; Kunisada, H.; Yuki, Y. Synthesis of Star Polystyrene by Radical Polymerization with 1,2,4,5-Tetrakis(P-Tert-Butylphenyl Selenomethyl)Benzene as a Novel Photoiniferter. *Eur. Polym. J.* **2003**, *39*, 1437−1441.

(174) Ding, C.; Fan, C.; Jiang, G.; Zhang, J.; Li, X.; Li, N.; Pan, X.; Zhang, Z.; Zhang, W.; Zhu, J.; et al. Diselenide Mediated Controlled Radical Polymerization under Visible Light Irradiation: Mechanism Investigation and α,ω-Ditelechelic Polymers. *Polym. Chem.* **2015**, *6*, 6416−6423.

(175) Zeng, J.; Zhu, J.; Zhang, Z.; Pan, X.; Zhang, W.; Cheng, Z.; Zhu, X. New Selenium-Based Iniferter Agent for Living Free Radical Polymerization of Styrene under UV Irradiation. *J. Polym. Sci., Part A: Polym. Chem.* **2012**, *50*, 2211−2218.

(176) Otsu, T.; Matsumoto, A.; Tazaki, T. Radical Polymerization of Methyl Methacrylate with Some 1,2-Disubstituted Tetraphenylethanes as Thermal Iniferters. *Polym. Bull.* **1987**, *17*, 323−330.

(177) Bledzki, A.; Braun, D.; Titzschkau, K. Initiation of Polymerization with Substituted Ethanes. 6. Polymerization of Methyl Methacrylate with Different Tetraphenylethanes. *Makromol. Chem.* **1983**, *184*, 745−754.

(178) Bledzki, A.; Braun, D. Initiation of Polymerization with Substituted Ethanes. 1. Polymerization of Methyl Methacrylate with 1,1,2,2-Tetraphenyl-1,2-Diphenoxyethane. *Makromol. Chem.* **1981**, *182*, 1047−1056.

(179) Zheng, X.; Yue, M.; Yang, P.; Li, Q.; Yang, W. Cycloketyl Radical Mediated Living Polymerization. *Polym. Chem.* **2012**, *3*, 1982−1986.

(180) Wang, J.-S.; Matyjaszewski, K. Controlled/"Living" Radical Polymerization. Atom Transfer Radical Polymerization in the Presence of Transition-Metal Complexes. *J. Am. Chem. Soc.* **1995**, *117*, 5614−5615.

(181) Matyjaszewski, K.; Xia, J. Atom Transfer Radical Polymerization. *Chem. Rev.* **2001**, *101*, 2921−2990.

(182) Kato, M.; Kamigaito, M.; Sawamoto, M.; Higashimura, T. Polymerization of Methyl Methacrylate with the Carbon Tetrachloride/Dichlorotris- (Triphenylphosphine)Ruthenium(II)/Methylaluminum Bis(2,6-Di-Tert-Butylphenoxide) Initiating System: Possibility of Living Radical Polymerization. *Macromolecules* **1995**, *28*, 1721−1723.

(183) Kamigaito, M.; Ando, T.; Sawamoto, M. Metal-Catalyzed Living Radical Polymerization. *Chem. Rev.* **2001**, *101*, 3689−3745.

(184) Xia, J.; Matyjaszewski, K. Controlled/"Living" Radical Polymerization. Homogeneous Reverse Atom Transfer Radical Polymerization Using Aibn as the Initiator. *Macromolecules* **1997**, *30*, 7692−7696.

(185) Gromada, J.; Matyjaszewski, K. Simultaneous Reverse and Normal Initiation in Atom Transfer Radical Polymerization. *Macromolecules* **2001**, *34*, 7664−7671.

(186) Jakubowski, W.; Matyjaszewski, K. Activator Generated by Electron Transfer for Atom Transfer Radical Polymerization. *Macromolecules* **2005**, *38*, 4139−4146.

(187) Tang, W.; Tsarevsky, N. V.; Matyjaszewski, K. Determination of Equilibrium Constants for Atom Transfer Radical Polymerization. *J. Am. Chem. Soc.* **2006**, *128*, 1598−1604.

(188) Tang, W.; Fukuda, T.; Matyjaszewski, K. Reevaluation of Persistent Radical Effect in NMP. *Macromolecules* **2006**, *39*, 4332−4337.

(189) Matyjaszewski, K. Atom Transfer Radical Polymerization (ATRP): Current Status and Future Perspectives. *Macromolecules* **2012**, *45*, 4015−4039.

(190) Jakubowski, W.; Matyjaszewski, K. Activators Regenerated by Electron Transfer for Atom-Transfer Radical Polymerization of (Meth)Acrylates and Related Block Copolymers. *Angew. Chem., Int. Ed.* **2006**, *45*, 4482−4486.

(191) Dong, H.; Tang, W.; Matyjaszewski, K. Well-Defined High-Molecular-Weight Polyacrylonitrile Via Activators Regenerated by Electron Transfer ATRP. *Macromolecules* **2007**, *40*, 2974−2977.

(192) Matyjaszewski, K.; Coca, S.; Gaynor, S. G.; Wei, M.; Woodworth, B. E. Zerovalent Metals in Controlled/"Living" Radical Polymerization. *Macromolecules* **1997**, *30*, 7348−7350.

(193) Matyjaszewski, K.; Jakubowski, W.; Min, K.; Tang, W.; Huang, J.; Braunecker, W. A.; Tsarevsky, N. V. Diminishing Catalyst Concentration in Atom Transfer Radical Polymerization with Reducing Agents. *Proc. Natl. Acad. Sci. U. S. A.* **2006**, *103*, 15309−15314.

(194) Percec, V.; Guliashvili, T.; Ladislaw, J. S.; Wistrand, A.; Stjerndahl, A.; Sienkowska, M. J.; Monteiro, M. J.; Sahoo, S. Ultrafast Synthesis of Ultrahigh Molar Mass Polymers by Metal-Catalyzed Living Radical Polymerization of Acrylates, Methacrylates, and Vinyl Chloride Mediated by Set at 25 °C. *J. Am. Chem. Soc.* **2006**, *128*, 14156−14165.

(195) Anastasaki, A.; Waldron, C.; Wilson, P.; Boyer, C.; Zetterlund, P. B.; Whittaker, M. R.; Haddleton, D. High Molecular Weight Block Copolymers by Sequential Monomer Addition Via Cu(0)-Mediated Living Radical Polymerization (SET-LRP): An Optimized Approach. *ACS Macro Lett.* **2013**, *2*, 896−900.

(196) Zhang, Q.; Wilson, P.; Li, Z.; McHale, R.; Godfrey, J.; Anastasaki, A.; Waldron, C.; Haddleton, D. M. Aqueous Copper-Mediated Living Polymerization: Exploiting Rapid Disproportionation of CuBr with Me₆tren. *J. Am. Chem. Soc.* **2013**, *135*, 7355−7363.

(197) Zhang, Q.; Li, M.; Zhu, C.; Nurumbetov, G.; Li, Z.; Wilson, P.; Kempe, K.; Haddleton, D. M. Well-Defined Protein/Peptide-Polymer Conjugates by Aqueous Cu-LRP: Synthesis and Controlled Self-Assembly. *J. Am. Chem. Soc.* **2015**, *137*, 9344−9353.

(198) Alsubaie, F.; Anastasaki, A.; Nikolaou, V.; Simula, A.; Nurumbetov, G.; Wilson, P.; Kempe, K.; Haddleton, D. M. Investigating the Mechanism of Copper(0)-Mediated Living Radical Polymerization in Aqueous Media. *Macromolecules* **2015**, *48*, 6421−6432.

(199) Alsubaie, F.; Anastasaki, A.; Nikolaou, V.; Simula, A.; Nurumbetov, G.; Wilson, P.; Kempe, K.; Haddleton, D. M. Investigating the Mechanism of Copper(0)-Mediated Living Radical Polymerization in Organic Media. *Macromolecules* **2015**, *48*, 5517−5525.

(200) Peng, C.-H.; Zhong, M.; Wang, Y.; Kwak, Y.; Zhang, Y.; Zhu, W.; Tonge, M.; Buback, J.; Park, S.; Krys, P.; et al. Reversible-Deactivation Radical Polymerization in the Presence of Metallic Copper. Activation of Alkyl Halides by Cu0. *Macromolecules* **2013**, *46*, 3803−3815.

(201) Konkolewicz, D.; Krys, P.; Góis, J. R.; Mendonça, P. V.; Zhong, M.; Wang, Y.; Gennaro, A.; Isse, A. A.; Fantin, M.; Matyjaszewski, K. Aqueous RDRP in the Presence of Cu⁰: The Exceptional Activity of CuⁱConfirms the SARA ATRP Mechanism. *Macromolecules* **2014**, *47*, 560−570.

(202) Konkolewicz, D.; Wang, Y.; Zhong, M.; Krys, P.; Isse, A. A.; Gennaro, A.; Matyjaszewski, K. Reversible-Deactivation Radical Polymerization in the Presence of Metallic Copper. A Critical Assessment of the SARA ATRP and SET-LRP Mechanisms. *Macromolecules* **2013**, *46*, 8749−8772.

(203) Zhong, M.; Wang, Y.; Krys, P.; Konkolewicz, D.; Matyjaszewski, K. Reversible-Deactivation Radical Polymerization in the Presence of Metallic Copper. Kinetic Simulation. *Macromolecules* **2013**, *46*, 3816−3827.

(204) Lin, C. Y.; Coote, M. L.; Gennaro, A.; Matyjaszewski, K. Ab Initio Evaluation of the Thermodynamic and Electrochemical Properties of Alkyl Halides and Radicals and Their Mechanistic Implications for Atom Transfer Radical Polymerization. *J. Am. Chem. Soc.* **2008**, *130*, 12762−12774.

(205) Harrisson, S.; Couvreur, P.; Nicolas, J. Comproportionation Versus Disproportionation in the Initiation Step of Cu(0)-Mediated Living Radical Polymerization. *Macromolecules* **2012**, *45*, 7388−7396.

(206) Wang, Y.; Zhong, M.; Zhu, W.; Peng, C.-H.; Zhang, Y.; Konkolewicz, D.; Bortolamei, N.; Isse, A. A.; Gennaro, A.; Matyjaszewski, K. Reversible-Deactivation Radical Polymerization in the Presence of Metallic Copper. Comproportionation-Disproportionation Equilibria and Kinetics. *Macromolecules* **2013**, *46*, 3793−3802.

(207) Ribelli, T. G.; Krys, P.; Cong, Y.; Matyjaszewski, K. Model Studies of Alkyl Halide Activation and Comproportionation Relevant to RDRP the Presence of Cu⁰. *Macromolecules* **2015**, *48*, 8428−8436.

(208) Tasdelen, M. A.; Uygun, M.; Yagci, Y. Studies on Photoinduced ATRP in the Presence of Photoinitiator. *Macromol. Chem. Phys.* **2011**, *212*, 2036−2042.

(209) Jiang, X.; Wu, J.; Zhang, L.; Cheng, Z.; Zhu, X. Highly Active Ppm Level Organic Copper Catalyzed Photo-Induced ICAR ATRP of Methyl Methacrylate. *Macromol. Rapid Commun.* **2014**, *35*, 1879−1885.

(210) Ciftci, M.; Tasdelen, M. A.; Li, W.; Matyjaszewski, K.; Yagci, Y. Photoinitiated ATRP in Inverse Microemulsion. *Macromolecules* **2013**, *46*, 9537−9543.

(211) Taskin, O. S.; Yilmaz, G.; Tasdelen, M. A.; Yagci, Y. Photoinduced Reverse Atom Transfer Radical Polymerization of Methyl Methacrylate Using Camphorquinone/Benzhydrol System. *Polym. Int.* **2014**, *63*, 902−907.

(212) Tasdelen, M. A.; Ciftci, M.; Yagci, Y. Visible Light-Induced Atom Transfer Radical Polymerization. *Macromol. Chem. Phys.* **2012**, *213*, 1391−1396.

(213) Murtezi, E.; Yagci, Y. Simultaneous Photoinduced ATRP and CuAAC Reactions for the Synthesis of Block Copolymers. *Macromol. Rapid Commun.* **2014**, *35*, 1782−1787.

(214) Yagci, Y.; Tasdelen, M. A.; Jockusch, S. Reduction of Cu(II) by Photochemically Generated Phosphonyl Radicals to Generate Cu(I) as Catalyst for Atom Transfer Radical Polymerization and Azide-Alkyne Cycloaddition Click Reactions. *Polymer* **2014**, *55*, 3468−3474.

(215) Gong, T.; Adzima, B. J.; Bowman, C. N. A Novel Copper Containing Photoinitiator, Copper(II) Acylphosphinate, and Its Application in Both the Photomediated CuAAC Reaction and in Atom Transfer Radical Polymerization. *Chem. Commun.* **2013**, *49*, 7950−7952.

(216) Da Silva, P. A. C.; David, P. G. Photoredox Chemistry of Copper(II) Perchlorate in Methanolic Medium. *Bull. Chem. Soc. Jpn.* **1982**, *55*, 2673−2674.

(217) David, P. G.; Correa da Silva, P. A. Photoredox Chemistry of Chloro and Bromo Complexes of Copper(II) in Methanolic Medium. *Bull. Chem. Soc. Jpn.* **1985**, *58*, 3566−3569.

(218) Tasdelen, M. A.; Uygun, M.; Yagci, Y. Photoinduced Controlled Radical Polymerization in Methanol. *Macromol. Chem. Phys.* **2010**, *211*, 2271−2275.

(219) Ciftci, M.; Tasdelen, M. A.; Yagci, Y. Sunlight Induced Atom Transfer Radical Polymerization by Using Dimanganese Decacarbonyl. *Polym. Chem.* **2014**, *5*, 600−606.

(220) Tasdelen, M. A.; Uygun, M.; Yagci, Y. Photoinduced Controlled Radical Polymerization. *Macromol. Rapid Commun.* **2011**, *32*, 58−62.

(221) Konkolewicz, D.; Schroder, K.; Buback, J.; Bernhard, S.; Matyjaszewski, K. Visible Light and Sunlight Photoinduced ATRP with ppm of Cu Catalyst. *ACS Macro Lett.* **2012**, *1*, 1219−1223.

(222) Fors, B. P.; Hawker, C. J. Control of a Living Radical Polymerization of Methacrylates by Light. *Angew. Chem., Int. Ed.* **2012**, *51*, 8850−8853.

(223) Guan, Z.; Smart, B. A Remarkable Visible Light Effect on Atom-Transfer Radical Polymerization. *Macromolecules* **2000**, *33*, 6904−6906.

(224) Bielawski, C. W.; Grubbs, R. H. Living Ring-Opening Metathesis Polymerization. *Prog. Polym. Sci.* **2007**, *32*, 1−29.

(225) Prier, C. K.; Rankic, D. A.; MacMillan, D. W. C. Visible Light Photoredox Catalysis with Transition Metal Complexes: Applications in Organic Synthesis. *Chem. Rev.* **2013**, *113*, 5322−5363.

(226) Delaude, L.; Delfosse, S.; Richel, A.; Demonceau, A.; Noels, A. F. Tuning of Ruthenium N-Heterocyclic Carbene Catalysts for Atrp. *Chem. Commun.* **2003**, 1526−1527.

(227) Ben-Asuly, A.; Aharoni, A.; Diesendruck, C. E.; Vidavsky, Y.; Goldberg, I.; Straub, B. F.; Lemcoff, N. G. Photoactivation of Ruthenium Olefin Metathesis Initiators. *Organometallics* **2009**, *28*, 4652−4655.

(228) Delaude, L.; Szypa, M.; Demonceau, A.; Noels, A. F. New in Situ Generated Ruthenium Catalysts Bearing N-Heterocyclic Carbene Ligands for the Ring-Opening Metathesis Polymerization of Cyclooctene. *Adv. Synth. Catal.* **2002**, *344*, 749−756.

(229) Karlen, T.; Ludi, A.; Muhlebach, A.; Bernhard, P.; Pharisa, C. Photoinduced Ring-Opening Metathesis Polymerization (PROMP) of Strained Bicyclic Olefins with Ruthenium Complexes of the Type [(η6-Arene(1))Ru(η6-Arene(2))](2+) and [Ru(Nc-R)(6)](2+). *J. Polym. Sci., Part A: Polym. Chem.* **1995**, *33*, 1665−1674.

(230) vanderSchaaf, P. A.; Hafner, A.; Muhlebach, A. Photoinduced Ring-Opening Metathesis Polymerization (PROMP) with Photochemi-

cally Generated Schrock-Type Catalysts. *Angew. Chem., Int. Ed. Engl.* **1996**, *35*, 1845−1847.

(231) Subbotina, I. R.; Shelimov, B. N.; Kazansky, V. B. Olefin Metathesis over Silica-Supported Molybdena Catalysts Activated by UV Irradiation in the Presence of Alkanes. *Kinet. Catal.* **1997**, *38*, 678−684.

(232) Tarasov, A. L.; Shelimov, B. N.; Kazansky, V. B.; Mol, J. C. Olefin Metathesis on Supported Rhenium Catalysts Activated by Gamma-Irradiation. *J. Mol. Catal. A: Chem.* **1997**, *115*, 219−228.

(233) Lalevee, J.; Blanchard, N.; Tehfe, M.-A.; Peter, M.; Morlet-Savary, F.; Gigmes, D.; Fouassier, J. P. Efficient Dual Radical/Cationic Photoinitiator under Visible Light: A New Concept. *Polym. Chem.* **2011**, *2*, 1986−1991.

(234) Zhang, G.; Song, I. Y.; Ahn, K. H.; Park, T.; Choi, W. Free Radical Polymerization Initiated and Controlled by Visible Light Photocatalysis at Ambient Temperature. *Macromolecules* **2011**, *44*, 7594−7599.

(235) Alfredo, N. V.; Jalapa, N. E.; Morales, S. L.; Ryabov, A. D.; Le Lagadec, R.; Alexandrova, L. Light-Driven Living/Controlled Radical Polymerization of Hydrophobic Monomers Catalyzed by Ruthenium-(II) Metalacycles. *Macromolecules* **2012**, *45*, 8135−8146.

(236) Dadashi-Silab, S.; Atilla Tasdelen, M.; Mohamed Asiri, A.; Bahadar Khan, S.; Yagci, Y. Photoinduced Atom Transfer Radical Polymerization Using Semiconductor Nanoparticles. *Macromol. Rapid Commun.* **2014**, *35*, 454−459.

(237) Dadashi-Silab, S.; Tasdelen, M. A.; Kiskan, B.; Wang, X.; Antonietti, M.; Yagci, Y. Photochemically Mediated Atom Transfer Radical Polymerization Using Polymeric Semiconductor Mesoporous Graphitic Carbon Nitride. *Macromol. Chem. Phys.* **2014**, *215*, 675−681.

(238) Kwak, Y.; Matyjaszewski, K. Photoirradiated Atom Transfer Radical Polymerization with an Alkyl Dithiocarbamate at Ambient Temperature. *Macromolecules* **2010**, *43*, 5180−5183.

(239) Li, B.; Yu, B.; Zhou, F. Spatial Control over Brush Growth through Sunlight-Induced Atom Transfer Radical Polymerization Using Dye-Sensitized TiO$_2$ as a Photocatalyst. *Macromol. Rapid Commun.* **2014**, *35*, 1287−1292.

(240) Yan, J.; Li, B.; Zhou, F.; Liu, W. Ultraviolet Light-Induced Surface-Initiated Atom-Transfer Radical Polymerization. *ACS Macro Lett.* **2013**, *2*, 592−596.

(241) Mosnacek, J.; Ilcikova, M. Photochemically Mediated Atom Transfer Radical Polymerization of Methyl Methacrylate Using ppm Amounts of Catalyst. *Macromolecules* **2012**, *45*, 5859−5865.

(242) Zhang, T.; Chen, T.; Amin, I.; Jordan, R. ATRP with a Light Switch: Photoinduced ATRP Using a Household Fluorescent Lamp. *Polym. Chem.* **2014**, *5*, 4790−4796.

(243) Anastasaki, A.; Nikolaou, V.; Zhang, Q.; Burns, J.; Samanta, S. R.; Waldron, C.; Haddleton, A. J.; McHale, R.; Fox, D.; Percec, V.; et al. Copper(II)/Tertiary Amine Synergy in Photoinduced Living Radical Polymerization: Accelerated Synthesis of ω-Functional and α,ω-Heterofunctional Poly(Acrylates). *J. Am. Chem. Soc.* **2014**, *136*, 1141−1149.

(244) Anastasaki, A.; Nikolaou, V.; Simula, A.; Godfrey, J.; Li, M.; Nurumbetov, G.; Wilson, P.; Haddleton, D. M. Expanding the Scope of the Photoinduced Living Radical Polymerization of Acrylates in the Presence of CuBr$_2$ and Me$_6$-Tren. *Macromolecules* **2014**, *47*, 3852−3859.

(245) Anastasaki, A.; Nikolaou, V.; Pappas, G. S.; Zhang, Q.; Wan, C.; Wilson, P.; Davis, T. P.; Whittaker, M. R.; Haddleton, D. M. Photoinduced Sequence-Control Via One Pot Living Radical Polymerization of Acrylates. *Chem. Sci.* **2014**, *5*, 3536−3542.

(246) Anastasaki, A.; Nikolaou, V.; Nurumbetov, G.; Truong, N. P.; Pappas, G. S.; Engelis, N. G.; Quinn, J. F.; Whittaker, M. R.; Davis, T. P.; Haddleton, D. M. Synthesis of Well-Defined Poly(Acrylates) in Ionic Liquids Via Copper(II)-Mediated Photoinduced Living Radical Polymerization. *Macromolecules* **2015**, *48*, 5140−5147.

(247) Ribelli, T. G.; Konkolewicz, D.; Pan, X.; Matyjaszewski, K. Contribution of Photochemistry to Activator Regeneration in Atrp. *Macromolecules* **2014**, *47*, 6316−6321.

(248) Ribelli, T. G.; Konkolewicz, D.; Bernhard, S.; Matyjaszewski, K. How Are Radicals (Re)Generated in Photochemical ATRP? *J. Am. Chem. Soc.* **2014**, *136*, 13303−13312.

(249) Frick, E.; Anastasaki, A.; Haddleton, D. M.; Barner-Kowollik, C. Enlightening the Mechanism of Copper Mediated Photordrp Via High-Resolution Mass Spectrometry. *J. Am. Chem. Soc.* **2015**, *137*, 6889−6896.

(250) Pan, X.; Malhotra, N.; Simakova, A.; Wang, Z.; Konkolewicz, D.; Matyjaszewski, K. Photoinduced Atom Transfer Radical Polymerization with Ppm-Level Cu Catalyst by Visible Light in Aqueous Media. *J. Am. Chem. Soc.* **2015**, *137*, 15430−15433.

(251) Yang, Q.; Dumur, F.; Morlet-Savary, F.; Poly, J.; Lalevee, J. Photocatalyzed Cu-Based ATRP Involving an Oxidative Quenching Mechanism under Visible Light. *Macromolecules* **2015**, *48*, 1972−1980.

(252) Nicewicz, D. A.; MacMillan, D. W. C. Merging Photoredox Catalysis with Organocatalysis: The Direct Asymmetric Alkylation of Aldehydes. *Science* **2008**, *322*, 77−80.

(253) Ischay, M. A.; Anzovino, M. E.; Du, J.; Yoon, T. P. Efficient Visible Light Photocatalysis of [2 + 2] Enone Cycloadditions. *J. Am. Chem. Soc.* **2008**, *130*, 12886−12887.

(254) Narayanam, J. M. R.; Tucker, J. W.; Stephenson, C. R. J. Electron-Transfer Photoredox Catalysis: Development of a Tin-Free Reductive Dehalogenation Reaction. *J. Am. Chem. Soc.* **2009**, *131*, 8756−8757.

(255) Tang, W.; Matyjaszewski, K. Effects of Initiator Structure on Activation Rate Constants in Atrp. *Macromolecules* **2007**, *40*, 1858−1863.

(256) Treat, N. J.; Fors, B. P.; Kramer, J. W.; Christianson, M.; Chiu, C.-Y.; Read de Alaniz, J.; Hawker, C. J. Controlled Radical Polymerization of Acrylates Regulated by Visible Light. *ACS Macro Lett.* **2014**, *3*, 580−584.

(257) Zhang, X.; Zhao, C.; Ma, Y.; Chen, H.; Yang, W. One-Pot Synthesis of PTFEMA-b-PMMA-b-PTFEMA by Controlled Radical Polymerization with a Difunctional Initiator in Conjugation with Photoredox Catalyst of Ir(ppy)3 under Visible Light. *Macromol. Chem. Phys.* **2013**, *214*, 2624−2631.

(258) Ma, W.; Chen, H.; Ma, Y.; Zhao, C.; Yang, W. Visible-Light-Induced Controlled Polymerization of Hydrophilic Monomers with Ir(ppy)3 as a Photoredox Catalyst in Anisole. *Macromol. Chem. Phys.* **2014**, *215*, 1012−1021.

(259) Liu, Q.; Liu, L.; Ma, Y.; Zhao, C.; Yang, W. Visible Light-Induced Controlled Radical Polymerization of Methacrylates with Perfluoroalkyl Iodide as the Initiator in Conjugation with a Photoredox Catalyst Fac-[Ir(ppy)]3. *J. Polym. Sci., Part A: Polym. Chem.* **2014**, *52*, 3283−3291.

(260) Lalevee, J.; Peter, M.; Dumur, F.; Gigmes, D.; Blanchard, N.; Tehfe, M.-A.; Morlet-Savary, F.; Fouassier, J. P. Subtle Ligand Effects in Oxidative Photocatalysis with Iridium Complexes: Application to Photopolymerization. *Chem. - Eur. J.* **2011**, *17*, 15027−15031.

(261) Lalevee, J.; Tehfe, M.-A.; Dumur, F.; Gigmes, D.; Blanchard, N.; Morlet-Savary, F.; Fouassier, J. P. Iridium Photocatalysts in Free Radical Photopolymerization under Visible Lights. *ACS Macro Lett.* **2012**, *1*, 286−290.

(262) Telitel, S.; Dumur, F.; Telitel, S.; Soppera, O.; Lepeltier, M.; Guillaneuf, Y.; Poly, J.; Morlet-Savary, F.; Fioux, P.; Fouassier, J.-P.; et al. Photoredox Catalysis Using a New Iridium Complex as an Efficient Toolbox for Radical, Cationic and Controlled Polymerizations under Soft Blue to Green Lights. *Polym. Chem.* **2015**, *6*, 613−624.

(263) di Lena, F.; Matyjaszewski, K. Transition Metal Catalysts for Controlled Radical Polymerization. *Prog. Polym. Sci.* **2010**, *35*, 959−1021.

(264) Pan, X.; Malhotra, N.; Zhang, J.; Matyjaszewski, K. Photoinduced Fe-Based Atom Transfer Radical Polymerization in the Absence of Additional Ligands, Reducing Agents, and Radical Initiators. *Macromolecules* **2015**, *48*, 6948−6954.

(265) Wang, Y.; Matyjaszewski, K. ATRP of MMA in Polar Solvents Catalyzed by FeBr2 without Additional Ligand. *Macromolecules* **2010**, *43*, 4003−4005.

(266) Nzulu, F.; Telitel, S.; Stoffelbach, F.; Graff, B.; Morlet-Savary, F.; Lalevee, J.; Fensterbank, L.; Goddard, J.-P.; Ollivier, C. A Dinuclear

Gold(I) Complex as a Novel Photoredox Catalyst for Light-Induced Atom Transfer Radical Polymerization. *Polym. Chem.* **2015**, *6*, 4605−4611.

(267) Cao, Y.; Xu, Y.; Zhang, J.; Yang, D.; Liu, J. Well-Controlled Atom Transfer Radical Polymerizations of Acrylates Using Recyclable Niobium Complex Nanoparticle as Photocatalyst under Visible Light Irradiation. *Polymer* **2015**, *61*, 198−203.

(268) Dalko, P. I.; Moisan, L. In the Golden Age of Organocatalysis. *Angew. Chem., Int. Ed.* **2004**, *43*, 5138−5175.

(269) Dondoni, A.; Massi, A. Asymmetric Organocatalysis: From Infancy to Adolescence. *Angew. Chem., Int. Ed.* **2008**, *47*, 4638−4660.

(270) Bertelsen, S.; Jorgensen, K. A. Organocatalysis-after the Gold Rush. *Chem. Soc. Rev.* **2009**, *38*, 2178−2189.

(271) MacMillan, D. W. C. The Advent and Development of Organocatalysis. *Nature* **2008**, *455*, 304−308.

(272) Seayad, J.; List, B. Asymmetric Organocatalysis. *Org. Biomol. Chem.* **2005**, *3*, 719−724.

(273) Ogawa, K. A.; Goetz, A. E.; Boydston, A. J. Metal-Free Ring-Opening Metathesis Polymerization. *J. Am. Chem. Soc.* **2015**, *137*, 1400−1403.

(274) Wang, D.; Wurst, K.; Knolle, W.; Decker, U.; Prager, L.; Naumov, S.; Buchmeiser, M. R. Cationic Ru-II Complexes with N-Heterocyclic Carbene Ligands for UV-Induced Ring-Opening Metathesis Polymerization. *Angew. Chem., Int. Ed.* **2008**, *47*, 3267−3270.

(275) Perkowski, A. J.; You, W.; Nicewicz, D. A. Visible Light Photoinitiated Metal-Free Living Cationic Polymerization of 4-Methoxystyrene. *J. Am. Chem. Soc.* **2015**, *137*, 7580−7583.

(276) Treat, N. J.; Sprafke, H.; Kramer, J. W.; Clark, P. G.; Barton, B. E.; Read de Alaniz, J.; Fors, B. P.; Hawker, C. J. Metal-Free Atom Transfer Radical Polymerization. *J. Am. Chem. Soc.* **2014**, *136*, 16096−16101.

(277) Pan, X.; Lamson, M.; Yan, J.; Matyjaszewski, K. Photoinduced Metal-Free Atom Transfer Radical Polymerization of Acrylonitrile. *ACS Macro Lett.* **2015**, *4*, 192−196.

(278) Miyake, G. M.; Theriot, J. C. Perylene as an Organic Photocatalyst for the Radical Polymerization of Functionalized Vinyl Monomers through Oxidative Quenching with Alkyl Bromides and Visible Light. *Macromolecules* **2014**, *47*, 8255−8261.

(279) Pan, X.; Fang, C.; Fantin, M.; Malhotra, N.; So, W. Y.; Peteanu, L. A.; Isse, A. A.; Gennaro, A.; Liu, P.; Matyjaszewski, K. Mechanism of Photoinduced Metal-Free Atom Transfer Radical Polymerization: Experimental and Computational Studies. *J. Am. Chem. Soc.* **2016**, *138*, 2411.

(280) Narayanam, J. M. R.; Stephenson, C. R. J. Visible Light Photoredox Catalysis: Applications in Organic Synthesis. *Chem. Soc. Rev.* **2011**, *40*, 102−113.

(281) Schultz, D. M.; Yoon, T. P. Solar Synthesis: Prospects in Visible Light Photocatalysis. *Science* **2014**, *343*, 985.

(282) Chen, M.; MacLeod, M. J.; Johnson, J. A. Visible-Light-Controlled Living Radical Polymerization from a Trithiocarbonate Iniferter Mediated by an Organic Photoredox Catalyst. *ACS Macro Lett.* **2015**, *4*, 566−569.

(283) Xu, J.; Jung, K.; Atme, A.; Shanmugam, S.; Boyer, C. A Robust and Versatile Photoinduced Living Polymerization of Conjugated and Unconjugated Monomers and Its Oxygen Tolerance. *J. Am. Chem. Soc.* **2014**, *136*, 5508−5519.

(284) Fu, C.; Xu, J.; Tao, L.; Boyer, C. Combining Enzymatic Monomer Transformation with Photoinduced Electron Transfer - Reversible Addition-Fragmentation Chain Transfer for the Synthesis of Complex Multiblock Copolymers. *ACS Macro Lett.* **2014**, *3*, 633−638.

(285) Lutz, J.-F.; Neugebauer, D.; Matyjaszewski, K. Stereoblock Copolymers and Tacticity Control in Controlled/Living Radical Polymerization. *J. Am. Chem. Soc.* **2003**, *125*, 6986−6993.

(286) Isobe, Y.; Fujioka, D.; Habaue, S.; Okamoto, Y. Efficient Lewis Acid-Catalyzed Stereocontrolled Radical Polymerization of Acryla-mides. *J. Am. Chem. Soc.* **2001**, *123*, 7180−7181.

(287) Shanmugam, S.; Boyer, C. Stereo-, Temporal and Chemical Control through Photoactivation of Living Radical Polymerization:

Synthesis of Block and Gradient Copolymers. *J. Am. Chem. Soc.* **2015**, *137*, 9988−9999.

(288) Iwai, K.; Uesugi, M.; Takemura, F. Tris(2,2′-Bipyridine)-Ruthenium(II)-Sensitized Photopolymerization of Acrylamide. *Polym. J.* **1985**, *17*, 1005−1011.

(289) Lalevee, J.; Telitel, S.; Xiao, P.; Lepeltier, M.; Dumur, F.; Morlet-Savary, F.; Gigmes, D.; Fouassier, J.-P. Metal and Metal-Free Photocatalysts: Mechanistic Approach and Application as Photoinitiators of Photopolymerization. *Beilstein J. Org. Chem.* **2014**, *10*, 863−876.

(290) Lalevee, J.; Blanchard, N.; Tehfe, M.-A.; Peter, M.; Morlet-Savary, F.; Fouassier, J. P. Household Led Irradiation under Air: Cationic Polymerization Using Iridium or Ruthenium Complex Photocatalysts. *Polym. Bull.* **2012**, *68*, 341−347.

(291) Xu, J.; Jung, K.; Boyer, C. Oxygen Tolerance Study of Photoinduced Electron Transfer-Reversible Addition-Fragmentation Chain Transfer (PET-RAFT) Polymerization Mediated by Ru-(bpy)$_3$Cl$_2$. *Macromolecules* **2014**, *47*, 4217−4229.

(292) Xu, J.; Jung, K.; Corrigan, N. A.; Boyer, C. Aqueous Photoinduced Living/Controlled Polymerization: Tailoring for Bio-conjugation. *Chem. Sci.* **2014**, *5*, 3568−3575.

(293) Horton, P.; Ruban, A. V.; Walters, R. G. Regulation of Light Harvesting in Green Plants. *Annu. Rev. Plant Physiol. Plant Mol. Biol.* **1996**, *47*, 655−684.

(294) Gilmore, A. M. Mechanistic Aspects of Xanthophyll Cycle-Dependent Photoprotection in Higher Plant Chloroplasts and Leaves. *Physiol. Plant.* **1997**, *99*, 197−209.

(295) Shanmugam, S.; Xu, J.; Boyer, C. Utilizing the Electron Transfer Mechanism of Chlorophyll a under Light for Controlled Radical Polymerization. *Chem. Sci.* **2015**, *6*, 1341−1349.

(296) Shanmugam, S.; Xu, J.; Boyer, C. Light-Regulated Polymerization under Near-Infrared/Far-Red Irradiation Catalyzed by Bacterio-chlorophyll A. *Angew. Chem., Int. Ed.* **2016**, *55*, 1036−1040.

(297) Balzani, V.; Juris, A.; Venturi, M.; Campagna, S.; Serroni, S. Luminescent and Redox-Active Polynuclear Transition Metal Complexes. *Chem. Rev.* **1996**, *96*, 759−833.

(298) Singh, S.; Aggarwal, A.; Bhupathiraju, N. V. S. D. K.; Arianna, G.; Tiwari, K.; Drain, C. M. Glycosylated Porphyrins, Phthalocyanines, and Other Porphyrinoids for Diagnostics and Therapeutics. *Chem. Rev.* **2015**, *115*, 10261−10306.

(299) Inoue, S.; Sugimoto, H.; Aida, T. Metalloporphyrin Catalysts for Living and Immortal Polymerizations. *Macromol. Symp.* **1996**, *101*, 11−18.

(300) Sugimoto, H.; Kuroki, M.; Watanabe, T.; Kawamura, C.; Aida, T.; Inoue, S. High-Speed Living Anionic Polymerization of Methacrylic Esters with Aluminum Porphyrin Initiators. Organoaluminum Compounds as Lewis Acid Accelerators. *Macromolecules* **1993**, *26*, 3403−3410.

(301) Simakova, A.; Mackenzie, M.; Averick, S. E.; Park, S.; Matyjaszewski, K. Bioinspired Iron-Based Catalyst for Atom Transfer Radical Polymerization. *Angew. Chem., Int. Ed.* **2013**, *52*, 12148−12151.

(302) Sigg, S. J.; Seidi, F.; Renggli, K.; Silva, T. B.; Kali, G.; Bruns, N. Horseradish Peroxidase as a Catalyst for Atom Transfer Radical Polymerization. *Macromol. Rapid Commun.* **2011**, *32*, 1710−1715.

(303) Shanmugam, S.; Xu, J.; Boyer, C. Exploiting Metalloporphyrins for Selective Living Radical Polymerization Tunable over Visible Wavelengths. *J. Am. Chem. Soc.* **2015**, *137*, 9174−9185.

(304) Avens, H. J.; Bowman, C. N. Mechanism of Cyclic Dye Regeneration During Eosin-Sensitized Photoinitiation in the Presence of Polymerization Inhibitors. *J. Polym. Sci., Part A: Polym. Chem.* **2009**, *47*, 6083−6094.

(305) Kizilel, S.; Perez-Luna, V. H.; Teymour, F. Photopolymerization of Poly(Ethylene Glycol) Diacrylate on Eosin-Functionalized Surfaces. *Langmuir* **2004**, *20*, 8652−8658.

(306) Farsari, M.; Filippidis, G.; Sambani, K.; Drakakis, T. S.; Fotakis, C. Two-Photon Polymerization of an Eosin Y-Sensitized Acrylate Composite. *J. Photochem. Photobiol., A* **2006**, *181*, 132−135.

(307) Xu, J.; Shanmugam, S.; Duong, H. T.; Boyer, C. Organo-Photocatalysts for Photoinduced Electron Transfer-Reversible Addi-

tion-Fragmentation Chain Transfer (Pet-RAFT) Polymerization. *Polym. Chem.* **2015**, *6*, 5615−5624.

(308) Xu, J.; Shanmugam, S.; Boyer, C. Organic Electron Donor-Acceptor Photoredox Catalysts: Enhanced Catalytic Efficiency toward Controlled Radical Polymerization. *ACS Macro Lett.* **2015**, *4*, 926−932.

(309) Patwa, A. N.; Tomer, N. S.; Singh, R. P. Visible Light-Induced Controlled/"Living" Radical Polymerization of Styrene. *J. Mater. Sci.* **2004**, *39*, 1047−1049.

(310) Rathore, K.; Reddy, K. R.; Tomer, N. S.; Desai, S. M.; Singh, R. P. Visible-Light-Induced Controlled/Living Radical Polymerization of Styrene with a Phenyl Seleno Group at One Terminal Chain End: 1-(Phenylseleno)Ethyl Benzene as a Photoiniferter. *J. Appl. Polym. Sci.* **2004**, *93*, 348−355.

(311) Barbey, R.; Lavanant, L.; Paripovic, D.; Schuwer, N.; Sugnaux, C.; Tugulu, S.; Klok, H.-A. Polymer Brushes Via Surface-Initiated Controlled Radical Polymerization: Synthesis, Characterization, Properties, and Applications. *Chem. Rev.* **2009**, *109*, 5437−5527.

(312) Kato, K.; Uchida, E.; Kang, E.-T.; Uyama, Y.; Ikada, Y. Polymer Surface with Graft Chains. *Prog. Polym. Sci.* **2003**, *28*, 209−259.

(313) Zhao, B.; Brittain, W. J. Polymer Brushes: Surface-Immobilized Macromolecules. *Prog. Polym. Sci.* **2000**, *25*, 677−710.

(314) Matsuda, T. Photoiniferter-Driven Precision Surface Graft Microarchitectures for Biomedical Applications. *Adv. Polym. Sci.* **2006**, *197*, 67−106.

(315) Ma, Y.; Liu, L.; Yang, W. Photo-Induced Living/Controlled Surface Radical Grafting Polymerization and Its Application in Fabricating 3-D Micro-Architectures on the Surface of Flat/Particulate Organic Substrates. *Polymer* **2011**, *52*, 4159−4173.

(316) Yang, P.; Yang, W. Surface Chemoselective Phototransformation of C-H Bonds on Organic Polymeric Materials and Related High-Tech Applications. *Chem. Rev.* **2013**, *113*, 5547−5594.

(317) Uchida, E.; Ikada, Y. Surface Modification of Polymers by UV-Induced Graft Polymerization. *Curr. Trends Polym. Sci.* **1996**, *1*, 135−146.

(318) Yang, W.; Ranby, B. Radical Living Graft Polymerization on the Surface of Polymeric Materials. *Macromolecules* **1996**, *29*, 3308−3310.

(319) Li, Y.; Desimone, J. M.; Poon, C.-D.; Samulski, E. T. Photoinduced Graft Polymerization of Styrene onto Polypropylene Substrates. *J. Appl. Polym. Sci.* **1997**, *64*, 883−889.

(320) Ma, H.; Davis, R. H.; Bowman, C. N. A Novel Sequential Photoinduced Living Graft Polymerization. *Macromolecules* **2000**, *33*, 331−335.

(321) Stachowiak, T. B.; Svec, F.; Frechet, J. M. J. Patternable Protein Resistant Surfaces for Multifunctional Microfluidic Devices Via Surface Hydrophilization of Porous Polymer Monoliths Using Photografting. *Chem. Mater.* **2006**, *18*, 5950−5957.

(322) Bai, H.; Huang, Z.; Yang, W. Visible Light-Induced Living Surface Grafting Polymerization for the Potential Biological Applications. *J. Polym. Sci., Part A: Polym. Chem.* **2009**, *47*, 6852−6862.

(323) de Boer, B.; Simon, H. K.; Werts, M. P. L.; van der Vegte, E. W.; Hadziioannou, G. "Living" Free Radical Photopolymerization Initiated from Surface-Grafted Iniferter Monolayers. *Macromolecules* **2000**, *33*, 349−356.

(324) Reddy, S. K.; Sebra, R. P.; Anseth, K. S.; Bowman, C. N. Living Radical Photopolymerization Induced Grafting on Thiol-Ene Based Substrates. *J. Polym. Sci., Part A: Polym. Chem.* **2005**, *43*, 2134−2144.

(325) Luo, N.; Hutchison, J. B.; Anseth, K. S.; Bowman, C. N. Synthesis of a Novel Methacrylic Monomer Iniferter and Its Application in Surface Photografting on Crosslinked Polymer Substrates. *J. Polym. Sci., Part A: Polym. Chem.* **2002**, *40*, 1885−1891.

(326) Luo, N.; Hutchison, J. B.; Anseth, K. S.; Bowman, C. N. Surface-Initiated Photopolymerization of Poly(Ethylene Glycol) Methyl Ether Methacrylate on a Diethyldithiocarbamate-Mediated Polymer Substrate. *Macromolecules* **2002**, *35*, 2487−2493.

(327) Yasutake, M.; Andou, Y.; Hiki, S.; Nishida, H.; Endo, T. Controlled Radical Polymerization of Vaporized Vinyl Monomers on Solid Surfaces under UV Irradiation. *Macromol. Chem. Phys.* **2004**, *205*, 492−499.

(328) He, D.; Ulbricht, M. Tailored "Grafting-from" Functionalization of Microfiltration Membrane Surface Photo-Initiated by Immobilized Iniferter. *Macromol. Chem. Phys.* **2009**, *210*, 1149−1158.

(329) Rahane, S. B.; Kilbey, S. M., II; Metters, A. T. Kinetics of Surface-Initiated Photoiniferter-Mediated Photopolymerization. *Macromolecules* **2005**, *38*, 8202−8210.

(330) Rahane, S. B.; Kilbey, S. M.; Metters, A. T. Kinetic Modeling of Surface-Initiated Photoiniferter-Mediated Photopolymerization in Presence of Tetraethylthiuram Disulfide. *Macromolecules* **2008**, *41*, 9612−9618.

(331) Rahane, S. B.; Metters, A. T.; Kilbey, S. M., II Modeling of Reinitiation Ability of Polymer Brushes Grown by Surface-Initiated Photoiniferter-Mediated Photopolymerization. *J. Polym. Sci., Part A: Polym. Chem.* **2010**, *48*, 1586−1593.

(332) Heeb, R.; Bielecki, R. M.; Lee, S.; Spencer, N. D. Room-Temperature, Aqueous-Phase Fabrication of Poly(Methacrylic Acid) Brushes by UV-LED-Induced, Controlled Radical Polymerization with High Selectivity for Surface-Bound Species. *Macromolecules* **2009**, *42*, 9124−9132.

(333) Li, A.; Benetti, E. M.; Tranchida, D.; Clasohm, J. N.; Schoenherr, H.; Spencer, N. D. Surface-Grafted, Covalently Cross-Linked Hydrogel Brushes with Tunable Interfacial and Bulk Properties. *Macromolecules* **2011**, *44*, 5344−5351.

(334) Li, A.; Ramakrishna, S. N.; Nalam, P. C.; Benetti, E. M.; Spencer, N. D. Stratified Polymer Grafts: Synthesis and Characterization of Layered 'Brush' and 'Gel' Structures. *Adv. Mater. Interfaces* **2014**, *1* (1−8), 1300007.

(335) Benetti, E. M.; Reimhult, E.; de Bruin, J.; Zapotoczny, S.; Textor, M.; Vancso, G. J. Poly(Methacrylic Acid) Grafts Grown from Designer Surfaces: The Effect of Initiator Coverage on Polymerization Kinetics, Morphology, and Properties. *Macromolecules* **2009**, *42*, 1640−1647.

(336) Navarro, M.; Benetti, E. M.; Zapotoczny, S.; Planell, J. A.; Vancso, G. J. Buried, Covalently Attached RGD Peptide Motifs in Poly(Methacrylic Acid) Brush Layers: The Effect of Brush Structure on Cell Adhesion. *Langmuir* **2008**, *24*, 10996−11002.

(337) Krause, J. E.; Brault, N. D.; Li, Y.; Xue, H.; Zhou, Y.; Jiang, S. Photoiniferter-Mediated Polymerization of Zwitterionic Carboxybetaine Monomers for Low-Fouling and Functionalizable Surface Coatings. *Macromolecules* **2011**, *44*, 9213−9220.

(338) Liu, Q.; Li, W.; Singh, A.; Cheng, G.; Liu, L. Two Amino Acid-Based Superlow Fouling Polymers: Poly(Lysine Methacrylamide) and Poly(Ornithine Methacrylamide). *Acta Biomater.* **2014**, *10*, 2956−2964.

(339) Liu, Q.; Singh, A.; Liu, L. Amino Acid-Based Zwitterionic Poly(Serine Methacrylate) as an Antifouling Material. *Biomacromolecules* **2013**, *14*, 226−231.

(340) Li, W.; Liu, Q.; Liu, L. Antifouling Gold Surfaces Grafted with Aspartic Acid and Glutamic Acid Based Zwitterionic Polymer Brushes. *Langmuir* **2014**, *30*, 12619−12626.

(341) Wong, E. H. H.; Guntari, S. N.; Blencowe, A.; van Koeverden, M. P.; Caruso, F.; Qiao, G. G. Phototriggered, Metal-Free Continuous Assembly of Polymers for the Fabrication of Ultrathin Films. *ACS Macro Lett.* **2012**, *1*, 1020−1023.

(342) Ma, J.; Luan, S.; Song, L.; Jin, J.; Yuan, S.; Yan, S.; Yang, H.; Shi, H.; Yin, J. Fabricating a Cycloolefin Polymer Immunoassay Platform with a Dual-Function Polymer Brush Via a Surface-Initiated Photoiniferter-Mediated Polymerization Strategy. *ACS Appl. Mater. Interfaces* **2014**, *6*, 1971−1978.

(343) Larsson, E.; Pendergraph, S. A.; Kaldeus, T.; Malmstroem, E.; Carlmark, A. Cellulose Grafting by Photoinduced Controlled Radical Polymerisation. *Polym. Chem.* **2015**, *6*, 1865−1874.

(344) Chen, H.; Zhao, C.; Li, R.; Ma, Y.; Liu, L.; Yang, W. A Facile Visible-Light-Induced Route to Functionalize Polymeric Substrates by Combining Controlled Radical Grafting Polymerization and Thiol-Yne Click Chemistry with Photoredox Catalyst Ir(ppy)3. *Macromol. Chem. Phys.* **2014**, *215*, 1378−1387.

(345) Meng, J.; Li, J.; Zhang, Y.; Ma, S. A Novel Controlled Grafting Chemistry Fully Regulated by Light for Membrane Surface Hydrophilization and Functionalization. *J. Membr. Sci.* **2014**, *455*, 405−414.

(346) Xiong, X.; Wu, Z.; Pan, J.; Xue, L.; Xu, Y.; Chen, H. A Facile Approach to Modify Poly(Dimethylsiloxane) Surfaces Via Visible Light-Induced Grafting Polymerization. *J. Mater. Chem. B* **2015**, *3*, 629−634.

(347) Xiong, X.; Liu, W.; Luan, Y.; Du, J.; Wu, Z.; Chen, H. A Versatile, Fast, and Efficient Method of Visible-Light-Induced Surface Grafting Polymerization. *Langmuir* **2014**, *30*, 5474−5480.

(348) Nie, Z.; Kumacheva, E. Patterning Surfaces with Functional Polymers. *Nat. Mater.* **2008**, *7*, 277−290.

(349) Olivier, A.; Meyer, F.; Raquez, J.-M.; Damman, P.; Dubois, P. Surface-Initiated Controlled Polymerization as a Convenient Method for Designing Functional Polymer Brushes: From Self-Assembled Monolayers to Patterned Surfaces. *Prog. Polym. Sci.* **2012**, *37*, 157−181.

(350) Chen, T.; Amin, I.; Jordan, R. Patterned Polymer Brushes. *Chem. Soc. Rev.* **2012**, *41*, 3280−3296.

(351) Bhat, R. R.; Tomlinson, M. R.; Wu, T.; Genzer, J. Surface-Grafted Polymer Gradients: Formation, Characterization, and Applications. *Adv. Polym. Sci.* **2006**, *198*, 51−124.

(352) Edmondson, S.; Osborne, V. L.; Huck, W. T. S. Polymer Brushes Via Surface-Initiated Polymerizations. *Chem. Soc. Rev.* **2004**, *33*, 14−22.

(353) Harris, B. P.; Kutty, J. K.; Fritz, E. W.; Webb, C. K.; Burg, K. J. L.; Metters, A. T. Photopatterned Polymer Brushes Promoting Cell Adhesion Gradients. *Langmuir* **2006**, *22*, 4467−4471.

(354) Sebra, R. P.; Reddy, S. K.; Masters, K. S.; Bowman, C. N.; Anseth, K. S. Controlled Polymerization Chemistry to Graft Architectures That Influence Cell-Material Interactions. *Acta Biomater.* **2007**, *3*, 151−161.

(355) Benetti, E. M.; Zapotoczny, S.; Vancso, G. J. Tunable Thermoresponsive Polymeric Platforms on Gold by "Photoiniferter"-Based Surface Grafting. *Adv. Mater.* **2007**, *19*, 268−271.

(356) Poelma, J. E.; Fors, B. P.; Meyers, G. F.; Kramer, J. W.; Hawker, C. J. Fabrication of Complex Three-Dimensional Polymer Brush Nanostructures through Light-Mediated Living Radical Polymerization. *Angew. Chem., Int. Ed.* **2013**, *52*, 6844−6848.

(357) Fors, B. P.; Poelma, J. E.; Menyo, M. S.; Robb, M. J.; Spokoyny, D. M.; Kramer, J. W.; Waite, J. H.; Hawker, C. J. Fabrication of Unique Chemical Patterns and Concentration Gradients with Visible Light. *J. Am. Chem. Soc.* **2013**, *135*, 14106−14109.

(358) Chen, Y.; Chen, D.; Ma, Y.; Yang, W. Multiple Levels Hydrophobic Modification of Polymeric Substrates by UV-Grafting Polymerization with TFEMA as Monomer. *J. Polym. Sci., Part A: Polym. Chem.* **2014**, *52*, 1059−1067.

(359) Lin, Z.; Ma, Y.; Zhao, C.; Chen, R.; Zhu, X.; Zhang, L.; Yan, X.; Yang, W. An Extremely Simple Method for Fabricating 3D Protein Microarrays with an Anti-Fouling Background and High Protein Capacity. *Lab Chip* **2014**, *14*, 2505−2514.

(360) Telitel, S.; Telitel, S.; Bosson, J.; Lalevee, J.; Clement, J.-L.; Godfroy, M.; Fillaut, J.-L.; Akdas-Kilig, H.; Guillaneuf, Y.; Gigmes, D.; et al. UV-Induced Micropatterning of Complex Functional Surfaces by Photopolymerization Controlled by Alkoxyamines. *Langmuir* **2015**, *31*, 10026−10036.

(361) Wang, Y.; Zhong, W.; Jiang, N.; Yang, W. Directly Fabricating Monolayer Nanoparticles on a Polymer Surface by UV-Induced MMA/DVB Microemulsion Graft Polymerization. *Macromol. Rapid Commun.* **2005**, *26*, 87−92.

(362) Wang, Y.; Deng, J.; Zhong, W.; Kong, L.; Yang, W. Facile Surface Superhydrophilic Modification: NVP/MBA Inverse Microemulsion Surface-Grafting Polymerization Initiated by UV Light. *Macromol. Rapid Commun.* **2005**, *26*, 1788−1793.

(363) Wang, Y.; Bai, Y.; Zhong, W.; Huang, W.; Yang, W. Direct Construction of Discrete Large Spherical Functional Particles onto Organic Material Surfaces by Photografting Polymerization. *Macromolecules* **2007**, *40*, 756−759.

(364) Tsuji, S.; Kawaguchi, H. Temperature-Sensitive Hairy Particles Prepared by Living Radical Graft Polymerization. *Langmuir* **2004**, *20*, 2449−2455.

(365) Liu, P.; Guo, J. Hg(II) Removal with Polyacrylamide Grafted Crosslinked Poly(Vinyl Chloride) Beads Via Surface-Initiated Controlled/"Living" Radical Polymerization. *J. Appl. Polym. Sci.* **2006**, *102*, 3385−3390.

(366) Derouet, D.; Thuc, C. N. H. Synthesis and Characterization of Poly(Methyl Methacrylate)-Grafted Silica Microparticles. *J. Appl. Polym. Sci.* **2008**, *109*, 2113−2127.

(367) Atmane, Y. A.; Sicard, L.; Lamouri, A.; Pinson, J.; Sicard, M.; Masson, C.; Nowak, S.; Decorse, P.; Piquemal, J.-Y.; Galtayries, A.; et al. Functionalization of Aluminum Nanoparticles Using a Combination of Aryl Diazonium Salt Chemistry and Iniferter Method. *J. Phys. Chem. C* **2013**, *117*, 26000−26006.

(368) Lee, D. H.; Tokuno, Y.; Uchida, S.; Ozawa, M.; Ishizu, K. Architecture of Polymer Particles Composed of Brush Structure at Surfaces and Construction of Colloidal Crystals. *J. Colloid Interface Sci.* **2009**, *340*, 27−34.

(369) Ishizu, K.; Kakinuma, H. Synthesis of Nanocylinders Consisting of Graft Block Copolymers by the Photo-Induced ATRP Technique. *J. Polym. Sci., Part A: Polym. Chem.* **2005**, *43*, 63−70.

(370) Bansal, A.; Kumar, A.; Kumar, P.; Bojja, S.; Chatterjee, A. K.; Ray, S. S.; Jain, S. L. Visible Light-Induced Surface Initiated Atom Transfer Radical Polymerization of Methyl Methacrylate on Titania/Reduced Graphene Oxide Nanocomposite. *RSC Adv.* **2015**, *5*, 21189−21196.

(371) Nugroho, R. W. N.; Odelius, K.; Hoeglund, A.; Albertsson, A.-C. Nondestructive Covalent "Grafting-from" of Poly(Lactide) Particles of Different Geometries. *ACS Appl. Mater. Interfaces* **2012**, *4*, 2978−2984.

(372) Balazs, A. C.; Emrick, T.; Russell, T. P. Nanoparticle Polymer Composites: Where Two Small Worlds Meet. *Science* **2006**, *314*, 1107−1110.

(373) Pecher, J.; Mecking, S. Nanoparticles of Conjugated Polymers. *Chem. Rev.* **2010**, *110*, 6260−6279.

(374) Elsabahy, M.; Wooley, K. L. Design of Polymeric Nanoparticles for Biomedical Delivery Applications. *Chem. Soc. Rev.* **2012**, *41*, 2545−2561.

(375) Kamaly, N.; Xiao, Z.; Valencia, P. M.; Radovic-Moreno, A. F.; Farokhzad, O. C. Targeted Polymeric Therapeutic Nanoparticles: Design, Development and Clinical Translation. *Chem. Soc. Rev.* **2012**, *41*, 2971−3010.

(376) Rao, J. P.; Geckeler, K. E. Polymer Nanoparticles: Preparation Techniques and Size-Control Parameters. *Prog. Polym. Sci.* **2011**, *36*, 887−913.

(377) Wang, Y.; Qiu, Z.; Yang, W. One-Pot Fabrication of Supramolecular Polymer Particles Via Situ Polymerization Stringed Assembly of a Two-Monomer Microemulsion. *Macromol. Rapid Commun.* **2006**, *27*, 284−288.

(378) Wang, Q.; Liu, L.; Yang, W. A Novel and Facile Approach for Preparing Composite Core-Shell Particles by Sequentially Initiated Grafting Polymerization. *Polymer* **2007**, *48*, 6581−6588.

(379) Liu, L.; Ren, M.; Yang, W. Preparation of Polymeric Janus Particles by Directional UV-Induced Reactions. *Langmuir* **2009**, *25*, 11048−11053.

(380) Lv, S.; Liu, L.; Yang, W. Preparation of Soft Hydrogel Nanoparticles with PNIPAM Hair and Characterization of Their Temperature-Induced Aggregation. *Langmuir* **2010**, *26*, 2076−2082.

(381) Liu, Y.; Liu, W.; Ma, Y.; Liu, L.; Yang, W. Direct One-Pot Synthesis of Chemically Anisotropic Particles with Tunable Morphology, Dimensions, and Surface Roughness. *Langmuir* **2015**, *31*, 925−936.

(382) Yoshida, E. Nitroxide-Mediated Photo-Controlled/Living Radical Dispersion Polymerization of Methyl Methacrylate. *Colloid Polym. Sci.* **2011**, *289*, 1625−1630.

(383) Yoshida, E. Giant Vesicles Prepared by Nitroxide-Mediated Photo-Controlled/Living Radical Polymerization-Induced Self-Assembly. *Colloid Polym. Sci.* **2013**, *291*, 2733−2739.

(384) Yoshida, E. Morphology Control of Giant Vesicles by Manipulating Hydrophobic-Hydrophilic Balance of Amphiphilic Random Block Copolymers through Polymerization-Induced Self-Assembly. *Colloid Polym. Sci.* **2014**, *292*, 763−769.

(385) Tan, J.; Zhao, G.; Lu, Y.; Zeng, Z.; Winnik, M. A. Synthesis of PMMA Microparticles with a Narrow Size Distribution by Photo-initiated RAFT Dispersion Polymerization with a Macromonomer as the Stabilizer. *Macromolecules* **2014**, *47*, 6856−6866.

(386) Yeow, J.; Xu, J.; Boyer, C. Polymerization-Induced Self-Assembly Using Visible Light Mediated Photoinduced Electron

Transfer-Reversible Addition-Fragmentation Chain Transfer Polymerization. *ACS Macro Lett.* **2015**, *4*, 984−990.

(387) McKenzie, T. G.; Wong, E. H. H.; Fu, Q.; Sulistio, A.; Dunstan, D. E.; Qiao, G. G. Controlled Formation of Star Polymer Nanoparticles Via Visible Light Photopolymerization. *ACS Macro Lett.* **2015**, *4*, 1012−1016.

(388) Yang, Y.; Urban, M. W. Self-Healing Polymeric Materials. *Chem. Soc. Rev.* **2013**, *42*, 7446−7467.

(389) Syrett, J. A.; Becer, C. R.; Haddleton, D. M. Self-Healing and Self-Mendable Polymers. *Polym. Chem.* **2010**, *1*, 978−987.

(390) Wu, D. Y.; Meure, S.; Solomon, D. Self-Healing Polymeric Materials: A Review of Recent Developments. *Prog. Polym. Sci.* **2008**, *33*, 479−522.

(391) Wojtecki, R. J.; Meador, M. A.; Rowan, S. J. Using the Dynamic Bond to Access Macroscopically Responsive Structurally Dynamic Polymers. *Nat. Mater.* **2011**, *10*, 14−27.

(392) Amamoto, Y.; Kamada, J.; Otsuka, H.; Takahara, A.; Matyjaszewski, K. Repeatable Photoinduced Self-Healing of Covalently Cross-Linked Polymers through Reshuffling of Trithiocarbonate Units. *Angew. Chem., Int. Ed.* **2011**, *50*, 1660−1663.

(393) Amamoto, Y.; Otsuka, H.; Takahara, A.; Matyjaszewski, K. Self-Healing of Covalently Crosslinked Polymers by Reshuffling Thiuram Disulfide Moieties in Air under Visible Light. *Adv. Mater.* **2012**, *24*, 3975−3980.

(394) Morris, R. E. The Sol-Gel Process: Uniformity. *Polymers and Applications*; Nova Science Pub Inc.: New York, 2011.

(395) Osada, Y.; Khokhlov, A. R. *Polymer Gels Networks*; Taylor & Francis: New York, 2002.

(396) Kloxin, C. J.; Scott, T. F.; Adzima, B. J.; Bowman, C. N. Covalent Adaptable Networks (CANS): A Unique Paradigm in Cross-Linked Polymers. *Macromolecules* **2010**, *43*, 2643−2653.

(397) Amamoto, Y.; Otsuka, H.; Takahara, A.; Matyjaszewski, K. Changes in Network Structure of Chemical Gels Controlled by Solvent Quality through Photoinduced Radical Reshuffling Reactions of Trithiocarbonate Units. *ACS Macro Lett.* **2012**, *1*, 478−481.

(398) Zhou, H.; Schön, E.-M.; Wang, M.; Glassman, M. J.; Liu, J.; Zhong, M.; Díaz Díaz, D.; Olsen, B. D.; Johnson, J. A. Crossover Experiments Applied to Network Formation Reactions: Improved Strategies for Counting Elastically Inactive Molecular Defects in PEG Gels and Hyperbranched Polymers. *J. Am. Chem. Soc.* **2014**, *136*, 9464−9470.

(399) Zhou, H.; Woo, J.; Cok, A. M.; Wang, M.; Olsen, B. D.; Johnson, J. A. Counting Primary Loops in Polymer Gels. *Proc. Natl. Acad. Sci. U. S. A.* **2012**, *109*, 19119−19124.

(400) Kawamoto, K.; Zhong, M.; Wang, R.; Olsen, B. D.; Johnson, J. A. Loops Versus Branch Functionality in Model Click Hydrogels. *Macromolecules* **2015**, *48*, 8980−8988.

(401) Spruell, J. M.; Hawker, C. J. Triggered Structural and Property Changes in Polymeric Nanomaterials. *Chem. Sci.* **2011**, *2*, 18−26.

(402) Braun, A. M.; Jakob, L.; Oliveros, E.; Oller do Nascimento, C. A. Up-Scaling Photochemical Reactions. *Adv. Photochem.* **1993**, *18*, 235−313.

(403) Braun, A. M.; Peschl, G. H.; Oliveros, E. Industrial Photochemistry. *CRC Handbook of Organic Photochemistry and Photobiology*, 3rd ed.; CRC Press: Boca Raton, FL, 2012; Vol. *1*, pp 1−19.10.1201/b12252-2

(404) Pastre, J. C.; Browne, D. L.; Ley, S. V. Flow Chemistry Syntheses of Natural Products. *Chem. Soc. Rev.* **2013**, *42*, 8849−8869.

(405) Yoshida, J.-i.; Takahashi, Y.; Nagaki, A. Flash Chemistry: Flow Chemistry That Cannot Be Done in Batch. *Chem. Commun.* **2013**, *49*, 9896−9904.

(406) Elvira, K. S.; Casadevall i Solvas, X.; Wootton, R. C. R.; de Mello, A. J. The Past, Present and Potential for Microfluidic Reactor Technology in Chemical Synthesis. *Nat. Chem.* **2013**, *5*, 905−915.

(407) McQuade, D. T.; Seeberger, P. H. Applying Flow Chemistry: Methods, Materials, and Multistep Synthesis. *J. Org. Chem.* **2013**, *78*, 6384−6389.

(408) Hessel, V.; Kralisch, D.; Kockmann, N.; Noel, T.; Wang, Q. Novel Process Windows for Enabling, Accelerating, and Uplifting Flow Chemistry. *ChemSusChem* **2013**, *6*, 746−789.

(409) Chan, N.; Cunningham, M. F.; Hutchinson, R. A. Copper-Mediated Controlled Radical Polymerization in Continuous Flow Processes: Synergy between Polymer Reaction Engineering and Innovative Chemistry. *J. Polym. Sci., Part A: Polym. Chem.* **2013**, *51*, 3081−3096.

(410) Wilms, D.; Klos, J.; Frey, H. Microstructured Reactors for Polymer Synthesis: A Renaissance of Continuous Flow Processes for Tailor-Made Macromolecules? *Macromol. Chem. Phys.* **2008**, *209*, 343−356.

(411) Schork, F. J.; Guo, J. Continuous Miniemulsion Polymerization. *Macromol. React. Eng.* **2008**, *2*, 287−303.

(412) Tonhauser, C.; Natalello, A.; Loewe, H.; Frey, H. Microflow Technology in Polymer Synthesis. *Macromolecules* **2012**, *45*, 9551−9570.

(413) Hornung, C. H.; von Kanel, K.; Martinez-Botella, I.; Espiritu, M.; Nguyen, X.; Postma, A.; Saubern, S.; Chiefari, J.; Thang, S. H. Continuous Flow Aminolysis of RAFT Polymers Using Multistep Processing and Inline Analysis. *Macromolecules* **2014**, *47*, 8203−8213.

(414) Gilmore, K.; Seeberger, P. H. Continuous Flow Photochemistry. *Chem. Rec.* **2014**, *14*, 410−418.

(415) Su, Y.; Straathof, N. J. W.; Hessel, V.; Noel, T. Photochemical Transformations Accelerated in Continuous-Flow Reactors: Basic Concepts and Applications. *Chem. - Eur. J.* **2014**, *20*, 10562−10589.

(416) Wenn, B.; Conradi, M.; Carreiras, A. D.; Haddleton, D. M.; Junkers, T. Photo-Induced Copper-Mediated Polymerization of Methyl Acrylate in Continuous Flow Reactors. *Polym. Chem.* **2014**, *5*, 3053−3060.

(417) Kermagoret, A.; Wenn, B.; Debuigne, A.; Jerome, C.; Junkers, T.; Detrembleur, C. Improved Photo-Induced Cobalt-Mediated Radical Polymerization in Continuous Flow Photoreactors. *Polym. Chem.* **2015**, *6*, 3847−3857.

(418) Chen, M.; Johnson, J. A. Improving Photo-Controlled Living Radical Polymerization from Trithiocarbonates through the Use of Continuous-Flow Techniques. *Chem. Commun.* **2015**, *51*, 6742−6745.

(419) Melker, A.; Fors, B. P.; Hawker, C. J.; Poelma, J. E. Continuous Flow Synthesis of Poly(Methyl Methacrylate) Via a Light-Mediated Controlled Radical Polymerization. *J. Polym. Sci., Part A: Polym. Chem.* **2015**, *53*, 2693−2698.

(420) Barnes, J. C.; Ehrlich, D. J. C.; Gao, A. X.; Leibfarth, F. A.; Jiang, Y.; Zhou, E.; Jamison, T. F.; Johnson, J. A. Iterative Exponential Growth of Stereo- and Sequence-Controlled Polymers. *Nat. Chem.* **2015**, *7*, 810−815.

(421) Leibfarth, F. A.; Johnson, J. A.; Jamison, T. F. Scalable Synthesis of Sequence-Defined, Unimolecular Macromolecules by Flow-IEG. *Proc. Natl. Acad. Sci. U. S. A.* **2015**, *112*, 10617−10622.

(422) Lutz, J.-F.; Ouchi, M.; Liu, D. R.; Sawamoto, M. Sequence-Controlled Polymers. *Science* **2013**, *341*, 628.

(423) Xu, J.; Shanmugam, S.; Fu, C.; Aguey-Zinsou, K.; Boyer, C. Selective Photoactivation: From a Single Unit Monomer Insertion Reaction to Controlled Polymer Architectures. *J. Am. Chem. Soc.* **2016**, DOI: 10.1021/jacs.5b12408.